Uplink OFDMA Resource Allocation using mobile Relays and Proportional Fairness

Salma Hamda Harchay

CONSERVATOIRE NATIONAL DES ARTS ET MÉTIERS | le cnam

École Doctorale du Conservatoire National des Arts et Métiers

Laboratoire CEDRIC/LAETITIA

THÈSE DE DOCTORAT

présentée par : **Salma HAMDA HARCHAY**

soutenue le : **21 mars 2016**

pour obtenir le grade de : **Docteur du Conservatoire National des Arts et Métiers**

Discipline / Spécialité : **Électronique / Télécommunications**

Uplink OFDMA Resource Allocation using mobile Relays and Proportional Fairness

THÈSE dirigée par

M. BOUALLEGUE Ridha	Professeur, SUP'COM (Tunisie)
Mme. PISCHELLA Mylène	Maître de conférence, CNAM
M. ROVIRAS Daniel	Professeur, CNAM

RAPPORTEURS

M. HAMDI Noureddine	Professeur, INSAT (Tunisie)
M. VANDENDORPE Luc	Professeur, Université Catholique de Louvain

EXAMINATEURS

M. BOUALLEGUE Ammar	Professeur, ENIT (Tunisie)
M. DEBBAH Mérouane	Professeur, CENTRALESUPELEC

Dedicaces

A mes chers parents, ma mère Jenina et mon père Nejib, qu'aucun mot ne pourrait décrire mon amour et mon respect pour eux, pour tout leur soutien et leur amour. J'espère qu'ils trouveront dans ce travail toute ma reconnaissance

A mes chers frères Fares et Sofien auxquels je souhaite tout le bonheur du monde

A mon cher mari Achraf pour son soutien perpétuel, j'espère qu'il trouvera dans ce travail toute ma gratitude et mon amour

A mon adorable fille Lyne, qui remplit ma vie de bonheur et que j'aime trop

A ma belle-famille. A ma belle-mère Amel et mon beau-père Hedi que j'aime et je respecte. A Haifa et Dhia que j'adore

A ma très chère grand-mère que j'aime tant

A toutes mes tantes et tous mes oncles particulièrement ma tante Emna et mon Oncle Mounir

A tous mes cousines et cousins spécialement Rim, Marwen et Mehdi, sur lesquels je peux toujours compter

A mes nouvelles amies du CNAM Iness, Hanen et Marwa, avec qui j'ai passé de très bons moments et qui ont su me remonté le moral à des périodes difficiles de la thèse

A mes chères amies Mariem, Lina, Mouna, Emna, Aicha, Anwaar, Marwa, Cyrine, Sihem, que j'aime beaucoup, même si je n'ai pas toujours l'occasion de passer beaucoup de temps avec elles.

A tous mes amis (es)..

Je dédie ce mémoire

Remerciement

Tout d'abord, je tiens à exprimer ma vive gratitude à mes encadrants de thèse. Je tiens à remercier tout particulièrement Professeur Daniel ROVIRAS du CNAM pour ses conseils constructifs et avisés et pour le temps qu'il m'a consacré malgré ses charges académiques et professionnelles. Je tiens également à remercier ma co-encadrante Mylène PISCHELLA, maître de conférence au CNAM, pour sa disponibilité, son enthousiame et sa réactivité tout au long de cette thèse. Mes vifs remerciement vont à mon directeur de thèse de l'ENIT à Tunis Professeur Ridha BOUALLEGUE pour son soutien. Je remercie tous mes encadrants pour leurs qualités humaines irréprochables, pour leur sens de l'écoute, sans oublier leurs méticuleuses lectures de ce mémoire.

Mes remerciement s'adressent à Mérouane DEBBAH, Professeur à CentraleSupelec, d'avoir accepté la présidence de mon jury et d'examiner mes travaux. Je remercie également Ammar BOUALLEGUE, Professeur à l'ENIT à Tunis et Noureddine HAMDI, Professeur à l'INSAT à tunis d'avoir accepté d'évaluer mes travaux et de faire le déplacement pour ma soutenance. J'associe également mes remerciement à Luc VANDENDORPE, Professeur à l'université catholique de Louvin, pour avoir accepté de faire partie de mon jury et d'examiner mes travaux.

Cette thèse s'est déroulée en cotutelle entre l'ENIT à Tunis et le CNAM à Paris, la majorité du temps étant sur Paris. J'adresse donc mes remerciement à tous mes collègues du CNAM et de l'ENIT aussi bien les chercheurs que le personnel administratif pour leur générosité et pour la bonne ambiance de travail qu'ils m'ont offert.

Salma HAMDA HARCHAY

Abstract

In wireless systems, resource allocation is still an important challenge to satisfy user requirements and to ensure good system performances with always greedy data applications. Multicarrier techniques especially the Orthogonal Frequency Division Multiplexing (OFDM) techniques are generally used to carry data into orthogonal subcarriers. Furthermore, relaying strategies are used to enhance cell edge performances. Many types of relays can be investigated as fix relays being part of the network infrastructure or mobile relays without additional deployment cost.
In this thesis, we mainly consider the resource allocation for an uplink Orthogonal Frequency Division Multiple Access (OFDMA) system for a cellular system model ensuring Quality of Service (QoS) requirements and fairness between users. The most used resource allocation algorithms are presented and a novel Weighted Proportional Fair (WPF) algorithm is proposed to approach upper bounds of both throughput and fairness. The WPF algorithm considers user weights to allocate more subcarriers in the cell center than in the cell edge keeping sufficient fairness between users. We establish a theoretical analysis to compare the behavior of the proposed WPF algorithm to the classical Proportional Fair (PF) algorithm. Then, we extend this WPF algorithm to a multi-cell system model where the Inter-Cell Interference (ICI) limits the system performance. Moreover, we study ICI mitigation strategies and propose a novel method to reduce the ICI based on Base Station (BS) cooperation and interference indicators. We propose the Enhanced Interference Indicator (EII) with integer values to be exchanged by the BSs indicating interference levels for the subcarriers. Function of these communicated EII values, each BS allocates dynamically subcarriers in order to reduce the ICI. Our contributions in the multi-cell system model are the WPF and the EII.
Moreover, we investigate in this dissertation the cooperative communication using mobile relays and propose multiple contributions. For this, simple mobile users with advantageous positions can relay cell edge users to carry data to the BS in addition to their own data. A Decode and Forward (DF) relay multiplex then its own data and relayed data before transmitting to the BS.

The resource allocation is formulated as an optimization problem aiming to minimize the system transmit power and respecting a required target data rate per user constraint. In a first time, we propose an initialization method for the paring step to associate source-relay pairs and propose an iterative heuristic to optimize both power and Resource Blocks (RB) allocations. In a second time, we consider the relay selection as an optimization variable in addition of power and RB allocations. For resolution, Lagrangian decomposition and Dual method are used and the global problem is divided into subproblems iterativelly resolved to approach the optimal solution. Finally, we extend this cooperative system model to a Multiple Input Multiple Output (MIMO) system model to study the influence of multiple antennas on the system transmit power. The features to optimize are relay selection, power and RBs allocation. Moreover, to allocate power in the different antennas for each user, both Equal Power Allocation (EPA) and beamforming are studied. Theoretical expressions are established and simulations results are presented to compare EPA, beamforming and non-cooperative system.

Key words

OFDMA, resource allocation, mobile relays, uplink, proportional fairness

Résumé

Dans les systèmes de communications sans fils, l'allocation de ressources reste toujours un défi considérable afin de satisfaire les demandes des utilisateurs et de fournir de bonnes performances avec une perpétuelle demande en applications gourmandes en ressources. Les techniques multiporteuses essentiellement les techniques dérivant de l'OFDM sont généralement utilisées pour transmettre les données dans des sous-porteuses orthogonales. De plus, de nouvelles stratégies de relayage sont proposées pour améliorer les performances en bordures de cellules. Plusieurs types de relais peuvent être sollicités comme les relais fixes faisant partie de l'infrastructure du système ou les relais mobiles qui ne nécessitent pas un coût additionnel de déploiement.

Dans cette thèse, nous étudions principalement l'allocation des ressources pour le sens montant d'un système cellulaire OFDMA assurant les exigences de qualité de service et l'équité entre les utilisateurs. Les algorithmes d'allocation de ressources les plus utilisés sont présentés et un nouvel algorithme se basant sur l'équité proportionnelle pondérée (WPF) est proposé afin d'approcher les bornes supérieures de débit et d'équité. L'algorithme WPF propose un poids variable par utilisateur permettant d'allouer un nombre plus élevé de sous-porteuses au centre de la cellule qu'en bordure tout en gardant une bonne équité entre les utilisateurs. Nous établissons une étude théorique afin de comparer l'algorithme proposé à l'algorithme classique d'équité proportionnelle (PF). Nous étendons ensuite l'algorithme WPF à un système multi-cellulaire où l'interférence inter-cellulaire (ICI) dégrade les performances du système. Enfin, nous étudions les stratégies d'annulation de l'ICI et proposons une nouvelle méthode pour réduire l'ICI en se basant sur la coopération entre les stations de base (BSs) et sur les indicateurs d'interférence. Nous proposons un nouvel indicateur d'interférence (EII) à valeurs entières échangé par les BSs pour indiquer les niveaux d'interférence des sous-porteuses. En prenant en compte les valeurs de EII échangées, chaque BS alloue dynamiquement les sous-porteuses de manière à éviter de fortes valeurs d'ICI.

Dans un deuxième temps, nous étudions la communication coopérative en utilisant des relais

mobiles. Pour cela, de simples utilisateurs mobiles ayant des positions avantageuses peuvent relayer d'autres utilisateurs en bordure de cellule en plus de transmettre leurs propres données. Un relai utilisant le protocole DF multiplexe ainsi ses propres données aux données relayées avant de transmettre à la BS. L'allocation de ressource est formulée sous forme d'un problème d'optimisation dont le but est de minimiser la puissance totale d'émission du système tout en assurant un débit cible par utilisateur. Dans un premier temps, nous proposons une méthode de sélection des relais comme phase d'initialisation et offrons une heuristique itérative pour optimiser l'allocation de puissance et des blocs de ressources radio (RBs). Dans un second temps, nous traitons la sélection des relais comme une variable d'optimisation additionnelle. Pour la résolution, la décomposition de Lagrange et la méthode duale sont utilisées et le problème global est divisé en sous problèmes résolus de manière itérative afin d'approcher la solution optimale. Enfin, nous étendons ce modèle coopératif à un modèle à antennes multiples (MIMO) afin d'étudier l'influence des antennes multiples sur la puissance totale de transmission. Les paramètres à optimiser sont la sélection des relais, l'allocation des puissances et l'allocation des RBs. Afin d'allouer la puissance sur les antennes d'un utilisateur, nous avons étudié la répartition égale des puissance (EPA) et le beamforming. Les expressions théoriques correspondantes sont établies et les résultats de simulation sont présentés pour comparer le modèle avec EPA et le modèle avec beamforming au modèle non coopératif.

Mots clés

OFDMA, allocation de ressources, relais mobiles, sens montant, équité proportionnelle

Résumé des travaux de thèse

Chapitre 1: Introduction

La perpétuelle évolution des applications mobiles de nos jours rend la gestion des réseaux mobiles cellulaires critique afin de répondre aux exigences des clients. En effet, en plus de la voix, les applications avec images et vidéos nécessitent une gestion de ressources plus efficace pour assurer la qualité demandée. Dans les systèmes de communication sans fil modernes, les techniques de multiplexage fréquentiel sont généralement adoptées spécialement l'OFDM (Orthogonal Frequency Division Multiplexing). L'idée principale de l'OFDM est de diviser la bande passante disponible en un ensemble de sous-porteuses orthogonales. La bande de chaque sous-porteuse doit être inférieure à la bande de cohérence du canal de propagation afin de réduire le fading par sous-porteuse. Avec l'orthogonalité entre les sous-porteuses, l'interférence inter-symboles peut être évitée. L'OFDMA présentant la variante multi-utilisateurs de l'OFDM est adoptée pour les standards Wimax [1] et LTE [2].

De plus, l'allocation de ressources dans les systèmes sans fils est l'élément principal pour satisfaire les demandes des clients avec la limitaion de la bande passante disponible. Dans la littérature, on peut trouver différents algorithmes selon l'objectif souhaité. L'algorithme maximisant la somme des débits présente la bande supérieure en terme de débit mais reste totalement inéquitable. Pour maximiser le débit du système, seuls les utilisateurs proches de la station de base (BS) sont servis et tous les autres sont ignorés. Ensuite, on trouve l'algorithme "max min" [3] avec l'objectif de maximiser à chaque fois le débit minimal dans le système. Cet algorithme est considéré comme la bande supérieure en équité entre utilisateurs mais il fournit un débit total du système

qui est faible. De plus, les algorithmes d'équité proportionnelle sont proposés dans la littérature comme un compromis entre le débit et l'équité [4][5].

L'allocation de ressource font l'objet de plusieurs recherches actuelles en particulier pour les prochaines générations de systèmes sans fils. De plus, les algorithmes proposés doivent offrir de bons résultats dans les systèmes multi-cellulaire et résister à l'interférence inter-cellulaire (ICI) [6] [2]. Dans un tel système, les algorithmes reposent généralement sur la réutilisation de fréquence ou sur la coopération entre les BS. La réutilisation de fréquence permet d'éviter l'ICI mais réduit la bande à utiliser dans chaque cellule. La coopération entre les BS peut réduire l'ICI mais peut engendrer un coût de communication important selon la quantité de données à échanger [7][8][9].

Afin d'améliorer les performances des systèmes, les statégies de relayages présentent de nos jours un sujet de recherche prometteur. Les relais peuvent être fixes ou mobile et la transmission peut s'effectuer sur un ou plusieurs sauts. Les relais fixes font partie du réseau et nécessitent un coût de déploiement tandis que les relais mobiles ne nécessitent aucun coût de déploiement mais sont totalement imprévisibles. Lorsque des relais sont utilisés, la transmission s'effectue en deux temps [10]: la source transmet au relai dans un premier temps et le relais transmet à la destination dans un second temp. Différents protocoles peuvent être utilisés au niveau des relais tels que le Decode and Forward (DF) et le Amplify and Forward (AF). Un relai utilisant le protocole DF décode le signal reçu, le ré-encode et le transmet à la destination. Un relai avec le protocole AF applique uniquement un facteur d'amplification au signal reçu avant de le transmettre à la destination. S'il n'existe pas de lien direct entre la source et la destination, les relais sont appelés des répéteurs. Si le lien direct existe, les relais peuvent être considérés comme un MIMO virtuel (Multiple Input Multiple Output)[11]. Dans les systèmes avec relais, la sélection du relai présente un élément supplémentaire pour l'allocation de ressources. Les relais fixes sont décrits et adoptés dans le standard LTE [12]. Les relais mobiles présentent un candidat sérieux pour la 5eme génération des systèmes sans fils.

Dans cette thèse, nous avons principalement considéré l'allocation de ressources pour le sens montant d'un système cellulaire OFDMA assurant les exigences de qualité de services et l'équité entre les utilisateurs. Les méthodes d'allocation proposées sont applicables dans les réseaux LTE Advanced et les réseaux de 5eme génération.

Chapitre 2: Contexte technique

Le contexte technique adopté dans cette thèse est introduit dans le chapitre 2. Les principales notions utilisées dans ce mémoire sont donc définies tel que l'OFDM, les aspects multi-cellulaires et les éléments mathématiques nécessaires pour formaliser et résoudre

des problèmes d'optimisation. Les modèles adoptés sont également détailles tel que le modèle de canal retrouvé dans tous les chapitres de contributions.

Chapitre 3: Allocation de ressources dans un système mono-cellulaire

Dans ce chapitre, l'allocation de ressources dans un système OFDMA multi-utilisateur est étudiée pour le sens montant des utilisateurs vers la BS. Les principaux algorithmes d'allocation de ressources sont étudiés et comparés et un nouvel algorithme se basant sur l'équité proportionnelle (PF) est proposé: l'algorithme à équité proportionnelle ponderée (WPF).

Modèle du système

On considère le sens montant d'un système de transmission OFDMA dans une cellule avec une BS, K utilisateurs et N sous-porteuses. Le canal est supposé sélectif en fréquence avec un évanouissement lent de Rayleigh et un bruit blanc gaussien (AWGN). Chaque sous-porteuse a une bande Δf et est exclusivement allouée à un utilisateur. Les utilisateurs sont répartis uniformément sur la cellule et chaque utilisateur subit un affaiblissement de propagation L_k et un affaiblissement causé par les obstacles S_k avec une loi log-normale. On appelle $\gamma_{k,j}^m$ le gain de canal pour un utilisateur k et une sous-porteuse **j** à l'instant m exprimé tel que:

$$\gamma_{k,j}^m = \frac{g_{k,j}^m}{L_k S_k \Delta f N_0} \tag{1}$$

avec $g_{k,j}^m$ le carré de l'évanouissement de Rayleigh et N_0 la puissance du bruit. Avec une puissance maximale P_k par utilisateur, le débit en bits/s de l'utilisateur k à l'instant m est exprimé tel que:

$$R_k^m = \Delta f \sum_{j=1}^{N} R_{k,j}^m = \Delta f \sum_{j=1}^{N} a_{k,j}^m \log_2 (1 + \gamma_{k,j}^m P_{k,j}^m) \tag{2}$$

avec $P_{k,j}^m$ la puissance allouée à la sous-porteuse j. $a_{k,j}^m$ est une variable booléenne égale à 1 si **j** est allouée à l'utilisateur k, 0 sinon. Les atténations sont supposées constantes pendant un intervalle de temps.

Algorithme à équité proportionnelle pondérée (WPF)

L'algorithme WPF est une évolution de l'algorithme classique à équité proportionnelle (PF) en ajoutant des priorités entre les différents utilisateurs. En effet, l'algorithme PF alloue approximativement le même nombre de sous-porteuses à tous les utilisateurs en commençant par le centre de la cellule. L'idée principale de notre nouvel algorithme est d'allouer plus de bande au centre de la cellule qu'en bordure afin de mieux exploiter

les bonnes conditions des utilisateurs au centre et par conséquent améliorer le débit du système. Pour ce, on introduit un poids par utilisateur indépendant des sous-porteuses. Ce poids est ajouté à la fonction d'utilité de chaque utilisateur afin de favoriser les utilisateurs au centre de la cellule sans ignorer ceux en bordure. L'utilité incrémentale de l'utilisateur k et la sous-porteuse **j** à l'instant m est exprimée tel que [5]:

$$U^{m}_{k,j} = \frac{R^{m}_{k,j}}{R^{m-1}_{k} + \sum_{i \in S^{m}_{sub,k}} R^{m}_{k,i}} [w_k]^{\beta} \quad (3)$$

où

$$w_k = \Delta f \log_2 \left(1 + \frac{P_k}{L_k S_k N_0 \Delta f} \right) \quad (4)$$

avec $S^{m}_{sub,k}$ l'ensemble des sous-porteuses allouées à l'utilisateur k à l'instant m et R^{m}_{k} le débit cumulé pour k jusqu'à l'intervalle de temps de transmission (TTI) m. w_k est le poids de l'utilisateur k et présente le débit moyen par utilisateur par sous-porteuse. $\beta \in [0;1]$, en posant $\beta = 0$, on retrouve l'algorithme PF classique. La sous-porteuse **j** est assignée à l'utilisateur maximisant l'utilité incrémentale $k^* = \arg\max_k U^{m}_{k,j}$

Etude théorique

Afin de comparer le comportement du nouvel algorithme proposé au PF classique, une étude théorique est réalisée. En considérant 2 utilisateurs, le premier au centre de la cellule et le deuxième en bordure, les probabilités d'affectation des sous-porteuses sont étudiées et calculées. Les résultats des équations analytiques sont ensuite comparés aux résultats de simulations comme présente la figure 1, N_k et U_k étant respectivement le nombre de sous-porteuses et l'utilité de l'utilisateur k.

Avec $\beta = 0$, la figure 1 montre bien qu'on retrouve le PF classique avec 50% de probabilité de chaque utilisateur pour gagner la sous-porteuse discutée quand $N_1 = N_2$. Quand $\beta \geq 0$, l'équité diminue et l'utilisateur 1 a plus de chance de gagner des sous-porteuses. Par exemple, pour $\beta = 1$ l'utilisateur 1 est favorisé avec $Pr(U_1 > U_2) \cong 1$ jusqu'à $N_1 - N_2 = 6$. C'est seulement à ce moment que l'utilisateur 2 peut gagner la prochaine sous-porteuse avec une probabilité de 50%.

Résultats de simulations

Pour les simulations, une cellule circulaire est considérée avec un rayon de 0.5 km. La bande totale considérée est de B = 1.4 MHz, K = 20 utilisateurs uniformément distribués et N = 72 sous-porteuses avec une bande par sous-porteuse Δf = 15 KHz. La puissance du bruit AWGN est $N_0 = -174$ dBm/Hz. Le shadowing suit une loi log-normale avec

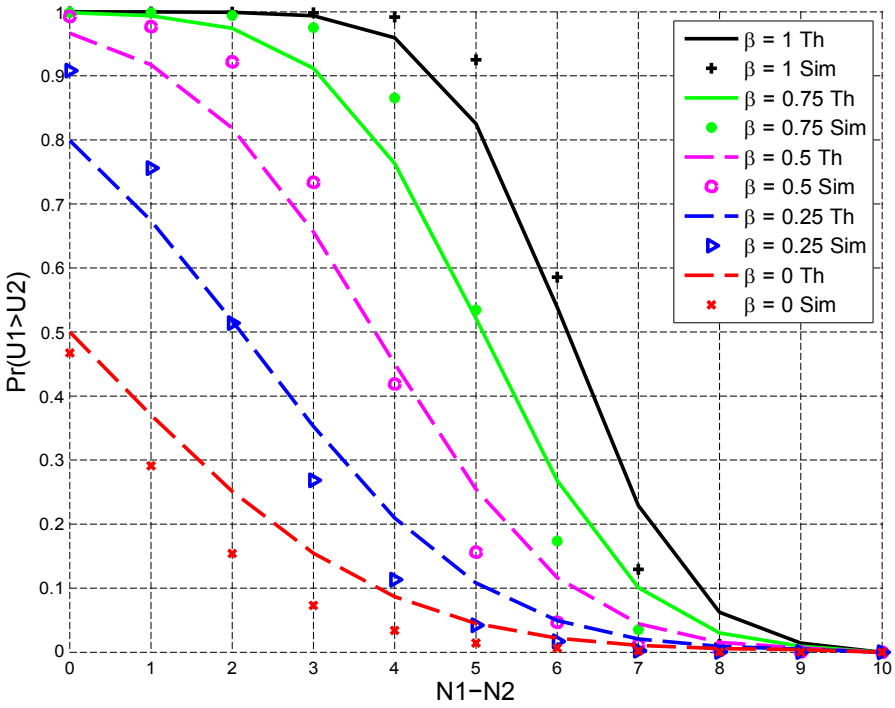

Figure 1: Probabilité $Pr(U_1 > U_2)$, $N_1 = 10$

un écart type de 6 dB et l'atténuation est considérée suivant le modèle LTE avec une fréquence de F = 2.6 GHz: $L_{k,dB}(d_k) = 128.1 + 37.6 \log_{10}(d_k)$ où d_k est la distance en km entre l'utilisateur k et la BS.

100 TTIs sont pris en compte pour l'algorithme WPF. Les résultats sont moyennés sur 500 simulations. Pour comparer avec les algorithmes existants dans la littérature, on note:

- **MaxSumRate:** L'algorithme qui maximise la somme de débits du système
- **WeightedPF:** Notre algorithme proposé WPF avec différentes valeurs de β
- **PF:** L'algorithme clasique PF ou le WPF avec β = 0
- **SameNbreSc:** L'algorithme allouant le même nombre de sous-porteuses par utilisateur
- **MaxMin:** L'algorithme qui vise d'assurer un débit minimal par utilisateur

Les résultats sont présentés en termes de débit et d'équité:

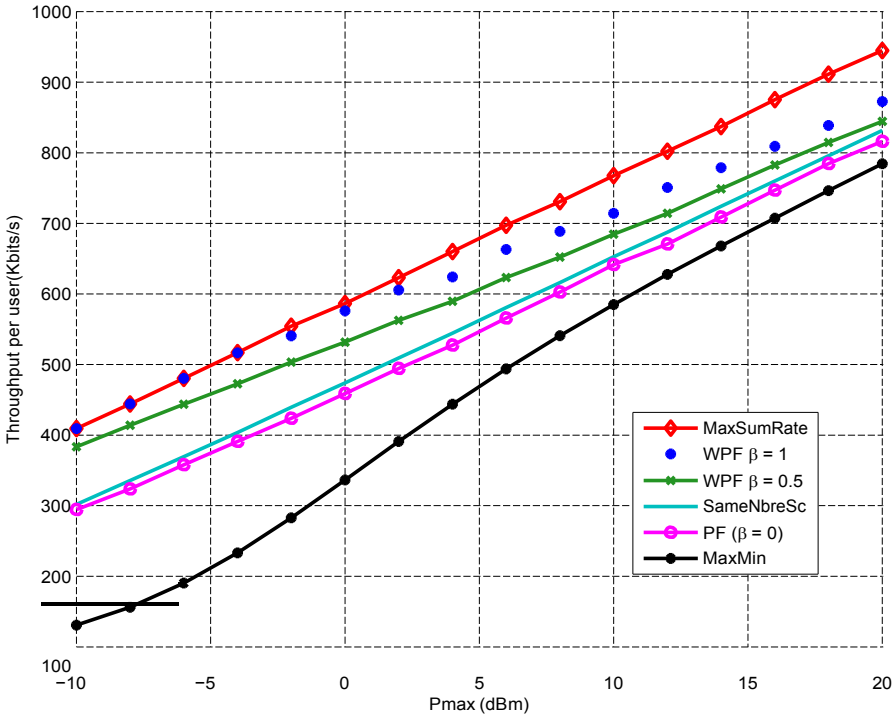

Figure 2: Débit du système

- **Débit** La figure 3.2 présente le débit du système en fonction des puissances de transmission. L'algorithme **MaxSumRate** est visiblement la borne supérieure du débit et l'algorithme **MaxMin** favorisant les utilisateurs en bordure de cellule présente les valeurs les plus faibles du débit. Les résultats de simulations confirment que l'algorithme **PF** alloue approximativement le même nombre de sous-porteuses par utilisateur. Si on ne considère pas l'algorithme totalement inéquitable **MaxSumRate**, notre algorithme proposé présente le meilleur débit système. En plus de son équité proportionnelle, l'algorithme **WPF** offre un débit élevé proche de la borne supérieure surtout en basses puissances de transmission. Comparant au **PF** classique, le **WPF** offre un gain qui croît avec β. Pour β = 0.5, le gain varie de 4% a 24%. Pour β = 0.5, le gain varie de 7% a 29%.

- **Equité:** Pour évaluer l'équité des différents algorithmes, l'indice d'équité (FI) [13] est adopté:

$$FI = \left(\sum_{k=1}^{K} R_k\right)^2 / K \sum_{k=1}^{K} R_k^2 \qquad (5)$$

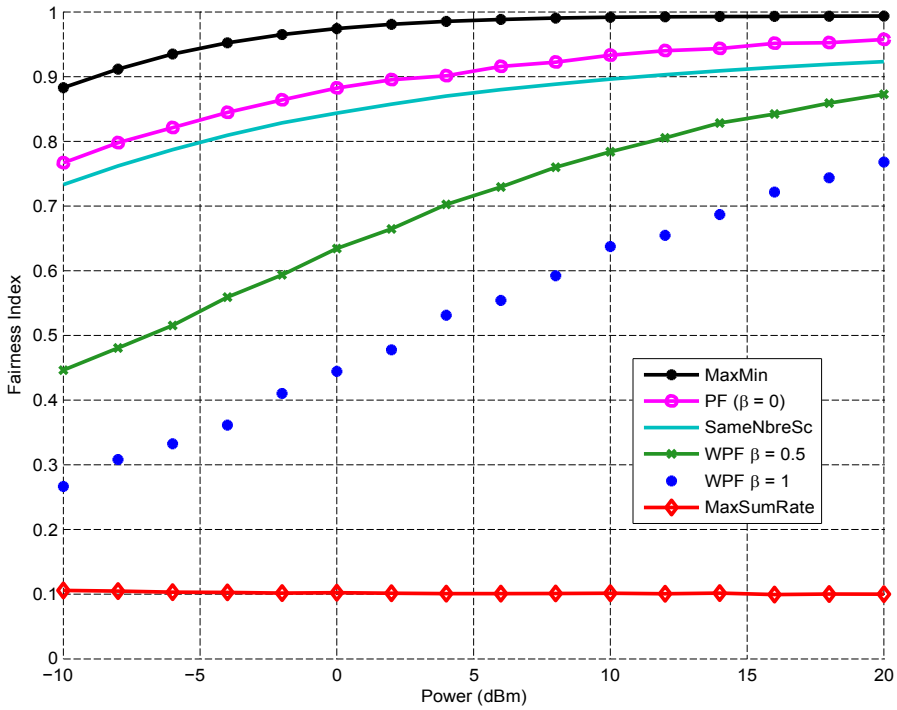

Figure 3: Indice d'équité

La figure 3 présente les indices d'équité des différents algorithmes étudiés. On peut remarquer que l'algorithme **MaxSumRate** est totalement inéquitable et que l'algorithme **MaxMin** présente la borne supérieure d'équité. Notre algorithme proposé atteint 87% d'équité pour $\beta = 0.5$ et 77% d'équité pour $\beta = 1$ pour les hautes valeurs de puissances. Comparant au **PF** classique, le **WPF** proposé perd de l'équité mais les résultats de simulation montrent que les utilisateurs en bordure perdent seulement 15% de leur débit tandis que ceux au centre arrivent à en gagner jusqu'à 45% du débit.

Selon la qualité de service souhaitée, l'algorithme **WPF** offre une flexibilité à travers le paramètre β. Pour une puissance $P = 21$ dBm et différentes valeurs de β, le tableau 1 présente les débits et les valeurs d'équité correspondantes. P est choisie égale à la puissance maximale de transmission d'un terminal mobile selon les caractéristiques d'un réseau cellulaire 4G [14].

Chapitre 4: Allocation de ressources dans un système multi-cellulaire

Dans ce chapitre, l'allocation de ressources est étudiée pour un système multi-cellulaire où l'ICI nuit aux performances du système. Les utilisateurs sont divisés en deux zones:

β	0.1	0.2	0.3	0.4	0.5
Débit (Kbits/s)	838.3	853.8	856.3	863	867.5
Indexe d'équité	0.94	0.93	0.91	0.89	0.87
β	0.6	0.7	0.8	0.9	1
Débit (Kbits/s)	869	877	876.5	886.2	890.8
Indexe d'équité	0.86	0.83	0.82	0.79	0.76

Table 1: Débits et Indices d'équité pour $\beta \in [0; 1]$

le centre et la bordure, comme c'est le cas dans certaines configurations de la norme LTE. Dans un premier lieu, l'algorithme WPF proposé dans le chapitre précédent est appliqué dans un système multi-cellulaire et comparé à l'algorithme de réutilisation de fréquence adopté en LTE. La comparaison est effectuée considérant une étude théorique et des simulations, et on considère le débit et l'équité. Dans un second lieu, la coopération entre les BSs est étudiée et un nouvel indicateur d'interférence est proposé (EII) pour chaque sous-porteuse par cellule afin d'indiquer le niveau d'interférence subie. L'allocation de sous-porteuse repose ainsi sur les valeurs de EII échangées dans le but de réduire l'interférence. Les résultats de simulations montrent qu'avec un coût de communication réduit, le EII peut améliorer les performances du systèmes.

L'algorithme WPF pour un modèle multi-cellulaire

Le facteur de réutilisation de fréquence (FFR) classique adopté en LTE [15][16] consiste à diviser équitablement les sous-porteuses en quatre ensembles F_1, F_2, F_3 et F_4. Le même ensemble F_1 est utilisé pour tous les centres des cellules alors qu'un $FFR = 3$ est utilisé en bordure avec le reste des ensembles (figure 4.1.a). On propose d'utiliser seulement deux ensembles de sous-porteuses F'_1 et F'_2 avec un nombre d'éléments $N_{F'_n} = \frac{N}{2}$ pour $n \in \{1, 2\}$. F'_1 est utilisé aux centres et F'_2 est utilisé en bordures (figure 4.1.b).

Dans chaque zone des cellules, l'allocation des sous-porteuses est établie selon l'algorithme WPF proposé dans le chapitre précédent avec un poids par utilisateur k et par cellule c exprimé tel que:

$$w_{k,c} = \log_2\left(1 + \frac{P_k}{L_{k,c} S_{k,c} (N_{sc} + I_0)}\right) \quad (6)$$

Les mêmes notations que les chapitre précédents sont utilisées en ajoutant l'indice c pour la cellule. I_0 est l'interférence moyenne par utilisateur par sous-porteuse qui peut être exprimée tel que:

$$I_0 = \frac{N_{interf} \; P \; K_b}{L_{interf} \; N_b} \quad (7)$$

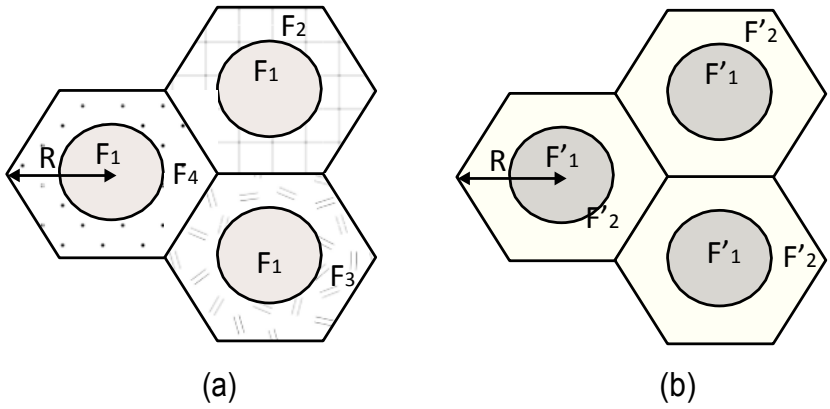

Figure 4: FFR dans LTE - FFR proposé

avec

- N_{interf}: Le nombre d'interféreurs. Dans notre système, 7 cellules sont considérées, le nombre d'interféreurs est donc considéré à 6.
- K_b: Le nombre d'utilisateurs en bordure de cellule $K_b \simeq \frac{K}{2}$.
- N_b: Le nombre de sous-porteuses en bordure de cellule $N_b = \frac{N}{2}$.
- P: La puissance de transmission par utilisateur. $\frac{P\ K_b}{N_b}$ est donc la puissance moyenne par sous-porteuse.
- L_{interf} l'atténuation correspondant au pire des interféreur situé à une distance $d_I = R$.

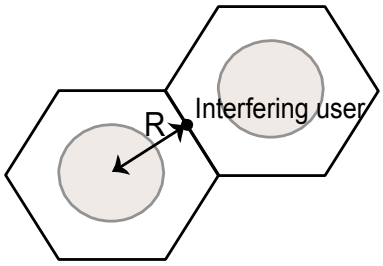

Figure 5: La position de l'utilisateur interféreur pris en compte

Résultats de simulation

Pour les simulations, 7 cellules hexagonales avec un rayon de 1 km sont considérées. Chaque cellule contient 20 utilisateurs uniformément distribués et 72 sous-porteuses. Chaque cellule comporte deux zones: le centre de cellule avec les utilisateurs à une distance $d < \frac{R}{\sqrt{2}}$ et la bordure de cellule avec le reste des utilisateurs. Les paramètres

d'atténuations sont les mêmes adoptés dans le chapitre précédent. Pour l'algorithme WPF, on considère 100 TTIs, 500 simulations et différentes valeurs de β. Les résultats de simulations sont étudiées en termes de débit et d'équité pour comparer le modèle proposé au FFR classique de 3.

- **Débit** Selon la figure 6, on peut remarquer que le modèle FFR3 est une fonction

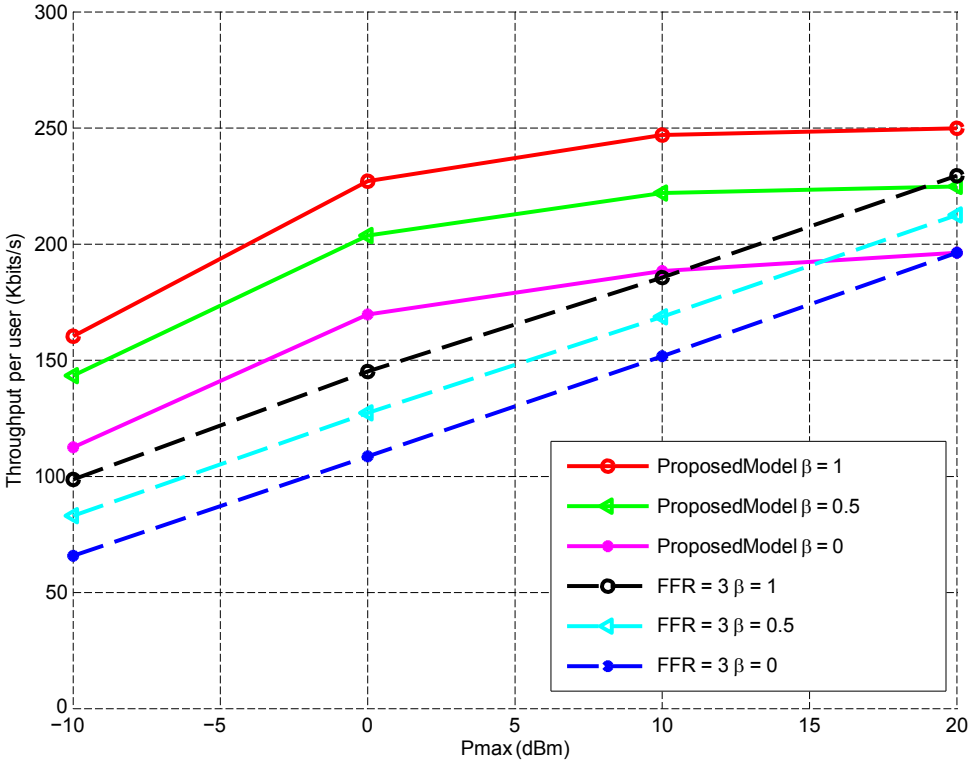

Figure 6: Débit du système

croissante de la puissance non affectée par l'ICI mais offre un débit inférieur à celui offert par le modèle proposé notamment pour les faibles puissances. Malgré l'ICI subie par notre modèle proposé, le débit du système reste inférieur ou égal au débit avec FFR3. La priorité entre les utilisateurs traduite par les différents poids permet un gain de 8% a 45% pour β = 1, de 5% à 41% pour β = 0.5 et atteint 38% pour β = 0 à faibles puissances.

- **Equité:** Pour évaluer l'équité, l'indice d'équité présenté dans l'equation 5 est adopté. Le tableau 4.1 compare les indices d'équité pour les deux modèles étudiés. On peut remarquer que le modèle proposé présente une diminution de valeur

d'équité mais que cette diminution reste légère.

$P_{max} = -10dBm$			
	$\beta = 0$	$\beta = 0.5$	$\beta = 1$
FFR = 3	0.57	0.42	0.31
ProposedModel	0.5	0.37	0.28
$P_{max} = 20dBm$			
	$\beta = 0$	$\beta = 0.5$	$\beta = 1$
FFR = 3	0.75	0.72	0.61
ProposedModel	0.7	0.59	0.5

Table 2: Indices d'équité en fonction des puissances de transmission

L'indicateur d'interférence amélioré EII

Dans cette partie chapitre 4, la coopération des BS est étudiées pour reduire l'ICI. Contrairement aux méthodes avec le FFR, toute la bande est utilisée dans toutes les cellules ce qui offre une meilleure diversité fréquentielle, par contre, la communication des BSs peut engendrer un coût élevé si la quantité de données échangée est grande.

Modèle du système

On conserve le même modèle du système multi-cellulaire avec 7 cellules et la moitié des utilisateurs dans chaque zone (centre ou bordure). Pour l'allocation de ressources, la moitié de la bande F_1 est utilisée aux centres et F_2 en bordures. L'allocation des sous-porteuses est effectuée selon l'algorithme PF. Pour l'allocation en bordure de cellules, les BSs échangent des valeurs de EII qui indiquent le niveau d'interférence pour chaque sous-porteuse dans le but d'éviter d'allouer les mêmes sous-porteuses dans des cellules voisines. Le EII est inspiré de l'indicateur d'interférence HII proposé par LTE [2] mais avec des valeurs entières afin de mieux évaluer les valeurs d'interférences.

Dans le modèle que nous proposons, la bordure de cellule est divisée en différents secteurs et une valeur EII est attribuée par sous-porteuse par cellule en fonction du secteur dans lequel la sous-porteuse est allouée. Comme nous nous intéressons au sens montant, l'interférence dépend de la distance entre l'utilisateur interféreur dans la cellule voisine et la BS de la cellule à étudier. Pour ce, afin de calculer les valeurs de EII, une analyse des dépendences entre les cellule est effectuée.

Comme exemple, la figure 7 présente les dépendances de la cellule centrale c1. Les utilisateurs en bordure de cette cellule seront fortement interférés s'ils gagnent les sous-porteuses déjà allouées dans les secteurs colorés en rouge (val_1). Ceci est dû à la faible

distance entre ces secteurs et la BS de la cellule centrale. Avec une valeur élevée val_1, les utilisateurs de la cellule centrale seront désavantagés pour gagner les sous-porteuses correspondantes. En effet, la meilleure allocation pour la cellule centrale est d'allouer les sous-porteuses déjà allouées dans les secteurs avec la plus faible valeur de EII val_4 (secteur 2 de la cellule 7 et secteur 3 de la cellule 2 par exemple). Pour compléter le même exemple, la figure 8 décrit l'allocation de la sous-porteuse **j** quand la cellule centrale est la dernière cellule à effectuer son allocation. Comme le montre la figure 8, **j** est déjà allouée dans les secteurs colorés. Pour les utilisateurs de la cellule centrale, la valeur de EII pour **j** est $EII_{j,1} = 2val_1 + 3val_2 + val_3$.

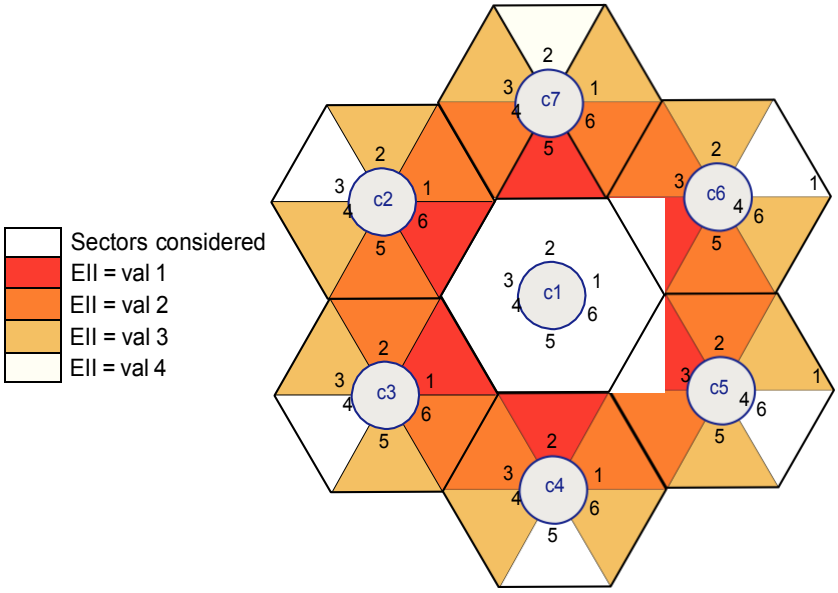

Figure 7: Exemple 1: Dépendances de la cellule centrale

La valeur de EII pour la sous-porteuse **j** dans la cellule c est exprimée de la façon suivante:

$$EII_{j,c} = \sum_{c'/=c} \sum_{s=1}^{S} b_{s,j,c'} \cdot eii_{s,c',c} \quad (8)$$

avec S = 6 le nombre de secteurs, $b_{s,j,c'}$ est une variable booléenne qui indique si **j** est allouée dans le secteur s de la cell c'. $eii_{s,c',c}$ est la valeur de EII du secteur s dans c' si c est la cellule étudiée. Les valeurs de EII sont calculées tel que $val_i = \frac{d}{d_1}^{-\alpha}$ (voir figure 9), $i \in [1..4]$ avec $\alpha = 3.76$ le coefficient de pathloss suivant le modèle LTE.

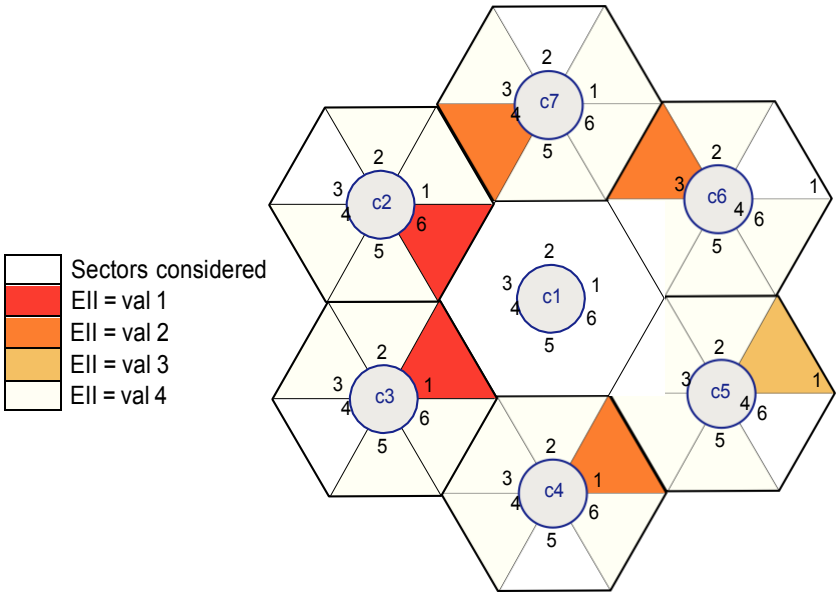

Figure 8: Exemple 2: La sous-porteuse **j** est déjà alouée dans les secteurs colorés

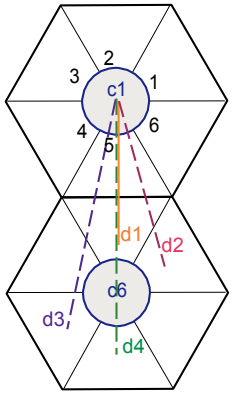

Figure 9: Distances: $d_1 = 1.3 \cdot R$; $d_2 = 1.56 \cdot R$; $d_3 = 1.98 \cdot R$; $d_4 = 2.16 \cdot R$

Les valeurs de EII sont utilisées dans l'estimation de l'interférence de la sous-porteuse **j** de la cell c tel que:

$$I_{j,c} = \frac{EII_{j,c}}{L_{interf}} \cdot \frac{P \cdot K_b}{N_b} \tag{9}$$

Les mêmes notations que dans l'équation (7) sont utilisées.

Résultats de simulation

Le modèle du système de la figure 7 est considéré avec 40 utilisateurs par cellule. Le reste des hypothèses du cas WPF en système multi-cellulaires sont maintenues. L'algorithme proposé avec EII est comparé à l'algorithme coopératif avec HII et au système non-coopératif.

- **Débit**

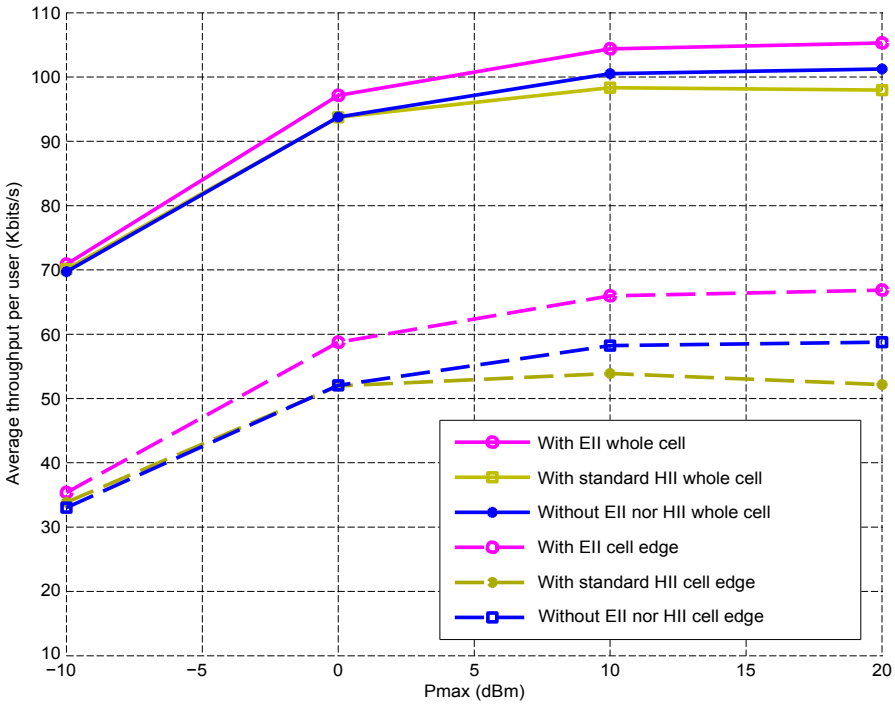

Figure 10: Débit du système

La figure 4.12 présente le débit moyen par utilisateur en fonction de la puissance de transmission pour 100 TTIs. On différencie les résultats en bordure de cellule où les indicateurs d'interférence sont utilisés de la moyenne de toute la cellule. Les simulations montrent que le HII ne présente pas toujours un gain en comparant avec le système sans coopération contrairement au EII proposé qui offre un gain jusqu'à 13% pour les forts SNR (figure 11).

- **Equité:** Le tableau 4.2 montre que l'indicateur EII proposé n'affecte que très légèrement les valeurs d'équité en le comparant au modèle sans coopération. Le EII améliore donc les performances du système sans pour autant affecter l'équité entre les utilisateurs.

Chapitre 5: Allocation de ressources dans un système OFDMA coopératif avec des relais mobiles

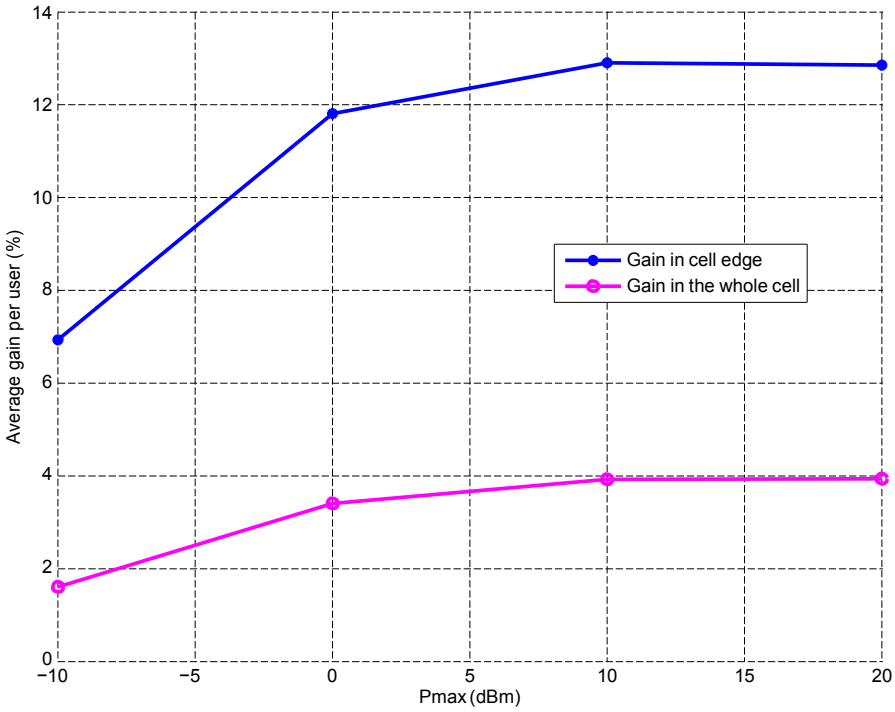

Figure 11: Gain moyen de l'algorithme proposé avec EII

	$P_{max} = -10$ dBm	$P_{max} = 20$ dBm
Sans EII	0.34	0.41
Avec EII	0.33	0.39

Table 3: Indices d'équité

Dans ce chapitre, le sens montant des utilisateurs vers la BS est étudié pour un système coopératif OFDMA avec des relais mobiles ayant leurs propres données à transmettre. En effet, on considère que de simples utilisateurs ayant des bonnes conditions de canal peuvent relayer d'autres utilisateurs en bordure de cellule, en plus de leurs propores données à transmettre. Les relais multiplexent alors leurs propres données aux données à relayer avant la transmission vers la BS. Le système étudié a comme objectif de minimiser la puissance totale de transmission afin de limiter les effets environmentaux. On considère également un débit minimal par utilisateur. L'allocation de ressources est formulée en tant qu'un problème d'optimisation visant à approcher la solution optimale. Les aspects à optimiser sont la sélection des relais, l'allocation des sous-porteuses et l'allocation des puissances.

Optimisation de l'allocation de sous-porteuse et des puissances

Dans cette partie, la sélection des relais est considérée comme une étape d'initialisation au problème d'optimisation. Chaque utilisateur peut ainsi transmettre en mode non-coopératif directement à la BS (figure 12a) ou en mode coopératif via un relai (figure 12b).

Les mêmes hypothèses pour un système mono-cellulaire avec K utilisateurs et N blocks

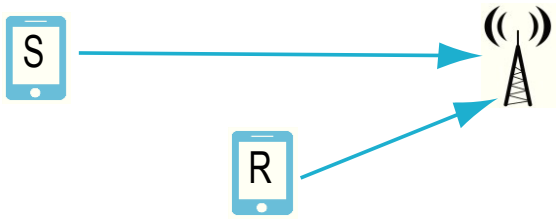

(a) Cas 1: Modèle non-cooperatif

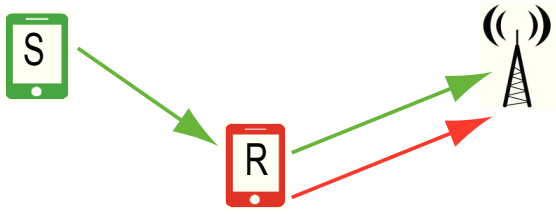

(b) Cas 2: Modèle cooperatif

Figure 12: Exemple 1: Schemas de transmission

de ressources (RB) sont maintenues. Les utilisateurs peuvent donc être des sources non relayées (NRS), des relais (R) ou des sources relayées (RS). Soit R le rayon de la cellule et $d_{k,k}$ la distance entre l'utilisateur user k et la BS. Afin de simplifier la sélection des relais, on pose:

- Les utilisateurs avec une distance $d_{k,k} < \frac{R}{3}$ sont proches de la BS et n'ont pas besoin d'être relayés. De plus, ils sont loin de la bordure et ne sont donc pas considérés en tant que relais. Ces utilisateurs sont considérés comme des sources non relayées et ne peuvent pas être relais.
- Les utilisateurs avec une distance $d_{k,k} > \frac{2R}{3}$ sont dans la bordure de la cellule et dont les performances peuvent être améliorées s'ils sont relayés par un utilisateurs à mi-chemin avec la BS. Ces utilisateurs sont considérés comme des sources relayées potentielles.

- Les utilisateurs avec une distance $\frac{R}{3} < d_{k,k} < \frac{2R}{3}$ peuvent relayer les utilisateurs avec $d_{k,k} > \frac{2R}{3}$. Comme leur distance vers la BS est relativement faible, ces utilisateurs ne seront pas relayés.
- Un utilisateur avec une distance $d_{k,k} > \frac{2R}{3}$ ne peut avoir qu'un seul relai afin de réduire le coût de signalisation.

D'abord, chaque utilisateur en bordure de cellule estime son meilleur relai et compare le débit qu'il peut atteindre avec son lien direct à la BS et son lien indirect via son relai. Il décide ainsi entre la transmission directe ou indirecte. Si l'utilisateur choisit de ne pas coopérer, il devient une NRS même s'il se situe en bordure de cellule. Un utilisateur se situant dans la zone des relais et qui n'est choisi par aucune RS devient également une NRS. A la fin de cette étape d'initialisation, résultent des ensembles initialisés de NRS, R et RS comme l'indique la figure 13. Les utilisateurs sont supposés half-duplex et les relais utilisent le protocole DF. La transmission est effectuée sur deux temps: Dans un premier temps, les NRS transmettent à la BS et les RS transmettent à leurs relais correspondants, les relais écoutent. Dans un second temp, les RS sont silencieuses, les NRS et les R transmettent à la BS. Les R multiplexent leurs propres données aux données à relayer avant la transmission à la BS.

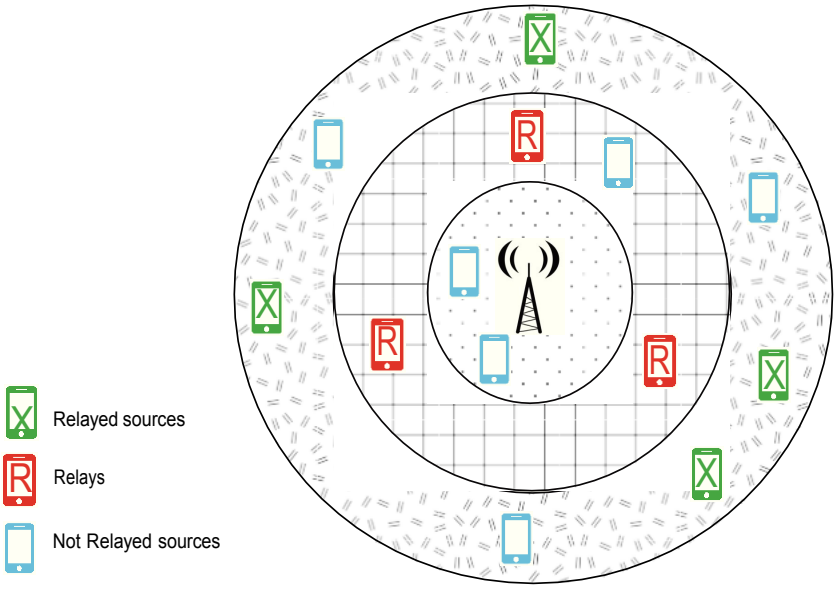

Figure 13: Exemple 2 : Modèle du système initialisé

La formulation du problème d'optimisation

Si on considère une NRS, une RS et un R ayant respectivement les RB j, j' et j''. le tableau 4 détaille la puissance de transmission consommée par utilisateur par TTI: Le problème d'optimisation global pour un système avec K utilisateurs et N RBs est

	NRS	RS	R
TTI 1	P_{NRS}^{j}	P_{RS}^{j}	0
TTI 2	P_{NRS}^{j}	0	$P_{R}^{j} + P_{R}^{j}$
Average Power per TTI	P_{NRS}^{j}	$\frac{1}{2}P_{RS}^{j}$	$\frac{1}{2}(P_{R}^{j'} + P_{R}^{j''})$

Table 4: La puissance de transmission consommée par utilisateur par TTI

exprimé tel que:

$$\underset{\mathbf{a},\mathbf{b},\mathbf{P}}{\text{minimiser}} \quad \sum_{k=1}^{K}\sum_{j=1}^{N}\left(1-\frac{b_k}{2}\right)a_{k,k}^{j}P_{k}^{j} + \frac{1}{2}\sum_{k=1}^{K}\sum_{r=1,r\neq k}^{N} b_k a_{k,r}^{j}\left(P_{k}^{j}+P_{r}^{j}\right) \tag{10a}$$

sous les contraintes

$$\sum_{k=1}^{K}\sum_{r=1}^{K} a_{k,r}^{j} \leq 1 \;\forall j, j = 1,..N \tag{10b}$$

$$\sum_{r=1}^{K}\sum_{j=1}^{N} a_{k,r}^{j}R_{k}^{j} \geq R_t \;\forall k, k = 1,..K \tag{10c}$$

$$a_{k,r}^{j} \in \{0,1\} \;\forall k, r, j \tag{10d}$$

$$b_k \in \{0,1\} \;\forall k \tag{10e}$$

$$P_{k}^{j} \geq 0 \;\forall k, j \tag{10f}$$

avec

- $\mathbf{b} = [b_1, b_2, ..., b_K]^T$ le vecteur des décisions de coopérations des utilisateurs
- $\mathbf{P}$ la matrices de puissances par utilisateur pour chaque RB
- $\mathbf{a}$ la matrice d'allocation du RB j par couple de (source, relai)
- La contrainte (10d) représente la décision de coopération pour l'utilisateur k. Si $b_k = 1$, k participe à une transmission coopérative (k est une RS ou un relai), sinon $b_k = 0$.

- Les contraintes (10b) et (10d) traduisent la contrainte d'allocation de RB. $a^j_{k,k} = 1$ veut dire que k transmet directement à la BS. $a^j_{k,r} = 1$ avec k /= r signifie que **j** est allouée à la transmission de l'utilisateur k vers le relai r au premier TTI et à la transmission des données relayées de r vers la BS au second TTI. Si $a^j_{k,r} = 1$, alors $b_k = 1$ et $b_r = 1$.
- La contrainte (10c) indique le débit cible par utilisateur R_t.
- La contrainte (10f) vérifie que toutes les puissances sont positives.
- Le premier terme du problème (10) représente la puissance de transmission pour une NRS pour les deux TTIs et la puissance de transmission nécessaire pour un relai pour transmettre ses propres données pour uniquement un seul TTI (d'où le facteur $\frac{1}{2}$). Le second terme du problème représente la puissance de transmission consommées pour les données relayées.

Résolution du problème

Considérant la sélection des relais comme une phase d'initialisation au problème d'optimisation, la résolution du problème consiste à résoudre itérativement les deux sous-problèmes:

1. Le problème sous-optimal d'allocation de puissances
2. Le problème sous-optimal d'allocation de RBs

La résolution est effectuée suivant la méthode duale et la décompsition de Lagrange afin d'approcher la solution optimale (figure 14).

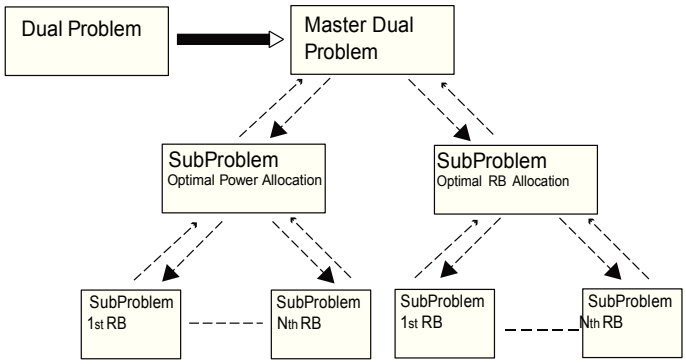

Figure 14: Hierarchie du problème duale décomposé

- **Allocation de puissances sous-optimale pour une allocation de RB donnée**

  Selon la nature des utilisateurs, les valeurs de puissances sont calculées tels que:

– k est une NRS ou un relai transmettant ses propres données dans le RB j:

$$P_k^j = \left[\frac{\lambda_k}{\ln(2)} - \frac{1}{\gamma_{k,k}^j}\right]^+ \tag{11}$$

avec $[x]^+ = \max\{0, x\}$.

– k est une source relayée par r

Dans une transmission coopérative, la puissance est minimisée quand la source et le relai envoient la même quantité de données. Par conséquent, le débit est le débit minimal des deux liens. Pour ce, on suppose que $P_k^j \gamma_{k,r}^j = P_r^j \gamma_{r,r}^j$ et on trouve:

$$P_k^j = \left[\frac{\lambda_k \gamma_{r,r}^j}{\ln(2)(\gamma_{k,r}^j + \gamma_{r,r}^j)} - \frac{1}{\gamma_{k,r}^j}\right]^+ \tag{12}$$

$$P_r^j = \left[\frac{\lambda_k \gamma_{k,r}^j}{\ln(2)(\gamma_{k,r}^j + \gamma_{r,r}^j)} - \frac{1}{\gamma_{r,r}^j}\right]^+ \tag{13}$$

- **Allocation sous optimale de RBs**

Utilisant les valeurs de puissances de l'étape précédente, seule la variable $a_{k,r}^j \; \forall \, k, r, j$ est à optimiser. En calculant le Lagrangian correspondant, la fonction duale g(λ) peut être exprimée tel que:

$$g(\boldsymbol{\lambda}) = \underset{\mathbf{a}}{\text{maximize}} \sum_{k=1}^{K} \sum_{r=1}^{K} a_{k,r}^j \, G_{k,r}^j - \sum_{k=1}^{K} \lambda_k \, R_t \tag{14}$$

avec $G = [G_{k,r}^j]$ est une matrice $K \times K \times N$ qui représente le gain éventuel du couple (k, r) s'il gagne le RB j.

– si k = r et k est une source non relayée:

$$G_{k,r}^j = \lambda_k \, \log_2 \left(1 + P_k^j \gamma_{k,k}^j\right) - P_k^j \tag{15}$$

– si k = r et k est un relai transmettant ses propres données via le RB j:

$$G_{k,r}^j = \frac{\lambda_k}{2} \log_2 \left(1 + P_k^j \gamma_{k,k}^j\right) - \frac{1}{2} P_k^j \tag{16}$$

– si k est une source relayée et k /= r:

$$G_{k,r}^j = \frac{\lambda_k}{2} \log_2 \left(1 + P_k^j \gamma_{k,r}^j - \frac{1}{2}(P_{k,r}^j + P_{r,r}^j)\right) \tag{17}$$

Les gains sont calculés pour chaque RB j, **j** est ensuite allouée au couple (k,r) maximisant le gain en j: $a^{j}_{k,r} = 1$ for $(k,r)^* = \arg\max_{(k,r)} G^{j}_{k,r}$

- **Mise à jour des variables de Lagrange**
  La dernière étape pour chaque itération de l'algorithme est la mise à jour des variables de Lagrange et le test de convergence de l'algorithme. Utilisant les résultats de l'itération t, λ de l'itération t + 1 est calculé tel que:

$$\lambda_k(t+1) = \left[\lambda_k(t) + \eta_k(t)\left[R_t - \sum_{r=1}^{K}\sum_{j=1}^{N} a^{j}_{k,r}(t) R^{j}(t)\right]\right]^{+} \quad (18)$$

avec η le pas adopté [17]. L'algorithme est considéré comme convergent si tous les utilisateurs atteignent le débit minimal exigé et si la variation de λ_k est négligeable pour tous les utilisateurs:

$$\frac{\lambda_k(t+1) - \lambda_k(t)}{\lambda_k(t+1)} < \varrho \ \forall k \quad (19)$$

avec ϱ proche de zero.

Résultats de simulations

Les paramètres de simulations utilisés dans les paragraphes précédents sont maintenus. Le pas pour la variable de Lagrange λ_k est fixé à $\eta_k = \frac{\lambda_k}{\sqrt{t}}$ pour $t < 2000$ avec t l'indice de l'itération. Quand t dépasse 2000, η_k devient invariant. ϱ est fixée à 0.001. R_t est varié lors des simulations dans l'intervalle [0.5..1.5] bits/s/Hz. Les simulations sont moyennées sur 1000 tirages afin d'avoir des résultats réalistes. Les figures 15 et 16 présentent les puissances de transmission du systèmes pour respectivement 18 et 30 utilisateurs avec différents nombre de RBs et différentes valeurs de R_t. Les cas avec relayage sont différenciés pour mieux montrer le gain effectif que propose notre algorithme. Pour 18 utilisateurs, 192 RBs et R_t = 1.5 bits/s/Hz, le gain offert par notre méthode proposée atteint 21% pour toutes les simulations confondues. Si on considère uniquement les cas avec relayage, le gain arrive à 51% pour les mêmes conditions. Les valeurs de gains sont présentée dans la figure 17.

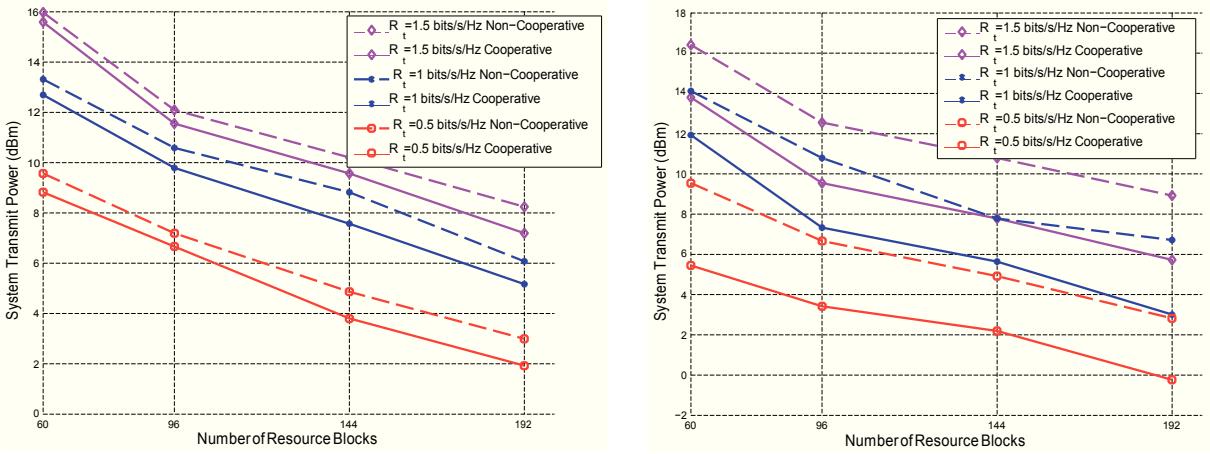

(a) All cases (b) Relaying cases only

Figure 15: Puissance de transmission pour 18 utilisateurs

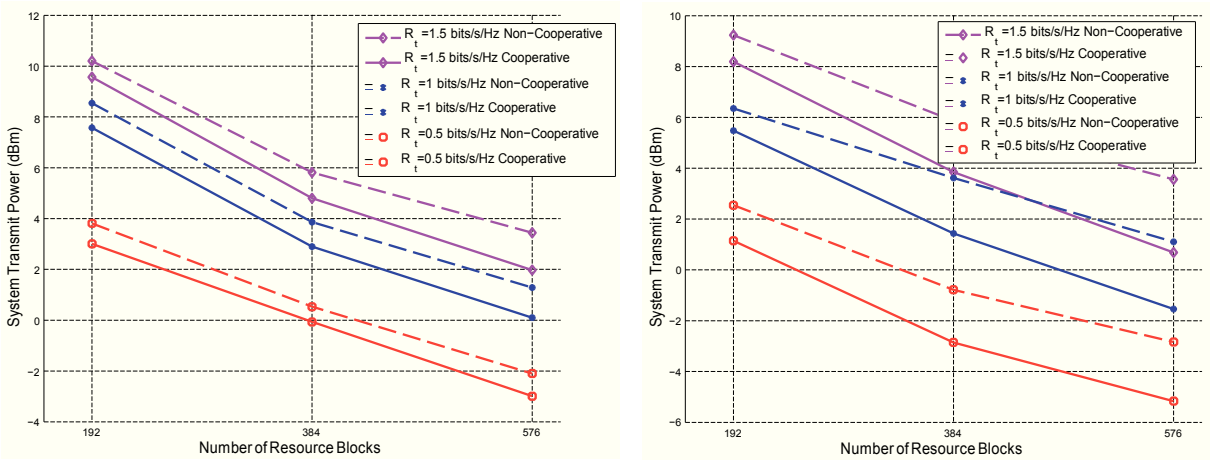

(a) All cases (b) Relaying cases only

Figure 16: Puissance de transmission pour 30 utilisateurs

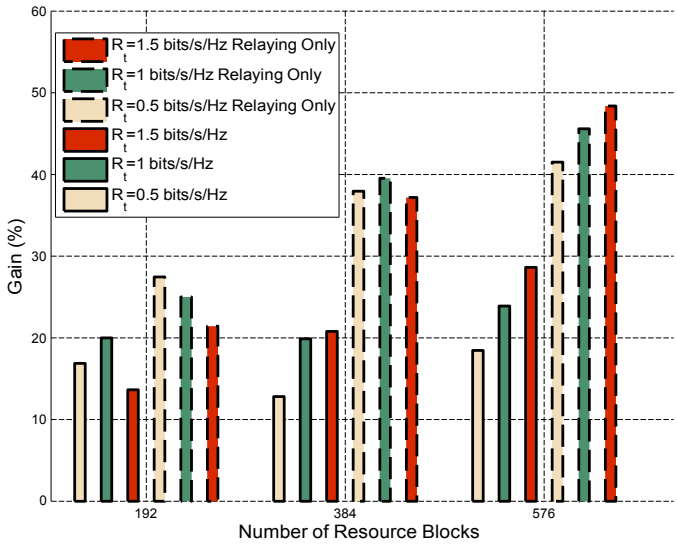

Figure 17: Gain pour 30 utilisateurs

Optimisation de sélection des relais, de l'allocation de sous-porteuse et des puissances

Modèle du système

Dans cette deuxième partie du chapitre, le but du problème d'optimisation d'allocation de ressources est d'optimiser la sélection des relais en plus des allocations des RBs et des puissances. Danc ce cas, un relai peut relayer une ou plusieurs sources relayées, une source relayée peut être relayée par un ou plusieurs relais mais dans des RBs différents. La transmission est étudiée pour deux cas: half-duplex et full-duplex (présentés par la figure 18). Le cas full-duplex est étudié pour avoir une borne supérieure du gain qu'on peut atteindre. On introduit la variable HF dans les équations pour différencier les deux cas (HF= 1 pour full-duplex et HF= $\frac{1}{2}$ pour half-duplex).

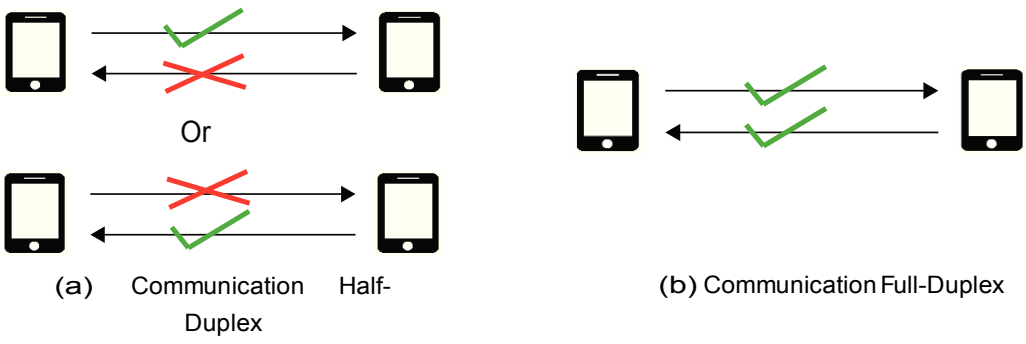

Figure 18: Communication Duplex

Comme exemple, le tableau 5 détaille la puissance consommée par utilisateur si on considère une NRS, une RS et un R ayant chacun un RB, respectivement j, j' et j''.

La formulation du problème d'optimisation

	Half-duplex			Full-duplex		
	NRS	RS	R	NRS	RS	R
TTI1	P_{NRS}^{j}	$P_{RS}^{j'}$	0	P_{NRS}^{j}	$P_{RS}^{j'}$	$P_{R}^{j''}$
TTI2	P_{NRS}^{j}	0	$P_{R}^{j} + P_{R}^{j}$	P_{NRS}^{j}	0	$P_{R}^{j} + P_{R}^{j}$

Table 5: Puissance consommée par utilisateur par TTI

Visant à minimiser la puissance totale du système en assurant un débit minimal par utilisateur, le problème global d'optimisation pour k utilisateurs et N RBs peut être exprimé tel que (on conserve les notations utilisées précédemment):

$$\underset{\mathbf{a,\ b,\ P}}{\text{minimier}} \sum_{k=1}^{K}\sum_{j=1}^{N}\left(1 - b_k(1 - HF)\right)a^{j}_{k,k}P^{j}_{k} + \frac{1}{2}\sum_{k=1}^{K}\sum_{r=1,r\neq k}^{K}\sum_{j=1}^{N} b_k a^{j}_{k,r}\left(P^{j}_{k} + P^{j}_{r}\right) \tag{20a}$$

sous les contraintes

$$\sum_{k=1}^{K}\sum_{r=1}^{K} i_{k,r} = 1 \ \forall j, j = 1,..N \tag{20b}$$

$$\sum_{r=1}^{K}\sum_{j=1}^{N} a^{j}_{k,r}R^{j}_{k} \geq R_t \ \forall k, k = 1,..K \tag{20c}$$

$$a^{j}_{k,r} \in \{0,1\} \ \forall k, r, j \tag{20d}$$

$$b_k \in \{0,1\} \ \forall k \tag{20e}$$

$$P^{j}_{k} \geq 0 \ \forall k, j \tag{20f}$$

La résolution de problème est basée sur la décomposition de Lagrange pour résoudre itérativement les deux sous problèmes suivants:

1. Le problème sous-optimal d'allocation de puissances
2. Le problème sous-optimal conjoint de sélection de relais et d'allocation de RBs

Résolution du problème

Pour résoudre le problème d'optimisation, les étapes Allocation de puissances sous-optimale et Mise à jour des variables de Lagrange sont équivalentes au paragraphe précédent. Par contre, l'allocation de RB sous-optimale est différente et est traitée conjointement avec la sélection des relais.

Solution sous optimale conjointe pour la sélection des relais et l'allocation de RBs

Utilisant les résultats de puissances sous optimales et en calculant la fonction duale correspondante g(λ), on peut ecrire:

$$g(\boldsymbol{\lambda}) = \underset{\mathbf{a}}{\text{maximize}} \sum_{k=1}^{\bar{K}} \sum_{r=1}^{\bar{K}} a^{j}_{k,r} G^{\mathbf{j}}_{k,r} - \sum_{k=1}^{\bar{K}} \lambda_k R_t \tag{21}$$

avec $G = [G^{j}_{k,r}]$ une matrice $K \times K \times N$ de gain eventuel si le couple (k, r)gagne le RB **j** . Les expressions de gain pour un RB **j** sont detaillées tel que:

- k est une source non relayée:

$$G^{j}_{k,k} = \lambda_k \log_2 \left(1 + P^{\mathbf{j}}_k \gamma^{\mathbf{j}}_{k,k}\right) - P^{\mathbf{j}}_k \tag{22}$$

- k un relai qui transmet ses propres données

$$G^{j}_{k,k} = HF\ \lambda_k \log_2 \left(1 + P^{\mathbf{j}}_k \gamma^{\mathbf{j}}_{k,k}\right) - HF\ P^{\mathbf{j}}_k \tag{23}$$

- k est une source relayée par r

$$G^{j}_{k,r} = \frac{\lambda_k}{2} \log_2 \left(1 + P^{\mathbf{j}}_{k,r} \gamma^{j}_{k,r}\right) - \frac{1}{2}\left(P^{\mathbf{j}}_{k,r} + P^{\mathbf{j}}_{r,r}\right) \tag{24}$$

Au début de l'algorithme, tous les utilisateurs sont considérés des NRS. Pour chaque RB j, les gains sont calculés pour toutes les combinaisons de couples source-relai possibles (s, r) et **j** est assignée au couple $(k, r)^*$ maximisant le gain: $a^{j}_{k,r} = 1$ pour $(k, r)^* = \arg\max_{(k,r)} G^{\mathbf{j}}_{k,r}$, sinon 0. Si k = r, la transmission est dite directe et $b_k = 0$. Sinon si k /= r, une coopération est utilisée, on a alors $b_k = 1$ et $b_r = 1$. Les natures des utilisateurs sont mises à jour à chaque allocation.

Résultats de simulation

Nous considérons les mêmes hypothèses de simulations que la première partie de ce

chapitre. La figure 19 présente la puissance de transmission consommée pour un système de 18 utilisateurs pour des valeurs différentes de débit cible. Les deux cas half et full-duplex sont étudiés. En comparant au système sans coopération, la solution proposée offre un gain considérable. Pour le cas half-duplex, l'algorithme proposé offre un gain de 36% pour R_t = 1.5 bits/s/Hz jusqu'à 49% pour R_t = 1 bits/s/Hz. Pour le cas full-duplex, l'algorithme proposé offre vers les 62% de gain pour R_t = 1.5 bits/s/Hz vers les 70% de gain pour R_t = 1 bits/s/Hz

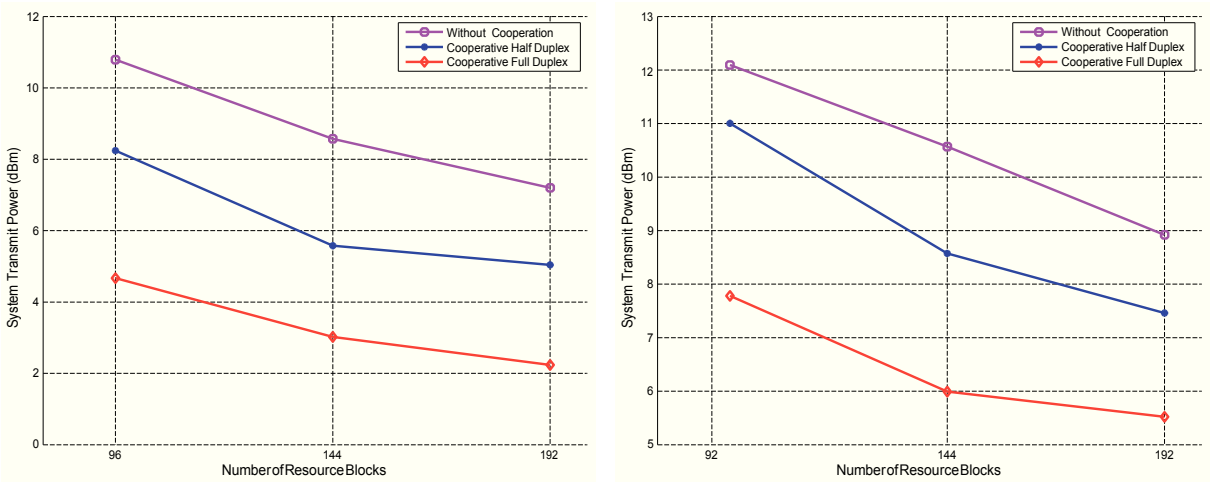

(a) R_t = 1 bis/s/Hz (b) R_t = 1.5 bis/s/Hz

Figure 19: Puissance de transmission du système avec 18 utilisateurs

Comparaison des méthodes d'optimisation proposées

Les deux méthodes d'optimisation proposées sont comparées:

1. méthode 1: Solution sous-optimale pour optimiser l'allocation des puissances et des RBs. On rappelle que pour cette méthode, la sélection des relais est effectuée comme une phase d'initialisation au problème d'optimisation.

2. méthode 2: Solution sous-optimale pour optimiser la sélection des relais, l'allocation des puissances et des RBs.

La comparaison est effectuée pour le cas des utilisateurs half-duplex pour un nombre variable de RBs pour comparer les deux méthodes proposées au système non-coopératif. Les résultats de simulations montrent que la méthode 2 offre des meilleures résultats que la méthode 1. Ceci peut être justifié par le fait qu'optimiser la sélection des relais peut réduire davantage la puissance du système que si on le fait avant l'optimsation.

L'optimisation de toutes les variables offre ainsi jusqu'à 40% de gain en comparant au modèle non comparatif. On note bien que la méthode 1 offre un gain significatif comparant au modèle non coopératif qui arrive jusqu'à 29%. Optimiser la sélection des relais offre un meilleur gain mais augmente de façon considérable la complexité du problème d'optimisation.

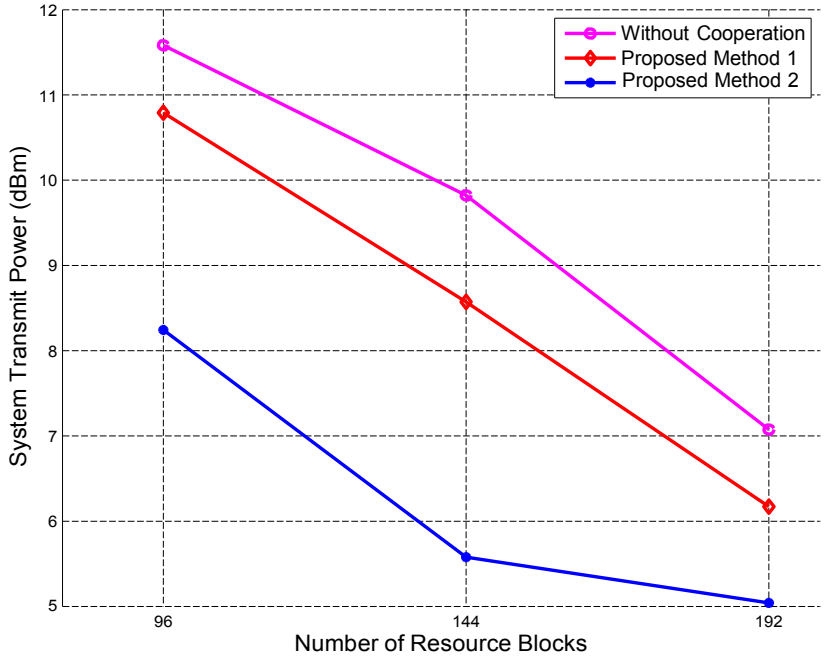

Figure 20: Puissance de transmission du système pour 18 utilisateurs, R_t = 1 bit-s/s/Hz

Chapitre 6: Allocation de ressources dans un système MIMO OFDMA coopératif avec des relais mobiles

Dans ce chapitre, l'optimisation de l'allocation des ressources avec des relais mobiles ayant leurs propres données à transmettre traité dans le chapitre précédent est étendue pour un système MIMO (Multiple Input Multiple Output). Le but est d'étudier l'influence des antennes multiples sur la puissance de transmission du système. Visant à minimiser la puissance consommée en garantissant un débit cible par utilisateur, le problème d'optimisation détermine la sélection des relais, l'allocation des puissances et des RBs. De plus, au niveau de chaque utilisateur, différentes stratégies d'allocation de puissance sont étudiées: la répartition égale de puissance sur les différentes antennes et le beamforming.

Formalisation du problème d'optimisation

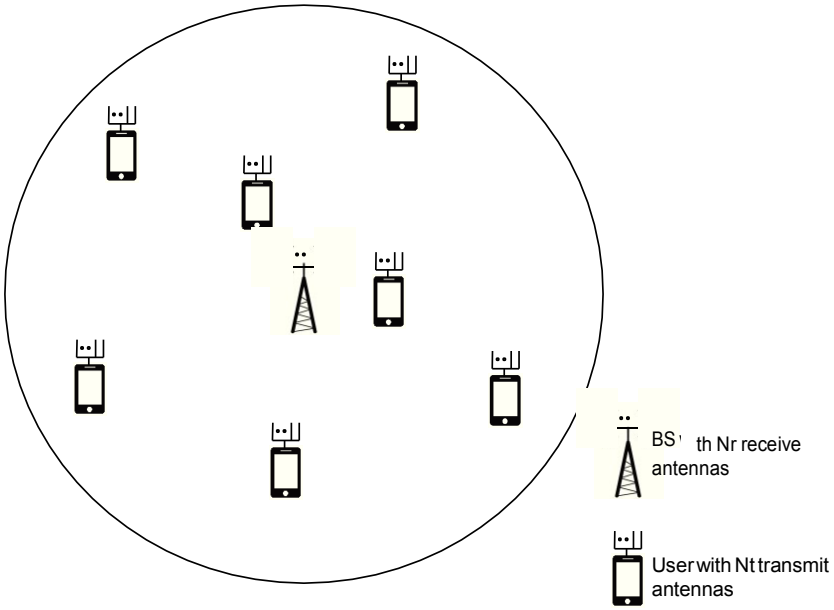

Figure 21: modèle du système MIMO

On traite le sens montant des utilisateurs avec L_t antennes de transmission vers la BS avec L_r antennes de réception et on suppose que $L_t = L_r = L$. Les utilisateurs sont supposés des utilisateurs half-duplex, ils ne peuvent donc pas écouter et transmettre en même temps. Pour le problème d'optimisation, la puissance par TTI est considérée en moyennant sur les deux TTIs. Pour K utilisateurs et N RBs, le problème d'optimisation peut être exprimé de la façon suivante:

$$\underset{\mathbf{a,\ b,\ P}}{\text{minimiser}} \quad \sum_{k=1}^{K}\sum_{j=1}^{N}\left(1-\frac{b_k}{2}\right)a^j_{k,k}P^j_k+\frac{1}{2}\sum_{k=1}^{K}\sum_{r\neq k=1}^{K}\sum_{j=1}^{N}b_k a^j_{k,r}\left(P^j_k+P^j_r\right) \quad (25a)$$

sous les contraintes

$$\sum_{k=1}^{K}\sum_{r=1}^{K} i_{k,r}=1 \ \forall j, \mathbf{j}=1,..N \quad (25b)$$

$$\sum_{r=1}^{K}\sum_{j=1}^{N}\sum_{l=1}^{L} a^j_{k,r}R^{jl}_k \geq R_t \ \forall k, k=1,..K \quad (25c)$$

$$a^j_{k,r}\in\{0,1\} \ \forall k, r, \mathbf{j} \quad (25d)$$

$$b_k\in\{0,1\} \ \forall k \quad (25e)$$

$$\sum_{l=1}^{L} P^{jl}_k \geq 0 \ \forall k, \mathbf{j} \quad (25f)$$

Les notations précédentes sont maintenues en ajoutant l'indice des directions des antennes l basées sur la décomposition en valeurs singulières.

Résolution du problème

Utilisant la décomposition de Lagrange, le problème global est divisé en sous problèmes pour résoudre l'allocation de puissances puis résoudre conjointement la sélection des relais et l'allocation des RBs. Ensuite, au niveau de chaque utilisateur, l'allocation des puissances pour les différentes antennes est effectuée selon deux méthodes:

- Répartition égale de puissances (EPA)

$$P^{j,l}_k=\frac{P^j_k}{L} \ \forall l \quad (26)$$

- Beamforming: l'utilisateur k alloue toute sa puissance à la meilleure direction d'antennes l* pour maximiser le débit

$$P^{j,l^*}_{k}=P^j_k \quad (27)$$

$$P^{j,l}_k=0 \ \forall l' \neq l^* \quad (28)$$

L'algorithme est résolu itérativement et à chaque itération, les conditions de convergence sont vérifiées et les variables de Lagrange sont mises à jour.

Résultats de simulations

Les conditions de simulation sont similaires au cas mono-antenne pour des utilisateurs half-duplex mais avec L = 2.

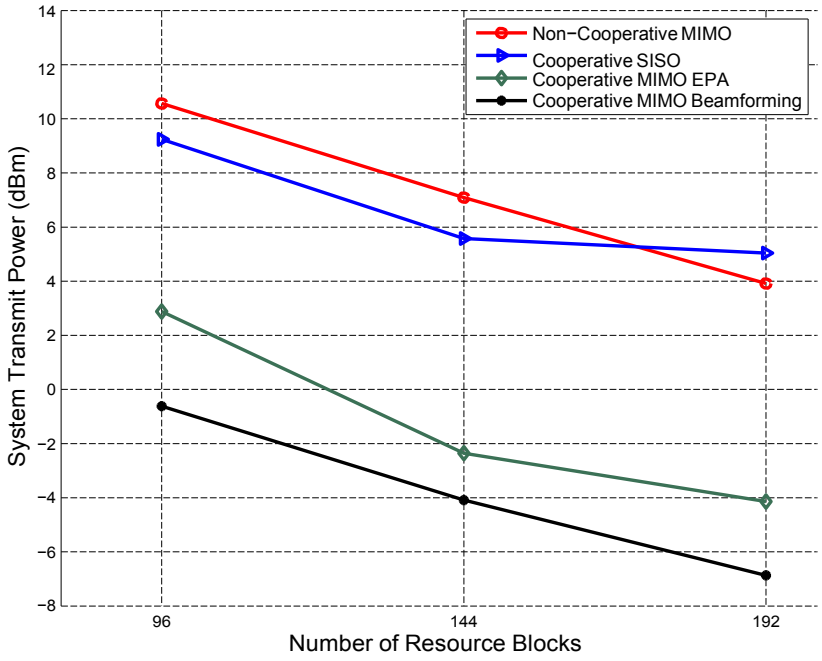

Figure 22: Puissance de transmission du système pour R_t = 1 bits/s/Hz

Les figures 22 et 23 présentent la puissance de transmission pour des débits cibles 1 bits/s/Hz et 1.5 bits/s/Hz en considérant 18 utilisateurs et 2 antennes par utilisateur. L'EPA et le beamforming sont comparés aux modèles SISO coopératif et MIMO non coopératif. Pour le modèle MIMO non coopératif, l'EPA est adoptée. Les résultats de simulations montrent que les modèles MIMO coopératifs offrent un gain considérable. En comparant au système MIMO non coopératif, le modèle coopératif permet un gain de 80% avec EPA et un gain de 90% avec le beamforming pour R_t = 1 bits/s/Hz. On peut également remarquer que le beamborming offre de meilleurs résultat que EPA, ceci est justifié par le fait que chaque utilisateur alloue toute sa puissance à la meilleur direction d'antennes et ne perd donc pas de la puissance dans des directions avec des conditions moins bonnes. Ensuite, en comparant au modèle SISO coopératif, le système MIMO coopératif offre un gain de 85% avec EPA et un gain de 90% avec le beamforming pour R_t = 1.5 bits/s/Hz. Ce gain est dû à la diversité spatiale offerte par le système MIMO.

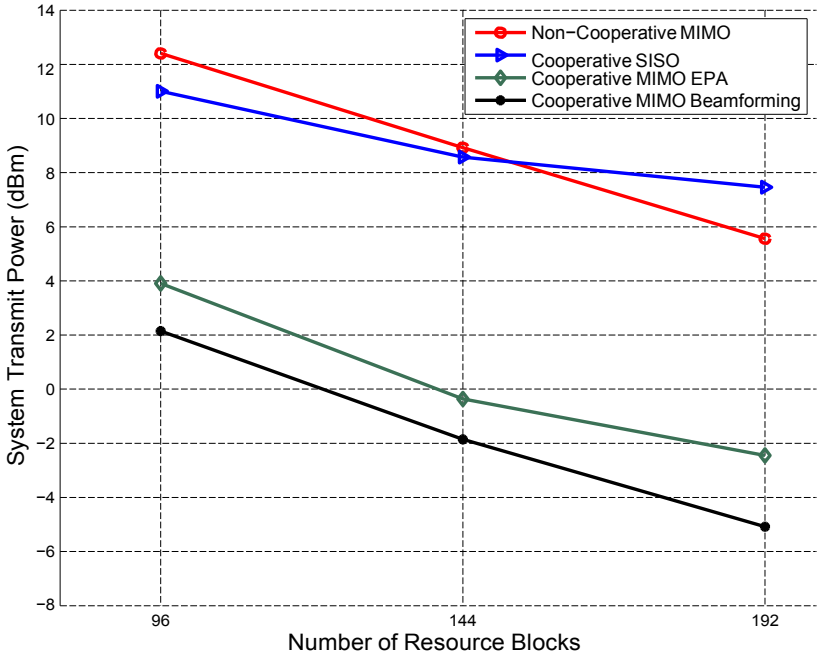

Figure 23: Puissance de transmission du système pour R_t = 1.5 bits/s/Hz

Chapitre 7: Conclusions et perspectives

Nous avons abordé dans cette thèse le problème d'allocation de ressources pour le sens montant d'un système OFDMA. Nous avons étudié les principaux algorithmes d'allocation de ressources existants pour un système mono-cellulaire et nous avons proposé l'algorithme WPF à équité proportionnelle pondérée comme compromis entre le débit et l'équité entre les utilisateurs. Une étude théorique a été réalisée afin d'étudier le comportement de cet algorithme proposé et de le comparer à l'algorithme classique PF. Ensuite, nous avons étudié l'algorithme WPF dans un contexte multi-cellulaire où l'interference nuit aux performances du système. En comparant au modèle de réutilisation de fréquence adopté en LTE, nous avons prouvé théoriquement et par simulations que notre algorithme proposé offre de meilleurs résultats. De plus, nous avons étudié les stratégies d'atténuation d'interférence basées sur la coopération entre les stations de bases (BS). Dans ce contexte, nous avons proposé un nouvel indicateur d'interférence (EII) qui permet, en utilisant des valeurs entières, d'indiquer le niveau d'interférence de chaque sous-porteuse en fonction de ses secteurs d'allocation dans les cellules voisines. L'allocation des sous-porteuses est donc effectuée dynamiquement en fonction des allocations dans les cellules voisines.

En outre, nous avons abordé dans la deuxieme partie de cette thèse l'allocation de

ressource coopérative en utilisant des relais mobiles. Pour ce, nous avons considéré que de simples utilisateurs ayant des bonnes conditions de canal peuvent relayer d'autres utilisateurs en bordure de cellule. Ayant également leurs propores données à transmettre, les relais multiplexent leurs données aux données à relayer avant la transmission à la BS. Visant à approcher la solution optimale, nous avons formulé le problème en un problème d'optimisation avec l'objectif de minimiser la puissance totale du système tout en assurant un débit minimal par utilisateur. Dans un premier temps, nous avons proposé une méthode d'association source-relai et nous avons proposé une solution sous-optimale pour l'allocation de puissance et des RBs. Dans un deuxième temps, nous avons traité la sélection de relai comme une variable d'optimisation additionnelle. Enfin, nous avons appliqué le problème étudié dans un système MIMO et nous avons étudié l'influence des antennes multiples sur la puissance consommée. La décomposition de Lagrange a été utilisée afin de résoudre les problèmes d'optimisations étudiés et des heuristiques itératives de résolution ont été proposées.

Comme perspectives pour ces travaux, nous envisageons d'étudier la faisabilité des différents algorithmes proposés pour un système où la connaissance du canal est partielle ou dans un système multi-cellulaire asynchrone. La robustesse et l'application de nos algorithmes dans des systemes réels peut donc être étudiée. Ensuite, il nous semble intéressant de quantifier l'échange de l'indicateur EII entre les BS et voir l'effet d'un échange périodique et non pas tous les TTIs. De plus, le cas de relais full-duplex étudié peut mériter plus d'attention. Il présente une borne supérieure et son application dans les réseaux modernes peut apporter un gain considérable.

Contents

List of Figures

List of Tables

Nomenclature

Abbreviations and Acronyms

AF	**A**mplify and **F**orward
AWGN	**A**dditive **W**hite **G**aussian **N**oise
BS	**B**ase **S**tation
CP	**C**yclic **P**refix
DF	**D**ecode and **F**orward
EII	**E**nhanced **I**nterference **I**ndicator
EPA	**E**qual **P**ower **A**llocation
FDMA	**F**requency **D**ivision **M**ultiple **A**ccess
FFR	**F**ractional **F**requency **R**euse
FFT	**F**ast **F**ourier **T**ransform
GPP	**G**eneration **P**artnership **P**roject
ICI	**I**nter-**C**ell **I**nterference
IFFT	**I**nverse **F**ast **F**ourier **T**ransform
KKT	**K**arush **K**uhn **T**ucker conditions
MIMO	**M**ultiple **I**nput **M**ultiple **O**utput
LTE	**L**ong **T**erm **E**volution
OFDMA	**O**rthogonal **F**requency **D**ivision **M**ultiple **A**ccess
PF	**P**roportional **F**air
QoS	**Q**uality **o**f **S**ervice
RB	**R**esource **B**lock
SINR	**S**ignal to **I**nterference plus **N**oise **R**atio
SISO	**S**ingle to **I**nput **S**ingle **O**utput
SNR	**S**ignal to **N**oise **R**atio
SVD	**S**ingle **V**alue **D**ecomposition
TTI	**T**ransmission **T**ime **I**nterval
WPF	**W**eighted **P**roportional **F**air
WiMAX	**W**orldwide **I**nteroperability for **M**icrowave **A**ccess

Notations

Vectors and matrices are denoted by bold letters (e.g X). Other notational conventions are summarized as follows:

C^n	The set of vector of length n with complex elements
R^n	The set of vector of length n with real elements
R^n_+	The set of vector of length n with real positive elements
R^n_{++}	The set of vector of length n with real strictly positive elements
$\ln(.)$	The natural logarithm
$\log_2(.)$	The base 2 logarithm
$\log_{10}(.)$	The base 10 logarithm
$L(.)$	Lagrangian of an optimization problem
∇f	The gradient of function f
$\|\Omega\|$	The cardinality of the set Ω. The number of elements in the finite set
$[x]^+$	The maximum between 0 and x
$E[.]$	The expectation operator
$var[.]$	The variance operator
C_n^k	The combination operator
$(.)^H$	The complex conjugate (Hermitian) transpose operator
$(.)^T$	The transpose operator
$(.)^*$	The optimal vector
I_n	The identity matrix of size n

Thesis specific notations

The following list consists of the most relevant notations used in the dissertation. This list is not exhaustive.

Notations applicable in all chapters:

K	The number of users
N	The number of subcarriers
B	The total available bandwidth
R	The cell radius
N_k	The number of subcarriers allocated to user k
R_t	The required target data rate per user
FI	The fairness index

Notations specific to chapter 2:

P_t	The transmit power
P_r	The received power
G_t	The antenna gains at the transmitter
G_r	The antenna gains at the receiver
R^n	The set of vector of length n of real elements
α	The pathloss exponent
B_c	The coherence bandwidth
T_{c0}	The coherence bandwidth
D_s	The multipath time delay spread
B_d	The Doppler bandwidth
c	The speed of light
V	The mobile speed
f_c	The carrier frequency

Notations specific to chapter 3:

N_0	The AWGN noise per subcarrier k
L_k	The pathloss of user k
S_k	The shadowing of user k
R_k	The data rate of user k
P_k	The maximum transmit power of user k
Δf	The bandwidth of a subcarrier
$P_{k,j}^m$	The power allocated for user k in subcarrier **j** at TTI m
$R_{k,j}^m$	The data rate of user k in subcarrier **j** at TTI m
$\alpha_{k,j}^m$	The square Rayleigh fading between user k and the BS in subcarrier **j** at TTI m
$a_{k,j}^m$	The boolean allocation variable for user k, subcarrier **j** at TTI m
$v_{k,j}^m$	The channel gain divided by the product of pathloss, shadowing and noise for user k, subcarrier **j** at TTI m.
w_k	The weight of user k
$S_{sub,k}^m$	The set of subcarriers assigned to user k at TTI m
$U_{k,j}^m$	The incremental utility for a user k and subcarrier **j** at time m
L_X	The probability distribution of random variable X
d_k	The distance of user k from the BS

Notations specific to chapter 4:

K_b The number of users in the cell border

K_c The number of users in the cell center

N_{cells} The number of cells

$R_{k,c}^m$ The data rate of user k in cell c at TTI m

$w_{k,c}$ The weight of user k in cell c

$v_{k,j,c}^m$ The channel gain divided by the product of pathloss, shadowing and noise for user k in cell c, subcarrier **j** at TTI m.

$\alpha_{k,j,c}^m$ The square Rayleigh fading between user k and the BS in cell c in subcarrier **j** at TTI m

L_k The pathloss of user k in cell c

S_k The shadowing of user k in cell c

$I_{j,c}$ The interference on subcarrier j for the cell c caused by the other cells $_{k,j,c}$

a^m The boolean allocation variable for user k in cell c, subcarrier **j** at TTI m

$t_{k,j,m}$ The incremental utility for a user k in cell c and subcarrier **j** at time m

$EII_{j,c}$ The EII value of subcarrier **j** in cell c

$eii_{s,c',c}$ The EII value of sector s in c' if the considered cell is c

$b_{s,j,c'}$ The boolean allocation variable of subcarrier **j** and sector s in cell c'

Notations specific to chapter 5 and chapter 6:

$d_{k,k}$ The distance of user k from the BS

$d_{k,k'}$ The distance between user k and user k'

gk, k^{j} The square Rayleigh fading between user k and the BS in subcarrier **j**

gk, k'^{j} The square Rayleigh fading between user k and user k' in subcarrier **j**

$L_{k,k}$ The pathloss of user k corresponding the direct link to the BS

$L_{k,k'}$ The pathloss of user k to user k'

$S_{k,k}$ The shadowing of user k corresponding the direct link to the BS

$S_{k,k'}$ The shadowing of user k to user k'

$vk^{j}_{,k}$ The channel gain for user k and the BS in subcarrier **j**

$vk^{j}_{,k'}$ The channel gain for user k and user k' in subcarrier **j**

$ak^{j}_{,k}$ The boolean allocation variable for subcarrier **j** for the direct link of user k to the BS

$ak^{j}_{,k'}$ The boolean allocation variable for subcarrier **j** for the indirect link of user k to user k'

b_k The boolean cooperation variable of user k

$Gk^{j}_{,k}$ The potential gain for the direct link of user k for subcarrier **j**

$Gk^{j}_{,k'}$ The potential gain for the pair (k, k') for the indirect link of user k through user k' for subcarrier **j**

L The number of antennas per user

L_t The number of transmit antennas per user

L_r The number of receive antennas per user

$Fk^{j}_{,k}$ The potential gain using EPA

$Fk^{j}_{,k}$ The potential gain using beamforming

Chapter 1

Introduction

1.1 Background and motivation

Today, we witness a high evolution of application for wireless systems. Thus, replying to quality of service requirements with always greedy data applications is still an important challenge. In fact, applications with images, music and videos require high data rate constraints which needs more efficient resource management in communication systems.

Multicarrier techniques have been introduced and adopted to achieve required data rates especially Orthogonal Frequency Division Multiplexing (OFDM). Actually, the main idea of OFDM multicarrier technology is to divide the wideband frequency selective communication channel into several orthogonal subcarriers. The bandwidth of each subcarrier has to be smaller than coherence bandwidth of the propagation channel, consequently, the fading experienced by each subcarrier is small and in addition to the orthogonality between subcarriers, the inter-symbol interference can be avoided. Orthogonal Frequency Division Multiple Access (OFDMA) is the multi-user variant of OFDM and is adopted for various standards as WiMAX [1] and LTE [2].

Moreover, resource allocation in wireless systems is is the key feature to satisfy

users requirements considering the limited available bandwidth. Multiple algorithms are proposed in the literature depending on the intended objective. Among the classical ones we find the sum rate maximization algorithm which is the upper bound of throughput. Besides, this algorithm is totally unfair while it serves only the minority of users near to the Base Station (BS). Then, we find the max min algorithm [3] with the main idea to maximize the lowest data rate in the system. This algorithm is considered as the upper bound of fairness between users but with which the system throughput is low. As a tradeoff between throughput and fairness, proportional fairness is investigated in the literature [4][5].

The importance of resource allocation especially for the next generation of wireless systems has motivated researches to develop alternative solutions and propose enhanced strategies to more efficiently manage the system resources. In addition, the behavior of resource allocation algorithms has to be robust in multi-cell systems where the Inter-Cell Interference (ICI) limits the system performance. The frequency reuse strategy is used in LTE to mitigate ICI but reduces the bandwidth per cell [6] [2]. Cooperation between BSs is also investigated in the literature to efficiently mitigate ICI with use of the total bandwidth in all cells. BS cooperation may reduce the ICI but, depending on the quantity of data to exchange, the cooperation cost may be significant [7][8][9].

Furthermore, relaying strategies have nowadays much attention to enhance systems performance. Relays can be fix or mobile and transmission may be established through one or more hops. If relays are fix, they are a part of the access network and a deployment cost is needed. On contrary, mobile relays do not necessitate any infrastructure cost but are totally unpredictable. The system can not know in advance the number of available potential relays. The transmission with relays is made in two time intervals [10] since the source has to transmit to its relay in a first time and the relay forwards data to the destination in a second time. Relay behavior is also investigated in literature and the classical scheme used in relays are Decode and Forward (DF) and Amplify and Forward (AF). A DF relay [18] decodes the received signal, encodes it and forwards it to destination. A AF relay simply amplify the received signal before transmission to destination. If no direct link is available between source and destination, relays are said repeaters. Relays may also be used as virtual Multiple Input Multiple Output (MIMO)[11].

In this case, combining techniques are needed in destination to extract the transmitted signal. For systems with relays, relay selection [19] is an additional feature to consider for resource allocation process. LTE standard [12] has adopted fixed relays. Mobile relays present an important candidate for 5^{th} generation (5G) of wireless systems.

1.2 Thesis objectives

In this thesis, we mainly consider the resource allocation for an uplink OFDMA system for a cellular system model ensuring Quality of Service (QoS) requirements and fairness between users. The proposed resource allocation methods are applicable to 4G LTE Advanced networks and future 5G networks. Parts of this study can also be applied to ad hoc type networks.
The main objectives of the studies performed in this thesis are:

- Study the resource allocation algorithm and evaluate their performance considering the system throughput and fairness between users. Propose an improved algorithm that approaches the upper bound of both system throughput and fairness.
- Extend the resource allocation in a multi-cell system model. Evaluate the multi-cell features especially the Inter-Cell Interference (ICI). Our aim is to mitigate the ICI to improve the system performances. We here investigate frequency reuse schemes as well as cooperation between BSs.
- Evaluate the potential gain offered by cooperation. In a system with mobile relays, and contributing to green communication, we take into account saving battery life and reducing environmental effects in resource allocation, in addition of QoS requirements. For this, resource allocation is formulated as a global optimization problem having the green objective to minimize the system transmit power and respecting QoS constraints. The aim is to approach the optimal solution and to provide the best allocation scheme.
- Study the influence of cooperation on reducing the system transmit power. We investigate multiple optimization features and study both half and full

duplex behavior users. Moreover optimize the resource allocation in a MIMO cooperative system model.

1.3 Thesis outline

Chapter 2 - Technical Background

Chapter 2 is devoted to introduce the basic element used in the rest of this dissertation. The technical background concerning OFDMA, LTE, wireless channel model, QoS and multi-cell features is presented. Then, mathematical tools for optimization formulation and resolution are depicted. Multi-cell system model will be studied in chapter 4. Optimization problems for resource allocation will be studied in chapters 5 and 6.

Chapter 3 - Resource Allocation in a single cell model

In chapter 3, we study the resource allocation for an uplink OFDMA system for one cell system model. The objective is to maximize the system throughput while ensuring fairness between users. First, we study the existing algorithms for resource allocation and study their effects on both throughput and fairness using utility functions. Then we propose a novel algorithm for resource allocation: the Weighted Proportional Fair (WPF) inspired from the classical PF algorithm. The main idea of the WPF algorithm is to add weights to the algorithm PF favoring users with good channel conditions. A theoretical analysis is performed to study the behavior of the WPF and to compare it to the classical PF algorithm. Simulation results show that the proposed algorithm approaches the upper bound of throughput while ensuring fairness between users.

Chapter 4 - Resource Allocation in a multi-cell system model

In chapter 4, we propose resource allocation strategies for a multi-cell system model where the performances are limited by the ICI. First, a resource allocation strategy based on Fractional Frequency Reuse (FFR) and WPF is proposed to mitigate the ICI. Resource allocation is made independently in each cell and thus no cooperation between BSs is needed. Theoretical study and simulation results compare the proposed algorithm to the classical FFR scheme used in the LTE standard and

show that performances can be improved with the proposed method especially in the cell center area concerning throughput. Moreover, the second part of this chapter proposes a mitigation ICI strategy based on cooperation between BSs. For this, the interference indicators are studied and a new Enhanced Interference Indicator (EII) is proposed. The EII is exchanged by BSs and consists to indicate the level of interference of RBs by integer values. The EII aims to improve resource allocation by considering allocations in neighboring cells. The EII values and the system dependencies are studied, and to reduce the high cost of BS cooperation, only integer EII values are communicated between BSs. Simulation results show that system performance are improved considering the proposed EII.

Chapter 5 - Resource Allocation in Cooperative OFDMA with Multiplexing Mobile Relays

In chapter 5, cooperative OFDMA system model is investigated. Uplink transmission from mobile users to the BS in a single cell are studied where half-duplex users can directly transmit data to the BS or cooperate with another user as Decode and Forward (DF) relay to carry data to the BS. A simple mobile user can then act as a Not Relayed Source (NRS), relayed source (RS) or relay (R). In all cases, all users have their own data to transmit, thus, a user acting as relay multiplex its own data to relayed data to the BS. The resource allocation is formulated as an optimization problem to find the optimal solution. For resolution, dual method and Lagrangian Decomposition are adopted and an iterative sub-optimal heuristic is proposed. In the first part of the chapter, the pairing step to associate RS to R is performed as an initialization with the assumption that a RS can be relayed by only one relay. The optimization problem aims to optimize Resource Block (RB) and power allocation while minimizing the system transmit power. A target data rate is also required by user. The objective is chosen for 5G communication in the context of green communication and for saving users battery life. The second part of this chapter, in addition to RB and power allocation, relay selection is considered as an optimization variable and solved dynamically. A RS can then be relayed by one or more relays in different RBs. With respect to the target data rate per user constraint and aiming to minimize the system transmit power, an iterative algorithm is proposed to find a sub-optimal solution for all resource allocation features. Both half and full-duplex user cases are studied and compared. Finally, we compare the two proposed methods.

Chapter 6 - Resource Allocation in Cooperative OFDMA MIMO system with Multiplexing Mobile Relays

In this chapter, we extend the cooperative resource allocation with multiplexing relays for a MIMO system model. The objective are always to minimize the system transmit power and to reduce the overall environmental effects, and the cooperative system has to ensure a target data rate per user using multiplexing relays. An optimization problem is formulated and solved theoretically to approach the optimal solution. The features to optimize are relay selection, RB allocation and power allocation. The MIMO system is studied and the global optimization problem is decomposed into sub-problems for resolution. Moreover, for each user, power allocation in the multiple antennas is studied. For this, two strategies are studied and compared. First, Equal Power Allocation (EPA) is investigated where the user equally divides its power in the antennas. Second, beamforming method is studied where each user uses all its power in the best direction to avoid directions with high signal attenuation. Theoretical expressions and simulation results are shown to compare the system performances with the two power allocation strategies.

Chapter 7 - Conclusions and Perspectives

Chapter 7 draws final conclusions of the thesis, summarizes the main obtained results and highlights the principle contributions of this dissertation. Finally, perspectives and possible future research direction are provided.

1.4 List of publication

Journal paper

1. S. Hamda, M. Pischella, D. Roviras, R. Bouallegue, “Uplink Resource Allocation in Cooperative OFDMA with Multiplexing Mobile Relays”, submitted.

Conference papers

1. S. Hamda, M. Pischella, D. Roviras, R. Bouallegue, “Analysis of Weighted Proportional Fair resource allocation for Uplink OFDMA”, IEEE Vehicular Technology Conference (VTC Fall), Sept. 2013, p1 - 5, Las Vegas USA.
2. S. Hamda, M. Pischella, D. Roviras, R. Bouallegue, “Fractional Frequency Reuse based on Weigthed Proportional Fair for Uplink OFDMA”, IEEE

Wireless Communications and Networking Conference (WCNC), Apr. 2014, p1456 - 1460, Istanbul, Turkey.

3. S. Hamda, M. Pischella, D. Roviras, R. Bouallegue, “Joint Enhanced Inter- ference Indicator and Proportional Fair allocation for Uplink OFDMA”, sub- mitted to World of Wireless, Mobile and Multimedia Networks (WoWMoM) 2016.

4. S. Hamda, M. Pischella, D. Roviras, R. Bouallegue, “Energy Efficient Re- source Allocation for Uplink OFDMA cooperative system using multiplexing half and full-duplex mobile relays”, IEEE Vehicular Technology Conference (VTC Spring), May 2016, Nanjing China.

5. S. Hamda, M. Pischella, D. Roviras, R. Bouallegue, “Cooperative Uplink OFDMA-MIMO Resource Allocation with Multiplexing Relays”, IEEE Wire- less Communications and Networking Conference (WCNC), Apr. 2016, Doha, Qatar.

Chapter 2

Technical Background

2.1 Introduction

This chapter aims to present the basic elements used in the rest of the document. First of all, we introduce the OFDM and OFDMA technologies adopted in the system models in the next chapters and we show how the LTE standard uses them. Then, we are interested to the wireless channel model given its importance in the transmission process. For this, we expose the different features to consider in a wireless channel as the pathloss, the fading, the noise, etc and present the system model adopted in the rest of the document. The quality of service for wireless systems is also defined in this chapter. Moreover, we focus on multi-cell systems where the Inter-Cell Interference (ICI) affects the system performance especially in the cell edge. We then present the classical methods to reduce the ICI as the Fractional Frequency Reuse (FFR) and the BS cooperation. Resource allocation in such system model is also described. Finally, we focus on mathematical tools to solve resource allocation problems. For this we present how to formulate an optimization problem, the associated constraints and the necessary steps to solve it.

2.2 Orthogonal Frequency Division Multiple Access (OFDMA)

OFDM is a multi-carrier modulation technique used for frequency selective channels to efficiently adapt the signal to the channel. The principle of OFDM is to transform a bradband multipath channel into a set of flat fading sub-channels for each subcarrier. The bandwidth of each subcarrier becomes small comparing to the coherence channel bandwidth. OFDM offers then simple channel equalization when it may be viewed as using many slowly-modulated narrowband signals rather than one rapidly-modulated wideband signal [20].

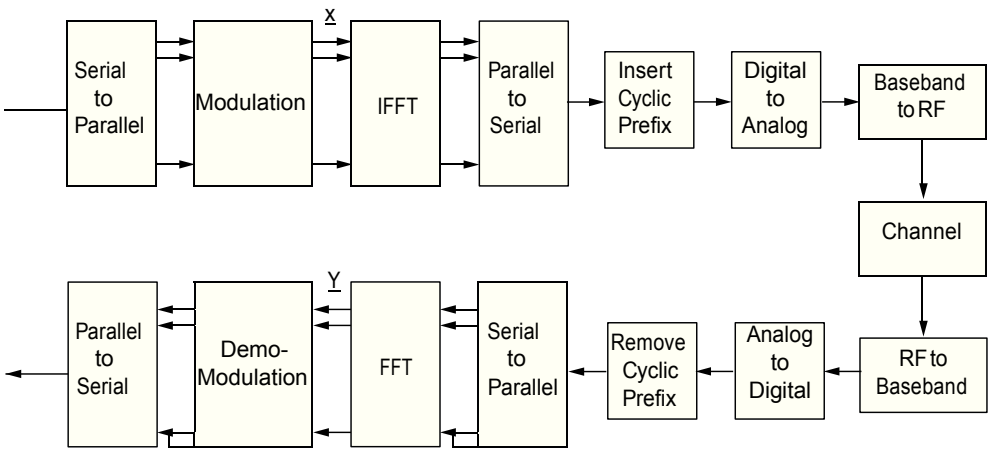

Figure 2.1: Implementation of an OFDM system

The orthogonality in OFDM is obtained by applying an Inverse Fast Fourier Transform (IFFT) at the transmitter and a Fast Fourier Transform (FFT) at the receiver (figure 2.1). To avoid inter-symbol interference, a Cyclic Prefix (CP) is added between OFDM symbols as a guard interval [20] (figure 2.2). OFDM is adopted for various standards as IEEE802.11a, WiMAX, LTE, DVB.

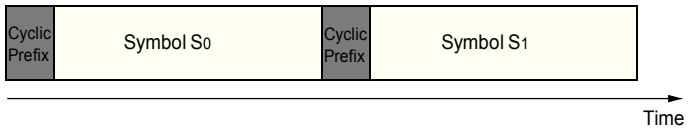

Figure 2.2: Cyclic prefix of an OFDM system

In a time invariant multipath channel, where CP is used, the input/output relation is given by:

$$\underline{Y} = H\underline{X} + \underline{W} \tag{2.1}$$

where:

- $\underline{X}$ is a vector of N complex symbols and is called an OFDM symbol,
- $\underline{Y}$ is a vector of N complex received symbols,
- N is the number of subcarriers and is equal to IFFT size,
- H is a diagonal $N \times N$ matrix where the diagonal elements are the channel complex gain for each subcarrier,
- $\underline{W}$ is a vector of size N with complex values and results from the additive noise.

OFDMA is the multi-user version of OFDM where different users can transmit simultaneously on different orthogonal subcarriers. The same subcarrier can then be used by different users but not at the same time (see figure 2.3). Comparing to TDMA and CDMA, the OFDMA is considered more advantageous since it offers flexibility, simplicity and robustness especially against inter-symbol interference and multi-path fading. OFDMA is also low sensitive to time synchronization errors. Many standards have adopted the OFDMA technology for resource allocation as IEEE 802.16 and LTE.

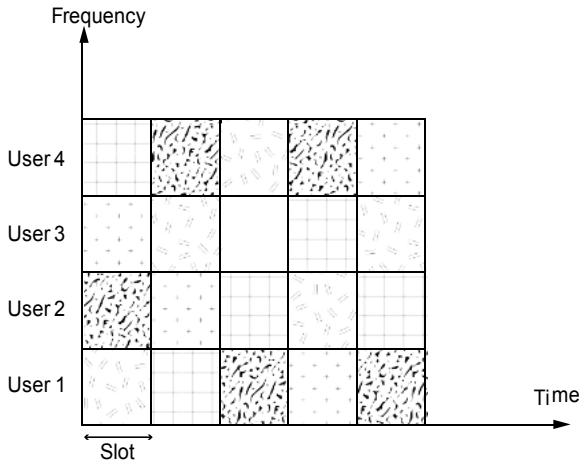

Figure 2.3: OFDMA

In figure 2.3, subcarrier allocation is varying from one time slot to an other. In LTE, the two time slot duration is called Transmission Time Interval (TTI) and is equal to 1ms.

2.3 Long Term Evolution (LTE)

LTE [21] is a wireless communication standard developed by the 3GPP (3rd Generation Partnership Project) and adopted since 2009. The evolution of LTE in the 4^{th} Generation (4G) in wireless networks is the LTE Advanced proposed on 2011 and widely adopted on 2014.

LTE takes advantageous of OFDMA and uses two different variants for downlink and uplink. For LTE, OFDM splits the frequency bandwidth into small subcarriers spaced at 15 kHz. LTE assigns subcarriers to users grouped in RB. A RB is composed by 12 subcarriers (see figure 2.4), it has then 180 kHz and is the smallest unit of subcarriers that can be allocated to users. Bandwidths from 1.4 MHz up to 20 MHz can be supported in LTE. The RBs not allocated are off in order to save power.

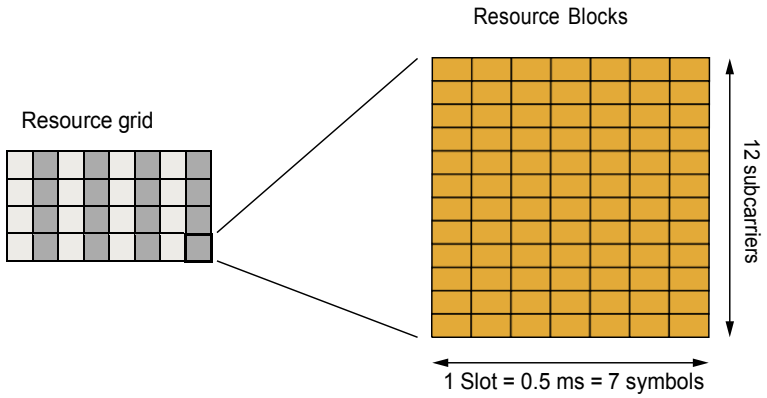

Figure 2.4: Resource Blocks

LTE uses the OFDMA technique for the downlink to carry data from the BS to the users. However, for the uplink from users to the BS, the Single Carrier FDMA (SC-FDMA) is used. For the SC-FDMA, an additional step with a Discrete Fourier Transform (DFT) is added before the conventional OFDMA processing, for this, SC-FDMA is also called Linearly precoded OFDMA (LP-OFDMA).
The comparison of SC-FDMA and OFDMA is studied in the literature [22][23][24]. The main advantage of SC-FDMA compared to OFDMA is that SC-FDMA offers lower Peak-to-Average Power Ratio (PAPR). This lower PAPR reduces battery power consumption and improves uplink coverage and cell-edge performance. In SC-FDMA, data are carried among multiple subcarriers and a complex receiver is needed contrary to OFDMA where each subcarrier transports data coming from one user only (see figure 2.5). SC-FDMA is used in LTE for the uplink while OFDMA with simple equalization at the receiver is adopted for the downlink.

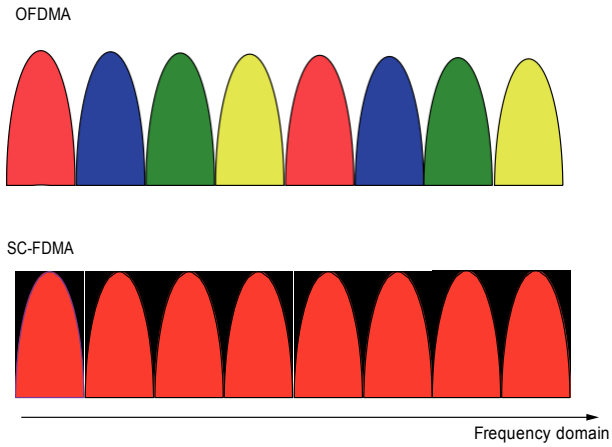

Figure 2.5: OFDMA vs SC-FDMA. Different users have different colors

2.4 Wireless Channel Model

The transmission chain can be simply presented by a transmitter and a receiver connected with a transmission medium called the channel. The transmitter adapts the signal to transmit corresponding to the channel characteristics. The channel is the principle cause of degradation that the received signal suffers from. It is consequently important to have a good knowledge of the channel to efficiently exploit it and offer high quality of transmission.

In wireless transmissions, the received signal is composed of several replicas of the emitted one due to obstacles. These different replicas are related to wave propagation phenomena like reflection, diffusion and scattering on obstacles. This is shown on figure 2.7. The multipath nature of the channel results in complex gains that are varying with the receiver or emitter position (emitter position in the case of figure 2.7 where we consider the uplink). The fading gain related to multipath is called small-scale fading. The small scale fading gain is frequency selective due to the multipath and is also time varying due to the mobility of the emitter, receiver or obstacles. An other attenuation of the received signal is due to the distance between emitter and receiver and to obstacles between them. Attenuation related to distance is the pathloss and attenuation due to obstacles is called shadowing. These two attenuations are called large-scale fading. Both large-scale fading and small-scale fading presented in figure 2.6 are time varying in

function of the relative position of the emitter and receiver. Nevertheless, small-scale fading varies where position varies of an order of magnitude of $\frac{\lambda}{2}$ (where λ is the wavelength of carrier frequency, few centimeters for used carrier frequency) and large-scale fading varies with position changes of the order of tens of meters. Due to the different orders of magnitude in distances, large-scale fading is generally kept constant for a user position while small-scale fading is considered as a time varying fading gain.

2.4.1 Large-scale fading

The large-scale fading considers essentially the pathloss and the shadowing (see figure 2.6).

- **Pathloss**
  The pathloss is the attenuation caused by the path from the transmitter to the receiver. The pathloss is modeled in function of the distance and models are different for various environments (indoor, outdoor, urban, etc.).
  Path loss when the antenna gains are included is given by:

$$PL(d) = 10\log_{10}\left(\frac{P_t}{P_r}\right) = 10\log_{10}\frac{1}{G_t G_r}\left(\frac{4\pi d}{\lambda}\right)^{\alpha} \tag{2.2}$$

  where P_t and P_r are respectively the transmit and the received powers. G_t and G_r are respectively the antenna gains at the transmitter and the receiver. d is the distance between the antennas. λ is the wavelength. d and λ are in meter. α is the pathloss exponent varying from 2 to 5 [25]. For a free space transmission, α is set to 2.

- **Shadowing**
  The shadowing fading is caused by the objects obstructing the propagation path between transmitter and receiver (generally buildings and hills). Generally, the shadowing is modeled by a log-normal random variable [26].

The large-scale fading are characterized to be frequency independent [27]. The pathloss and the shadowing are considering as large-scale fading because they occur over relatively large distances.

2.4.2 Small-scale fading

The fading is an attenuation that wireless signal suffers from. It can be due to multipath propagation and named multipath induced fading [28]. Figure 2.7 shows an example of multipath environment for a system with one mobile user as transmitter and one BS as receiver. Since the BS is surrounded by obstacles, many replicas of the original signal reach the BS from different paths with different delays.
Small-scale fading can be frequency selective in function of the delay spread of the channel. So, different frequencies or subcarriers will experiment different attenuations. two main parameters are used for characterizing the small-scale fading: Coherence Bandwidth B_c and Coherence Time T_{c_0}. Coherence bandwidth characterizes the time varying nature of the small-scale fading gain and is principally related to the mobility (speed) of emitter or receiver.
Many distribution functions can be used for modeling and designing fading gain in wireless communication systems [28]. The most used ones are Rayleigh and Ricean distributions. We can also find Nakagami and Weibull distributions.

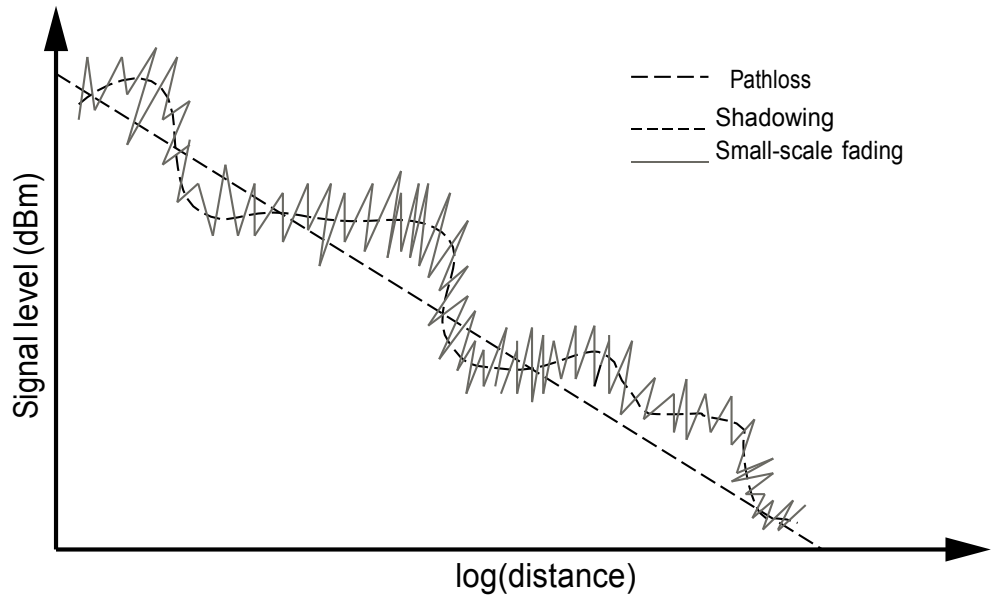

Figure 2.6: Fading types

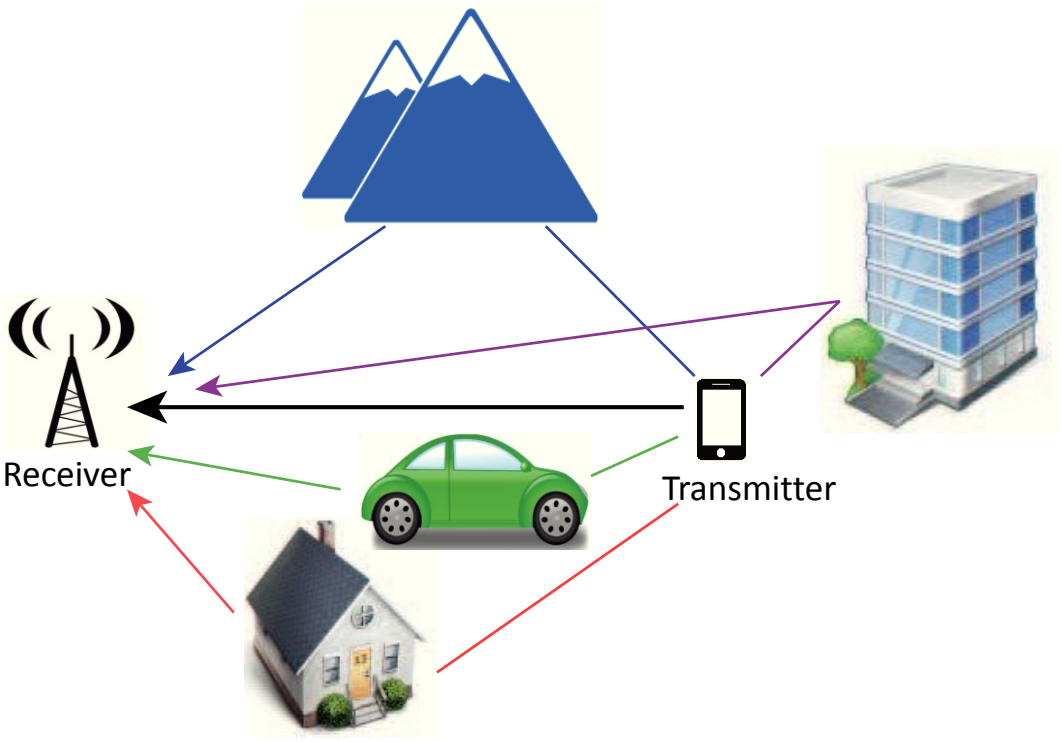

Figure 2.7: Mobile propagation environment (rural area)

2.4.3 Coherence Bandwith

The coherence bandwidth B_c is considered as the bandwidth over which the channel gain can be considered as constant. When transmitted bandwidth is much lower than the coherence bandwidth, B_c, the channel is called “flat fading” and all frequencies or subcarriers are multiplied by the same gain. On the contrary, when the transmitted bandwidth is larger than B_c, the channel is called “frequency selective”. For classical systems, the channel is always frequency selective. Using OFDM with the right number of subcarriers permits to have a flat fading channel for each of the subcarriers. B_c depends on the delay spread multipath time that is the difference of the time of arrival between the earliest and the latest signals considering multiple paths. B_c in Hz can be expressed as:

$$B_c \approx \frac{1}{D_s}$$

where D_s is the multipath time delay spread and is expressed in seconds.

2.4.4 Coherence Time

Because mobility of emitter, receiver and obstacles, the small scale fading is true varying. The coherence time T_{c_0} is the time duration where we can consider the channel as invariant in the time domain. T_{c_0} is given as:

$$T_{c_0} \approx \frac{1}{B_d} = \frac{c}{2Vf_c}$$

where:

- B_d is called the Doppler bandwidth,
- c is the speed of light,
- V is the mobile speed,
- f_c is the carrier frequency.

When symbol duration is lower than T_{c_0} we say that we are in “slow fading” situation, meaning that channel can be considered as constant for many successive symbols. On the contrary, when symbol duration is higher than T_{c_0}, we say that we are in “fast fading” situation and the channel varies within a symbol duration. Figure 2.8 illustrates the time and frequency channel small scale fading gain for a vehicular channel, a mobile speed of 20 km/h and a carrier frequency f_c = 1.86 Hz.

2.4.5 Noise

The noise can be defined as an unwanted signal interfering with the desired signal. The noise is generally modeled as a Gaussian process considering the central limit theorem [29] and called Additive Gaussian White Noise (AWGN). It is summed to the transmitted signal. If **x** is the transmitted complex vector, H is the channel coefficient matrix and **W** the noise complex vector, the received signal can be expressed as:

$$Y = X H + W$$

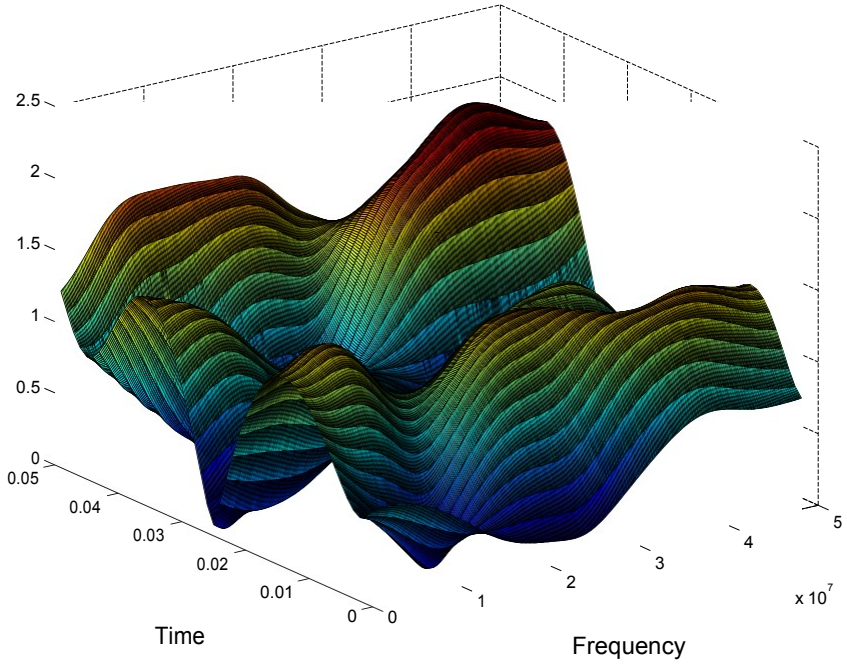

Figure 2.8: Channel frequency response

2.4.6 Our Channel Model

In all system models studied along this PhD, some assumptions are made. Mobile users are considered suffering from both pathloss and shadowing. The shadowing is considered having a log-normal distribution with variance 6 dB and the pathloss is considered according to the LTE model with frequency F = 2.6 GHz: $L_{k,dB}(d_k) = 128.1 + 37.6 \log_{10}(d_k)$ where d_k is the distance in km of user k from the BS.
Then, Rayleigh slow fading is considered and the channel is assumed constant for a period of an OFDM symbol. Independent Rayleigh gains are randomly drawn for each subcarrier. The system considers also an AWGN noise with power density $N_0 = -174$ dBm/Hz.

2.5 Quality of Service

In wireless communications, QoS is needed to measure users satisfaction. Actually, QoS is specified by policies as system management to ensure some level of metrics considering delay constraints, reliability and data rate. In wireless networks,

QoS is affected by many factors as attenuation, interference, noise, time varying channel, user mobility, etc. The traffic management efficiency is then necessary for getting good QoS and good resource utilization.
The parameters of QoS are defined by the users and the network manages its bandwidth to satisfy the request. The most considered QoS parameters are delay, jitter, packet loss and throughput [30]. Fairness is also a QoS parameter of interest.
In chapters 3 and 4, we study resource allocation with proportional fairness objective, a period of time with M TTIs is considered, the QoS parameter considered is fairness between users among the assumed period. In chapters 5 and 6, we resolve optimization problems for resources allocation respecting a target data rate constraint per user. This constraint traduces the required QoS.

2.6 Multi-cell features

In a multi-cell network, users are divided into several cells according to a regular shape. Hexagonal cells as presented in figure 2.9 are conventional. Each cell is covered by one Base Station (BS) to efficiently serve users (figure 2.9). Cells can have different sizes: we can find macro cells with a radius up to 30 km, pico cells solving a street issue with a radius between 200m and 2000m or femto cells covering a home with a radius minor than 200m. Reducing the cell size allows to increase the user capacity and to decrease the power consumption in mobile terminal but needs a high number of handovers per user. Nowadays, wireless networks have heterogeneous nature combining multiple cell types as presented in figure 2.10.

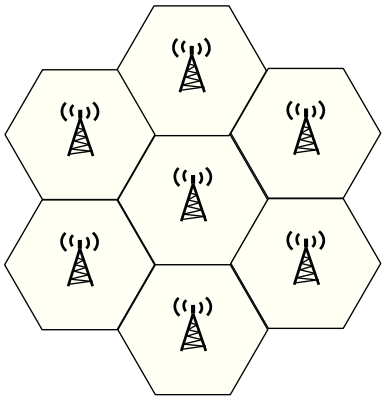

Figure 2.9: Multi-cell system model

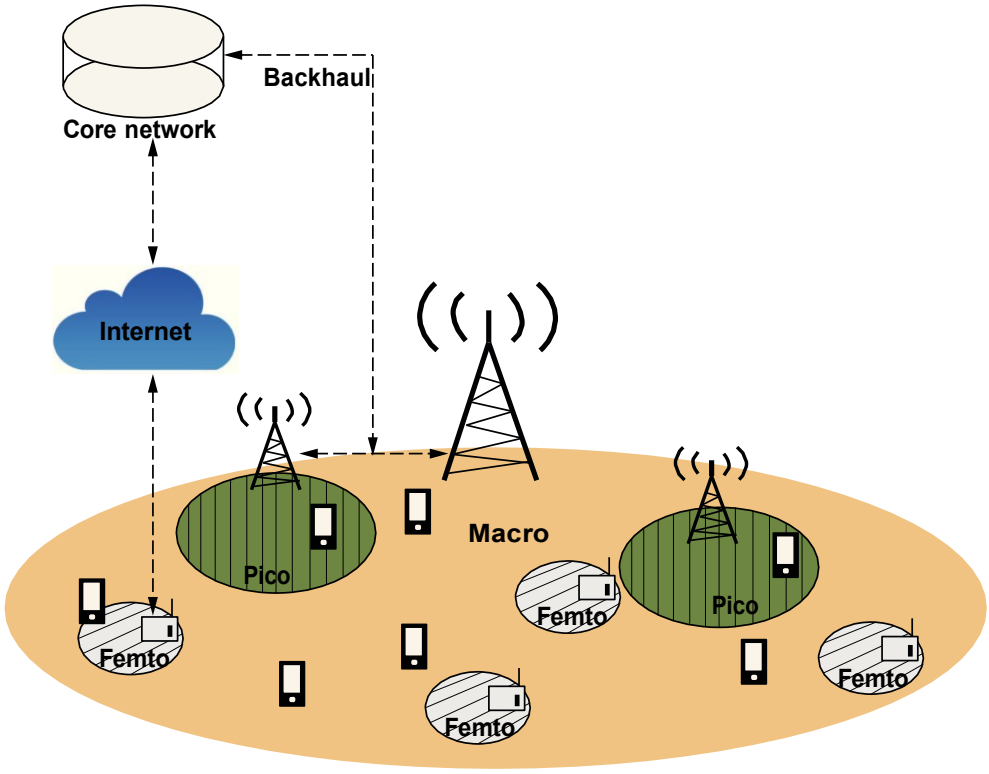

Figure 2.10: Heterogeneous Network

The resource allocation in a multi-cell system is critical due to the reuse of frequency and consequently to the caused interference. In fact, a cellular network is composed by clusters where a cluster can contain one or more cells. The available bandwidth is then reused in each cluster as presented in section 2.6.2. When two users transmit data to two different destinations in the same frequency, each of

them causes interference for the other.
In the next sections, we detail the interference channel, the most used methods to avoid its effects: the fractional frequency reuse and the cooperation between BS and we present the resource allocation in a multi-cell system model.

2.6.1 Inter-Cell Interference

For a multi-cell system model, the ICI is the key feature limiting the network capacity since the same frequency can be used in neighboring cells. In fact, the interference is caused when N independent transmitters carry their seperate data to N independent receivers through a common channel. The case with N = 2 is shown in figure 2.11.

In cellular networks and OFDMA, a frequency is allocated to only one user by

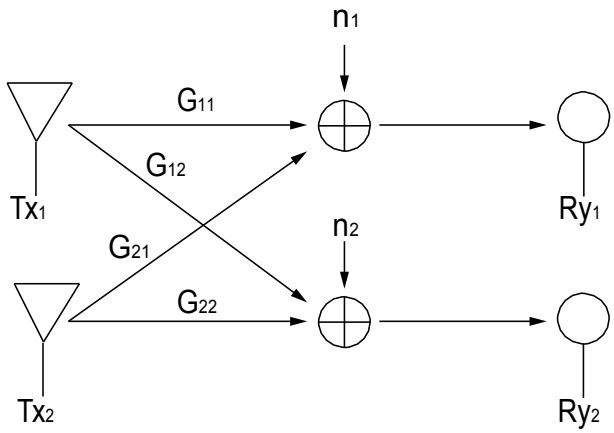

Figure 2.11: Interference channel

cluster and subcarriers are orthogonal. Then, there is no intra-cell interference, only inter-cell interference is considered. To mitigate ICI, many methods are proposed in the literature but the most common are the FFR and the cooperation between BS.

2.6.2 Fractional Frequency Reuse

The FFR method aims to avoid ICI especially in the cell edge by dividing the available subcarriers into multiple subsets and using different subsets in neighboring cells. Figure 2.12 shows the examples of FFR = 3 and FFR = 7. The LTE

standard adopts FFR = 3 in the cell border, users in the cell center use the same subset of subcarriers whereas users in cell edges use different subsets of subcarriers as presented in figure 2.13. According to the considered FFR, the total bandwidth is divided which implies the decrease of available resources per area but the ICI is avoided in the cell edge. An optimal FFR is studied in [6]. In [31], the authors study dynamic FFR schemes. FFR use in LTE standard is depicted in [32].

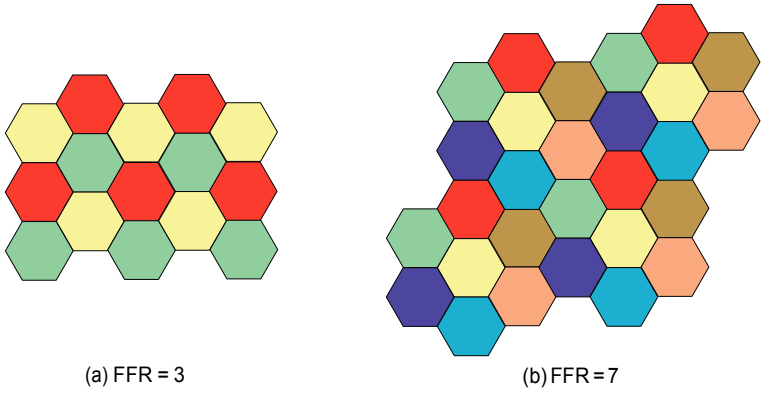

Figure 2.12: Frequency reuse

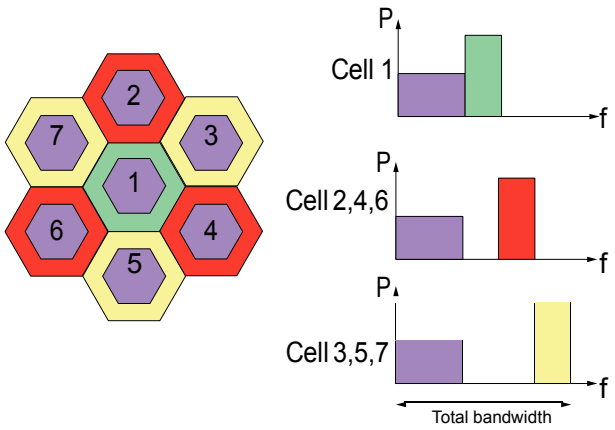

Figure 2.13: Frequency reuse in LTE

2.6.3 BS cooperation

In addition to FFR, cooperation between BS is investigated to mitigate ICI without decrease of the bandwidth [7]. BSs may exchange transmitted or received data to better estimate the ICI. Since BS communication needs high signaling and affects then system performance, it is generally established through backhaul

communication. Wireline communication can also be reduced to adjacent cells only [33]. Moreover, a BS controller can be adopted where all BSs communicate with, this can decrease communications between BS [34].
Moreover, interference indicators are offered by the LTE standard [21] to reduce the high cost needed for BS cooperation. Instead of exchanging transmitted data, BSs have only to communicate boolean indicators to highlight interfering subcarriers. These indicators can impact the resource allocation to avoid assigning interfering subcarriers in the cell edge. Interference indicators are more detailed in chapter 4.

2.6.4 Resource allocation for a multi-cell system

In a multi-cell system, resource allocation can be performed according to different methods:

- Centralized resource allocation: A BS controller that has information from all system entities and knows positions and channel characteristics of all BSs and users is responsible to allocate the resources in the system. A high signaling cost is needed for a such system model. However, interference can be reduced. This kind of resource allocation will be used in chapters 5 and 6.
- Distributed resource allocation: The resource allocation is made for each cell independently. No signaling is required since each cell ignores allocation in neighboring cells and the interference level can be high. This kind of resource allocation will be used in chapters 3 and 4.
- Hybrid resource allocation: The resource allocation is made for each cell considering the allocation in neighboring cells. The BSs cooperate and exchange information to reduce the ICI. The signaling cost depends on the communicated data (users transmitted signals, interference indicators, etc.). This kind of resource allocation will be used in chapter 4 (section 4.5).

2.7 Optimization elements

In the second part of the dissertation (chapters 5 and 6), the resource allocation is studied and formulated as an optimization problem. The resolution is established using mathematical tools to solve optimization problems. In fact, the problems dealt with in the thesis can be decomposed into convex optimization problems. Convex problems have the advantages to offer a unique global optimum, formulating a resource allocation as an optimization problem leads then to the best allocation scheme. In the studied problems, we aim to optimize multiple variables which adds complexity to the resolution process. In this case, at the expense of some loss of performance, iterative methods are adopted to compute the variables independently and sub-optimal heuristics are proposed.
In this section, we present the general formalization of convex optimization problem with the main objective and the associated constraints (section 2.7.1). Then, we explain in section 2.7.2 the duality theory allowing to solve optimization problems using Lagrangian and Karush–Kuhn–Tucker (KKT) conditions. Our main reference for convex optimization and dual method is Boyd & Vandenberghe [35].

2.7.1 Convex Optimization

A mono-objective optimization problem is formulated as follows:

$$\begin{aligned} &\underset{\mathbf{x}}{\text{minimize}}\ f_0(x) \\ &\text{subject to}\ \ f_i(x) \leq 0, i = 1..m \\ &\qquad\qquad h_i(x) = 0, i = 1..p \end{aligned} \tag{2.3}$$

Where $x = [x_1, .., x_n]^T$ is the optimization variable. $f_0 : R^n \rightarrow R$ is the objective function, $f_i : R^n \rightarrow R, \forall i \in \{1, ..., m\}$ are the inequality constraint functions and $h_i : R^n \rightarrow R, \forall i \in \{1, ..., p\}$ are the equality constraint functions. A vector x^* is optimal if it has the smallest objective value among all the vectors satisfying the constraints. When $m = 0$ and $p = 0$, the minimization problem is said unconstrained. If $m = 0$ and $p \geq 0$, it is an equality constrained minimization problem and when $m \geq 0$ and $p = 0$, the problem is said an inequality constrained one.

An optimization problem expressed in the form (2.3) is convex when the objective and the inequality constraint functions are convex and the equality constraint functions are affine. The main property of a convex problem is that it has only one global optimum. For an unconstrained problem, the global optimum is obtained when the gradient of the objective function is null:

$$\nabla f_0(x) = 0$$

Convex sets and convex functions are defined as:

- **Convex sets**
  A convex set C contains line segment between any two points in the set.

$$\forall x_1, x_2 \in C, 0 \leq \theta \leq 1, \theta\, x_1 + (1 - \theta)\, x_2 \in C \tag{2.4}$$

- **Convex functions**
  A function $\mathbf{f} : R^n \rightarrow R$ is convex over a set domf if and only if domf is convex and for all $x, y \in$ domf and $0 \leq \theta \leq 1$, we have:

$$\mathbf{f}(\theta\, x + (1 - \theta)y) \leq \theta\, \mathbf{f}(x) + (1 - \theta)f(y) \tag{2.5}$$

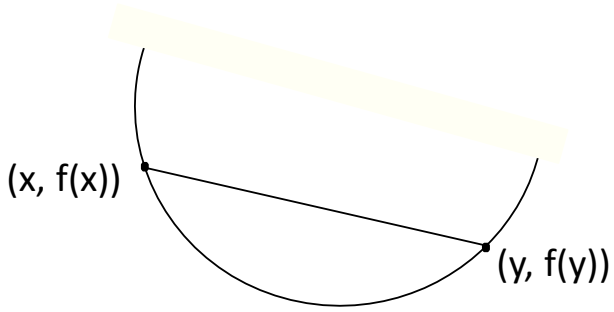

Figure 2.14: Convex function

If $\mathbf{f}$ is convex then $-f$ is concave. For example, on R, exponential functions are convex and logarithmic functions are concave. Affine functions can be considered convex and concave. Power function x^α on R_{++} is convex for $\alpha \geq 1$ or $\alpha \leq 0$. x^α on R_{++} is concave for $0 \leq \alpha \leq 1$.

In the next section, we explain the duality method used in the dissertation for optimization resolution.

2.7.2 Duality theory

We consider an optimization problem expressed in the form (2.3) and its non-empty domain $D = \bigcap_{i=0}^{m} \mathrm{dom} f_i \cap \bigcap_{i=0}^{p} \mathrm{dom} h_i$. This initial problem is called the primal problem. The associated Lagrangian $L : R^n \times R^m \times R^p \rightarrow R$ is expressed as follows:

$$L(\mathbf{x}, \lambda, v) = f_0(x) + \sum_{i=1}^{m} \lambda_i f_i(x) + \sum_{i=1}^{p} v_i h_i(x) \tag{2.6}$$

with $\mathrm{dom} L = D \times R^m \times R^p$, vectors λ and v are the dual variables or Lagrangian multiplier vectors associated to problem (2.3). λ_i is the Lagrangian multiplier associated with the i^{th} inequality constraint $f_i(x) \leq 0$ and v_i is the Lagrangian multiplier associated with the i^{th} equality constraint $h_i(x) = 0$.
The Lagrangian dual function $g : R^m \times R^p \rightarrow R$ is defined as the minimum value of the Lagrangian over $x \in D$, for $\lambda \in R^m$ and $v \in R^p$:

$$g(\lambda, v) = \min_D L(\mathbf{x}, \lambda, v) = \min_D \left(f_0(x) + \sum_{i=1}^{m} \lambda_i f_i(x) + \sum_{i=1}^{p} v_i h_i(x) \right) \tag{2.7}$$

Since the dual function is the minimum of a set of affine functions of (λ, v), it is always concave independently of the nature of the primal problem (2.3). Consequently, we can approximate the optimal value of the primal problem by solving the Lagrangian dual problem expressed as follows:

$$\begin{aligned} &\max_{\{\lambda, v\}} \; g(\lambda, v) \\ &\text{subject to} \;\; \lambda_i \geq 0 \;\; \forall i \in \{1, ..., m\} \end{aligned} \tag{2.8}$$

The problem (2.8) is a convex optimization problem. Its solution is a unique global optimal one. The solution (λ^*, v^*) are called optimal Lagrange multiplier or dual optimal multiplier. If $d^* = g(\lambda^*, v^*)$ is the optimal value of the dual problem and p^* is the optimal value of primal problem, we have the important inequality $d^* \leq p^*$. This inequality holds even the primal problem is convex or not. The difference $p^* - d^*$ is called the optimal duality gap of the original problem. When

p^* and d^* are infinite, the duality is considered weak and the primal problem is considered infeasible. However, if the duality gap is equal to zero, the duality is called strong, the optimal solution can then be found by solving the dual problem. To find the optimal solution for the primal or the dual problem, Karush Kuhn Tucker (KKT) conditions are generally used. If x^* and (λ^*, v^*) are respectively the primal and dual optimal points, for any optimization problem with differentiable objective and constraint functions and for which the strong duality is verified, optimal points must satisfy the KKT conditions as explained in equation (2.9). Optimization problem can be decomposed into multiple sub-problems in the dual space. Some constraints can also be relaxed. Dual decomposition is generally used when the optimization problem has coupling variables. Decomposition methods and their application are detailed in [36].

$$\begin{aligned} & f_i(x^*) \leq 0, \ \forall i \in \{1, ..., m\} \\ & h_i(x^*) = 0, \ \forall i \in \{1, ..., p\} \\ & \lambda_i^* \geq 0, \ \forall i \in \{1, ..., m\} \\ & \lambda_i^* f_i(x^*) = 0, \ \forall i \in \{1, ..., m\} \\ & \nabla f_0(x^*) + \sum_{i=1} \lambda_i^* \nabla f_i(x^*) + \sum_{i=1} v^* \nabla h_i(x^*) = 0 \end{aligned} \tag{2.9}$$

In this dissertation, optimization problems are used to solve resource allocation in chapters 5 and 6. The primal problems are non convex, some relaxations are made to formulate the resources allocation problems in a resolvable form. Then, dual Lagrangian method [37] and decomposition theory [38][39] are investigated to propose sub-optimal heuristics and to approach the optimal solution.

2.8 Conclusion

In this state of the art chapter, we have presented first OFDMA which is the multiple access method used throughout the thesis. Next, we have presented the channel model that will be used in all following chapters. The channel model has a pathloss with pathloss exponent equal to 3.76 and a log normal shadowing with standard deviation of 6 dB. Considering small-scale fading, independent Rayleigh gains are affecting each subcarrier. Coherence time of the channel is supposed to

be higher than OFDM symbol duration (Slow fading condition).
Inter-Cell Interference mitigation procedures have been presented with the FFR of LTE that will be used in the following chapters. Finally, some basic concepts on optimization problems have been presented and further used in chapters 5 and 6. Distributed resource allocation techniques will be studied in chapter 3 (single cell model) and 4 (multi-cell model). In chapter 4, cooperation between cells using interference indicators will be presented. Centralized resource allocation techniques are studied in chapter 5 with multiplexing mobile relays and SISO transmissions. MIMO systems are investigated in chapter 6.

Chapter 3

Resource Allocation in a single cell model

3.1 Introduction

In this chapter, we investigate the resource allocation problem for an uplink OFDMA multiuser system. We study resource allocation algorithms for comparison with as principal comparative features the throughput and the fairness between users. We focus on the Proportional Fairness (PF) approach which aims to maximize the system throughput while ensuring fairness between users. Then, we propose a Weighted Proportional Fair algorithm for resource allocation that introduces priorities between users to better exploit good channel conditions in the cell center. We also perform a theoretical analysis to compare both standard and weighted proportional fair algorithms. Simulation results, compared to existing algorithms, show that the proposed algorithm approaches the max sum rate upper bound but still maintains sufficient fairness between users.

3.2 State of the art

OFDMA technology is widely used in the context of resources allocation for wireless data systems for its multiple strengths since it offers the simplicity of the

receiver and avoids complicate equalizers [40]. In the literature, resource allocation in OFDMA systems is discussed by a large number of authors for both downlink and uplink. Resource allocation consists in subcarrier and power allocations which can be performed statically or dynamically [41]. Moreover, utility functions are used to measure users satisfaction depending on the goal to reach. In [42] the same authors present several resource allocation algorithms. Mathematical formulations for the resource allocation problems are derived in [43] with several objectives and constraints. Actually, the system is totally unfair if it aims to maximize the system throughput. Some kind of fairness can be introduced in terms of allocated subcarriers or in terms of user rates with the Max-Min fairness criterion [44]. Resource allocation problems can also be formulated with game theory. In that case, the resolution is to achieve a Nash Bargaining [5]. Furthermore, PF algorithms are used to guarantee a tradeoff between throughput and fairness by considering previous allocations and can be improved by adding users priorities.

3.2.1 Utility functions

Resource allocation for wireless networks is based on efficiency and fairness as principal features. Spectral efficiency is estimated by the system throughput that can be unfair especially for users with bad channel conditions or cell edge users. On the other hand, ensuring absolute fairness leads to low bandwidth efficiency. Consequently, a tradeoff between efficiency and fairness is necessary for resource allocation in wireless systems. In this context, utility theory [45] has been introduced as an important concept by the economists to estimate the benefits from using some resources and to measure user satisfaction. Moreover, utility functions are used in communication networks to evaluate the system behavior depending on quality of service requirements. Utility functions considering flow control and routing are introduced for wireline networks. In fact, an utility function is defined as an increasing function of the throughput, it may consider some other measurements to better evaluate users satisfaction [45] such as waiting delays or queuing sizes [40]. Theoretical analysis for different utility functions are given in [46], especially for Max-Min fairness and Proportional Fairness.

3.2.2 Existing algorithm for Resource Allocation

In this section, the most used resource allocation algorithms are presented. We differentiate the efficiency of them by considering two principal features: the throughput and the fairness.

- **Max Sum Rate**
  The sum rate maximization consists in maximizing the sum of users' throughput without considering the rate of each user separately. In this case, users with good channel conditions thus those near to the BS are advantaged and earn all subcarriers. Consequently, users remote to the BS are totally ignored. Allocation with the max sum rate maximize the system throughput but the majority of users have a rate equal to zero. This allocation is then totally unfair. The corresponding utility function in this case is simply the user rate. With K users, the system objective is to maximize the total system utility as follows:

$$\text{maximize} \sum_{k=1}^{K} R_k$$

- **Max Min**
  The system with the Max Min criteria aims to ensure a minimal rate per user. Contrary to the Max Sum Rate described above, this method favors users with bad channel condition to earn a high number of subcarriers to achieve the required data rate. The total system throughput decreases comparing to the previous allocation but the local user throughput increases [3]. The max min allocation is considered totally fair. The utility function for the max min algorithm is still the data rate. The difference with the previous algorithm is that the system objective has to respect a required minimal data rate constraint per user as follows:

$$\text{maximize} \sum_{k=1}^{K} R_k$$
$$\text{subject to } R_k \geq R_t \ \forall k$$

  where R_t is the required target data rate per user.

- **Proportional Fair**
  The Proportional Fair allocation is a resource allocation method which considers both throughput and fairness. It therefore allows maximizing the total throughput of the system without ignoring users with bad channel conditions. In [4], the proportional fairness is defined as: a feasible rate vector $R^m = (R^m_1, R^m_2, ..., R^m_K)$ is proportional fair if for any other feasible rate vector R^{m*}, the aggregate of proportional changes is negative:

$$\sum_{k=1}^{K} \frac{R^{m*}_k - R^m_k}{R^m_k} \leq 0$$

  Where R^m_k is the cumulative rate of user k at the end of the m^{th} TTI.
  The proportional fair algorithm considers a period of time, it can be unfair at a considered TTI but after m TTIs, all users are served considering a proportional fair manner. If the instantaneous rate is considered for the PF algorithm, the natural logarithm function is considered as a utility function. The system objective can the be expressed as:

$$\text{maximize} \sum_{k=1}^{K} \log(R_k)$$

3.3 Chapter Structure

In this chapter, we focus on the PF algorithm and we propose a weight depending on the average SNR experienced by users to improve the classical PF allocation. Such weights in our proposed algorithm favor users with good channel conditions but still maintains proportional fairness. In fact, adjusting the number of allocated subcarriers according to channel conditions offers a higher system throughput and proportional fairness criterion keeps fairness between users.
This chapter is organized as follows: section 3.4 describes the system model and defines some essential used concepts, section 3.5 presents the proposed algorithm for Weighted PF resource allocation and offers a theoretical analysis comparing standard PF and WPF and section 3.6 depicts simulation results. Finally, section 3.7 concludes the chapter.

3.4 System Model

We consider an uplink OFDMA transmission system in a single cell system model with one BS, K users and N subcarriers. We assume that the channel is a frequency-selective Rayleigh fading channel with slow fading and the noise is AWGN. We also assume that the subcarriers are not shared by different users and each subcarrier has a bandwith Δf. Users have an uniform distribution in the cell and each user k experiences a pathloss L_k and a shadowing S_k with log-normal distribution. The channel gain coefficients for a user k and a subcarrier **j** at TTI m can be expressed as:

$$\gamma_{k,j}^{m} = \frac{g_{k,j}^{m}}{L_k S_k \Delta f N_0} \tag{3.1}$$

Where $g_{k,j}^{m}$ is the square Rayleigh fading between user k and the BS in subcarrier **j** and N_0 is the noise power density. With a maximum power P_k for user k, the total throughput in bits/s of this user is given by:

$$R_k^m = \Delta f \sum_{j=1}^{k,j} R^m = \Delta f \sum_{j=1}^{k,j} a^m \log_2 (1 + \gamma^m P^m) \tag{3.2}$$

Where $P_{k,j}^{m}$ is the power allocated in subcarrier j. $a_{k,j}^{m}$ is a boolean variable which equals 1 if the subcarrier **j** is assigned to user k, 0 otherwise. We assume that pathloss, shadowing and $g_{k,j}^{m}$ do not vary during the considered time frame.
In this chapter, the PF algorithm is studied and improved. In the next section, the proposed algorithm Weighted PF is presented and compared to the classical PF one.

3.5 Proposed Weighted PF

In this section, we explain the principle of our proposed WPF algorithm. Then, we perform a theoretical analysis for both PF and WPF to compare the behavior of each method.

3.5.1 Principle

Although the PF algorithm provides fairness between users, it can be improved by priorities depending on the users positions in the cell. Actually, it may be better for users with unfavorable channel conditions to acquire a smaller number of subcarriers to avoid wasting power. Users in the cell center can then take advantage by having more subcarriers and increase the network throughput. To exploit good channel conditions more efficiently in the cell center, we introduce in this chapter a weighted PF algorithm. We propose a weight expression depending essentially on the average SNR of the users. The proposed weight will be included in the utility expression and will allow cell center users to earn more subcarriers than cell edge users. The incremental utility for a user k and subcarrier **j** at time m can then be expressed as [5]:

$$U^{m}_{k,j} = \frac{R^{m}_{k,j}}{R^{m-1}_{k} + \sum_{i \in S^{m}_{sub,k}} R^{m}_{k,i}} [w_k]^{\beta} \tag{3.3}$$

and

$$w_k = \Delta f \log_2 \left(1 + \frac{\frac{P_k}{N}}{L_k S_k N_0 \Delta f}\right) \tag{3.4}$$

Where $S^{m}_{sub,k}$ is the set of subcarriers assigned to user k at the current m and R^{m}_{k} the cumulative rate for user k until TTI m. w_k is the weight of user k and traduces the average data rate per user per subcarrier. $\beta \in [0;1]$, setting $\beta = 0$ we find the standard PF. Subcarrier **j** is then allocated to the user with the highest incremental utility:

$$k^{*} = \arg\max_{k} U^{m}_{k,j} \tag{3.5}$$

After all subcarriers have been allocated in the cell, the power is equally assigned to each users subcarriers. With $|S^{m}_{sub,k}|$ the cardinal of $S^{m}_{sub,k}$, $P^{m}_{k,j} = \frac{P_k}{|S^{m}_{sub,k}|} \; \forall j \in S^{m}_{sub,k}$, 0 otherwise. The rate is finally calculated with equation (3.2).

3.5.2 Theoretical Analysis

In this section, we study theoretically the behavior of the PF and the WPF to proof the influence of the weight introduced in the WPF. To demonstrate that users in the cell center have more chances to earn subcarriers than the cell border

users, we perform a theoretical analysis at the first TTI (m = 1) with 2 users and N subcarriers. To simplify notations, we set $\gamma_{k,j} = \alpha_k.g_{k,j}$ in (equation (3.1)). We assume that user 1 is near to the BS and user 2 is at the cell border, therefore $\alpha_1 >> \alpha_2$ and that $P_1 = P_2 = P$. We consider both standard Proportional Fair ($\beta = 0$) and Weighted PF ($\beta \neq 0$) algorithms for comparison. $_k$ is set to R^0
$\varrho << 1 \ \forall k \in \{1,2\}$.
In the following, to simplify notations, we have dropped the time index m.

3.5.2.1 Standard PF algorithm

Here, we use the proposed algorithm but considering the incremental utility (equation (3.3)) without the weigth $[w_k]^\beta$ to analyse the traditional PF (or with $\beta = 0$).

- For the subcarrier **j** = 1

$$U_{k,1} = \frac{\Delta f \ \log_2(1 + \alpha_k g_{k,1} P)}{R_k^0}; \ \forall k \in \{1,2\}$$

$U_{1,1} > U_{2,1}$ with probability close to 1 because $\alpha_1 >> \alpha_2$, thus subcarrier **j** = 1 is allocated to user 1 with probability close to 1.

- For the subcarrier **j** = 2

$$U_{1,2} = \frac{\Delta f \ \log_2(1 + \alpha_1 g_{1,2} \frac{P}{2})}{R^0_{\ 1} + \Delta f \ \log_2(1 + \alpha_1 g_{1,1} \frac{P}{2})};$$

$$U_{2,2} = \frac{\Delta f \ \log_2(1 + \alpha_2 g_{2,2} P)}{R_2^0}$$

Since $R_k^0 = \varrho << 1$, $U_{2,2} > U_{1,2}$ then subcarrier **j** = 2 is allocated to user 2 with probability close to 1.

In the general case, the utility for user $k \in \{1,2\}$ and subcarrier **j** is expressed as:

$$U_{k,j} = \frac{\Delta f \ \log_2(1 + \alpha_k g_{k,j} \frac{P}{N_k})}{R_k^0 + \Delta f \ \sum_{i \in S_{sub,k}} \log_2(1 + \alpha_k g_{k,i} \frac{P}{N_k})};$$

$N_k - 1$ is the number of subcarriers already allocated to user k.

- If the two users have the same number of subcarriers,

Comparing the two utilities is equivalent to compare two random variables

X_1 and Y_1 with the same probability distribution. $Pr(X_1 > Y_1) = 0.5$ and the current **j** is then randomly allocated.

Proof:

By neglecting $R_k^0 = \varrho << 1$, we have:

$Pr(U_{1,j} > U_{2,j}) = Pr(X_1 > Y_1)$ with:

$$X_1 = \sum_{i' \in S_{sub,2}} \log_2\left(1 + \alpha_1 g_{1,j} \frac{P}{N_1}\right) \quad \log_2\left(1 + \alpha_2 g_{2,i'} \frac{P}{N_2}\right)$$

$$Y_1 = \sum_{i \in S_{sub,1}} \log_2\left(1 + \alpha_2 g_{2,j} \frac{P}{N_2}\right) \quad \log_2\left(1 + \alpha_1 g_{1,i} \frac{P}{N_1}\right)$$

$N_1 = |S_{sub,1}|$ and $N_2 = |S_{sub,2}|$. $S_{sub,1}$ and $S_{sub,2}$ have the same number of elements, then, X_1 and Y_1 are two independent random variables with the same Cumulative distribution function $F_{X1}(x)$ and the same Probability density function $p_{X1}(x)$.

Using:

$$Pr\left(\frac{X}{Y} \le \gamma_{th}\right) = \int_0^\infty F_X(\gamma_{th} y)\, p_Y(y)\, dy \tag{3.6}$$

We have:

$$\begin{aligned} Pr(U_{1,j} > U_{2,j}) &= Pr(X_1 > Y_1) \\ &= \int_0^\infty F_{Y1}(y)\, p_{X1}(y)\, dy \\ &= \int_0^\infty F_{X1}(y)\, p_{Y1}(y)\, dy \\ &= Pr(U_{2,j} > U_{1,j}) \end{aligned}$$

Consequently: $Pr(U_{1,j} > U_{2,j}) = 0.5$

- If user 1 has more subcarriers than user 2,

$$Pr(U_{1,j} > U_{2,j}) = Pr(X_1 > Y_1 + Z_1)$$

With $Z_1 > 0$ and X_1 and Y_1 defined as before.

Consequently, $Pr(U_{1,j} > U_{2,j}) < 0.5$ and user 2 has more chances to earn the subcarrier j.

To sum up, the classical PF assigns subcarriers to users sorted by pathloss considering mainly the number of previously allocated subcarriers. With this allocation method, all users eventually have nearly the same number of sucarriers. However, reducing the number of subcarriers at the cell border region will improve system throughput which is the behavior of our proposed algorithm.

3.5.2.2 Weigthed PF

As with classical PF, **j** = 1 is allocated to user 1 and **j** = 2 is allocated to user 2 with probability close to 1.

- **j** > 2, $\forall k \in \{1, 2\}$:

$$U_{k,j} = \frac{\Delta f \ \log_2(1 + \alpha_k g_{k,j} \frac{P}{N_k})}{R_k^0 + \Delta f \sum_{i \in S_{sub,k}} \log_2(1 + \alpha_k g_{k,i} \frac{P}{N_k})} [w_k]^\beta ;$$

If $N_k - 1$ is the number of subcarriers already allocated to user k, $Pr(U_{1,j} > U_{2,j})$ can be expressed as $Pr(X_2 > Y_2)$ with:

$$X_2 = \left(\frac{w_1}{w_2}\right)^\beta B \quad \text{and} \quad Y_2 = A$$

$$B = \sum_{i' \in S_{sub,2}} \log_2\left(1 + \alpha_1 g_{1,j} \frac{P}{N_1}\right) \log_2\left(1 + \alpha_2 g_{2,i'} \frac{P}{N_2}\right) \tag{3.7}$$

$$A = \sum_{i \in S_{sub,1}} \log_2\left(1 + \alpha_2 g_{2,j} \frac{P}{N_2}\right) \log_2\left(1 + \alpha_1 g_{1,i} \frac{P}{N_1}\right) \tag{3.8}$$

$$Pr(U_{1,j} > U_{2,j}) = Pr\left(\left(\frac{w_1}{w_2}\right)^\beta B - A > 0\right)$$
$$= Pr(C > 0)$$

Where again we have neglected $R_k^0 = \varrho << 1$.
We have to express the probability distributions of A and B to evaluate the probability distribution of C.
We assume that we are in high SNR and we use the approximation $\log_2(1 + a) \approx \log_2(a)$, then:

$X = \log_2(\alpha_1 g_{1,j} P)$ follows a distribution $L_X(\mu_1, {\sigma_1}^2)$ with mean μ_1 and variance ${\sigma_1}^2$. Similarly:

$$Y = \log_2(\alpha_2 g_{2,j} P) \sim L_Y(\mu_2, {\sigma_2}^2)$$

$$Z = \log_2(\alpha_1 g_{1,j} P)\log_2(\alpha_2 g_{2,j} P) \sim L_Z(\mu_3, {\sigma_3}^2)$$

As $g_{1,j}$ and $g_{2,j}$ are independent, X and Y are independent which implies: $E[X.Y] = E[X].E[Y]$ and

$$\begin{aligned} var(X.Y) = var(X)var(Y) + var(X)[E(Y)]^2 \\ + var(Y)[E(X)]^2 \end{aligned}$$

we have:

$$\begin{aligned} &\mu_3 = \mu_1 \mu_2; \\ &{\sigma_3}^2 = {\sigma_1}^2 {\sigma_2}^2 + {\sigma_1}^2 \mu_2^2 + {\sigma_2}^2 \mu_1^2 \end{aligned}$$

Applying the central limit theorem [47], A and B follow normal distributions with means μ_A and μ_B and variances ${\sigma_A}^2$ and ${\sigma_B}^2$ expressed as:

$$\begin{aligned} &\mu_A = N_1 \mu_0 \\ &\mu_B = N_2 \mu_0 \end{aligned}$$

$$\text{where } \mu_0 = \mu_3 - \mu_2 \log_2(N_1) - \mu_1 \log_2(N_2) + \log_2(N_1)\log_2(N_2) \qquad (3.9)$$

Where:

$$\begin{aligned} \frac{{\sigma_A}^2}{N_1} &= {\sigma_1}^2 {\sigma_2}^2 + N_1 {\sigma_2}^2 {\mu_1}^2 - 2N_1 \mu_1 {\sigma_2}^2 \log_2(N_1) + N_1 {\sigma_2}^2 \log_2(N_1)^2 \\ &+ {\sigma_1}^2 {\mu_2}^2 - 2\mu_2 {\sigma_1}^2 \log_2(N_2) + {\sigma_1}^2 \log_2(N_2)^2 \qquad (3.10) \\ \frac{{\sigma_B}^2}{N_2} &= {\sigma_1}^2 {\sigma_2}^2 + {\sigma_2}^2 {\mu_1}^2 - 2\mu_1 {\sigma_2}^2 \log_2(N_1) + {\sigma_2}^2 \log_2(N_1)^2 \\ &+ N_2 {\sigma_1}^2 {\mu_2}^2 - 2N_2 \mu_2 {\sigma_1}^2 \log_2(N_2) + N_2 {\sigma_1}^2 \log_2(N_2)^2 \qquad (3.11) \end{aligned}$$

The computation of these equations is detailed in appendix A.

Finally, the random variable C follows then a normal distribution with mean

μ_C and variance σ_C^2 calculated as:

$$\mu_C = \left(\frac{w_1}{w_2}\right)^{\beta} N_2\mu_0 - N_1\mu_0 \tag{3.12}$$

$$\sigma_C{}^2 = \left(\frac{w_1}{w_2}\right)^{2\beta} N_2\sigma_B{}^2 + N_1\sigma_A{}^2 \tag{3.13}$$

Consequently:

$$\begin{aligned} Pr(U_{1,j} > U_{2,j}) &= Pr(C > 0) \\ &= \int_0^{\infty} \frac{1}{\sigma_C\sqrt{2\pi}} \exp\left(-\frac{(x-\mu_C)^2}{2\sigma_C{}^2}\right) dx \\ &= Q\left(-\frac{\mu_C}{\sigma_C}\right) \end{aligned} \tag{3.14}$$

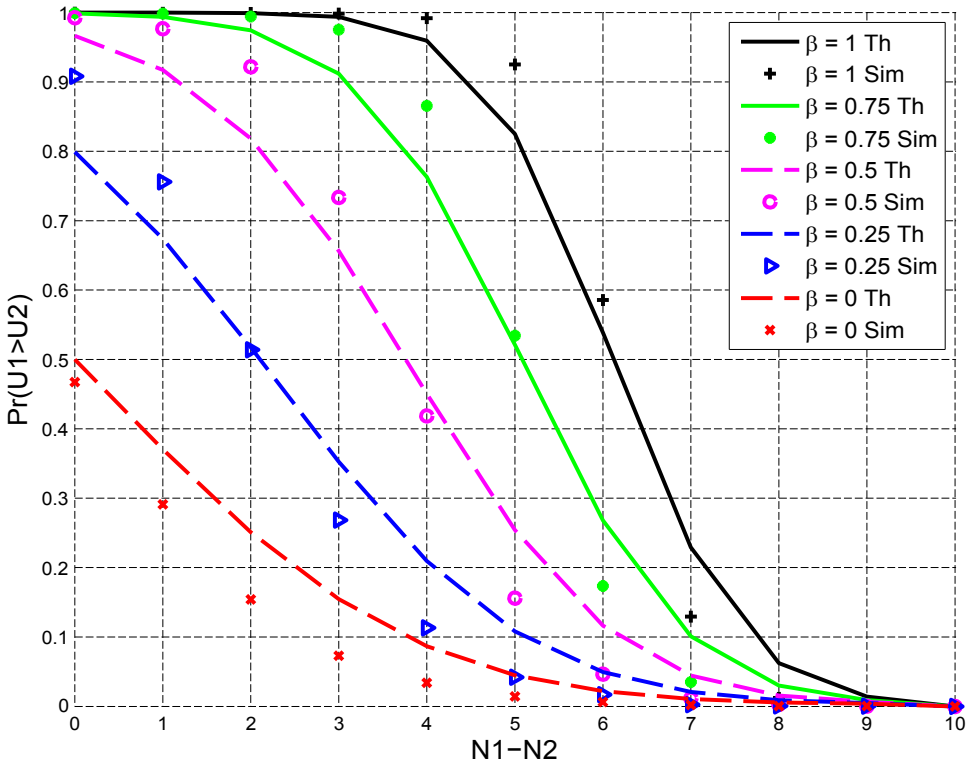

Figure 3.1: Probability $Pr(U_1 > U_2)$, $N_1 = 10$

The behavior of the WPF algorithm is tested to verify that it matches with equation (3.14). Simulations are made to compare the WPF to the equation (3.14). Figure 3.1 shows the probability that user 1 acquires the discussed subcarrier **j**

with theoretical expression (equation (3.14)) (Th) and simulations (Sim) when $N_1 = 10$. To calculate theoretical results, we evaluate μ_1, μ_2, σ_1^2 and σ_2^2 by simulation. We can remark that theoretical results are more closed to simulations for $\beta = 1$, this is due to the high value of N_1.
With $\beta = 0$, we find the standard PF algorithm and for $N_1 = N_2$, as proved in the previous section, the two users have the same chances to obtain the next subcarrier: $Pr(U_1 > U_2) = 0.5$. Moroever, when β increases, the fairness decreases and user 1 earns a higher number of subcarriers. We can see for example for $\beta = 1$, user 1 is favored to get subcarriers with $Pr(U_1 > U_2) \cong 1$ until $N_1 - N_2 = 6$. Only at this moment user 2 can win the next subcarrier in 50% of cases. Then, for $N_1 - N_2 \rangle 7$, the next subcarrier is certainly allocated to user 2. Figure 3.1 shows also that the necessary difference $N_1 - N_2$ corresponding to $Pr(U_1 > U_2) = 0.5$ grows with β. For different values of N_1, table 3.1 shows the minimum difference $N_1 - N_2$ to have the same chances for the two users to acquire the discussed subcarrier:

	$N_1 - N_2$ **for**			
N_1	$\beta = 0.25$	$\beta = 0.5$	$\beta = 0.75$	$\beta = 1$
$N_1 = 5$	1	1	2	3
$N_1 = 10$	2	3	5	6
$N_1 = 15$	3	5	7	9
$N_1 = 20$	4	7	10	12

Table 3.1: $N_1 - N_2$ for $Pr(U_1 > U_2) = 0.5$

3.6 Performance Evaluation

In the simulations, we consider a circular cell with radius of 0.5 km. We assume a total bandwith B = 1.4 MHz, K = 20 users uniformly distributed and N = 72 subcarriers. The bandwith per subcarrier is $\Delta f = 15$ KHz. We consider Rayleigh channels with Slow Fading and AWGN noise with power density $N_0 = -174$ dBm/Hz . The Shadowing has a log-normal distribution with standard deviation 6 dB and the Pathloss is considered according to the LTE model with frequency F = 2.6 GHz: $L_{k,dB}(d_k) = 128.1 + 37.6 \log_{10}(d_k)$ where d_k is the distance in km of user k from the BS.

We consider 100 TTIs for the WPF algorithm. 500 simulations are made and averaged to have the results in the figures below. To compare with existing algorithms, we denote by:

- **MaxSumRate:** The algorithm that aims to maximize the total system throughput.
- **WeightedPF:** Our proposed algorithm Weighted Proportional Fairness with different values of β.
- **PF:** The standard PF or the WPF for $\beta = 0$.
- **SameNbreSc:** The algorithm which assigns the same number of subcarriers to all users.
- **MaxMin:** The algorithm that aims to achieve a minimal throughput per user.

3.6.1 throughput

Figure 3.2 shows the average system throughput for low and high transmit powers. The **MaxSumRate** algorithm is obviously the upper bound for system throughput. Then, by favoring cell border users, the **MaxMin** algorithm has the lowest system throughput. Simulation results confirm that the **PF** algorithm assigns nearly the same number of subcarriers for all users. If we do not consider the **MaxSumRate** which is completely unfair, our proposed **WeightedPF** algorithm has the best throughput. In addition to its proportional fairness, the figure shows that the proposed algorithm offers high throughput near to the upper bound especially for low transmit powers. Compared to the standard PF, the relative gain of the WPF grows with β. For $\beta = 0.5$, this gains varies from 4% to 24% and for $\beta = 1$, it counts 7% until 29%.

Figure 3.3 shows the average throughput depending on the positions of users. We note that the throughput at cell border is almost the same for **PF**, **SameNbreSc** and **WeightedPF** algorithms. It is slightly higher for the **MaxMin** thanks to the high number of subcarriers assigned in this region which disadvantages users in the cell center and consequently the total system throughput as shown in Fig

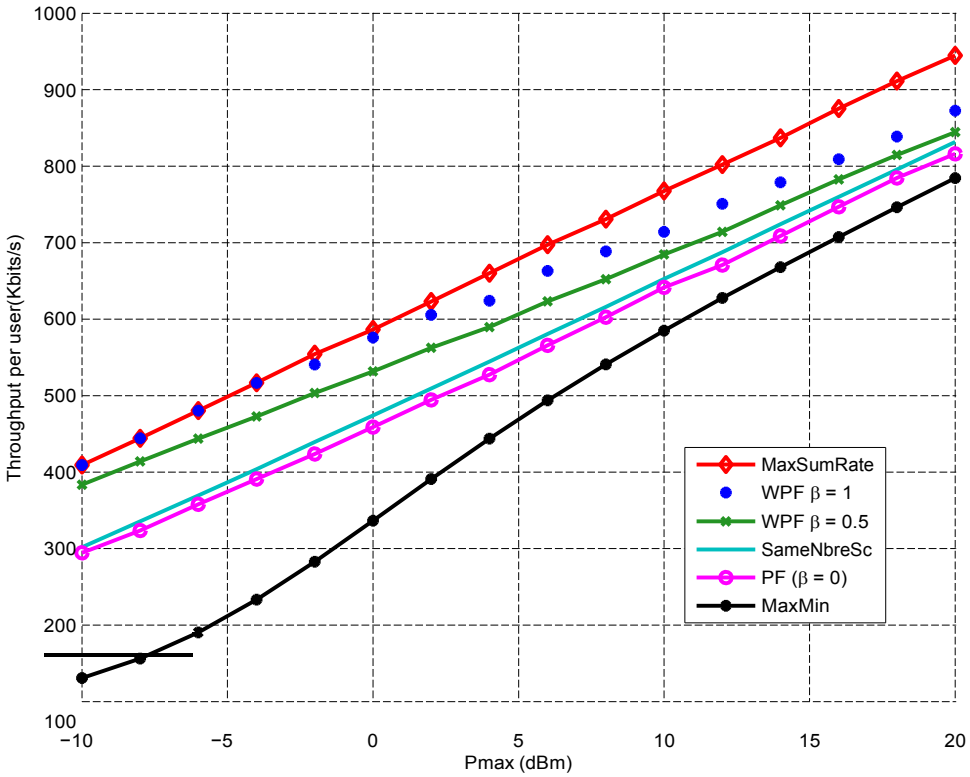

Figure 3.2: System Throughput

3.2. Moreover, we have not traced the **MaxSumRate** algorithm for a better readability of the figure, it is clearly unfair in favoring users in the cell center (20000 Kbits/s for d = 0.02 Km) and in ignoring users in the border cell (0 Kbits/s for d > 0.36 Km).

3.6.2 fairness

To evaluate the fairness of our algorithm, we adopt the Fairness Index (FI) [13], The algorithm is more fair when its FI approaches 1:

$$FI = \left(\sum_{k=1}^{K} R_k \right)^2 / K \sum_{k=1}^{K} R_k^2 \qquad (3.15)$$

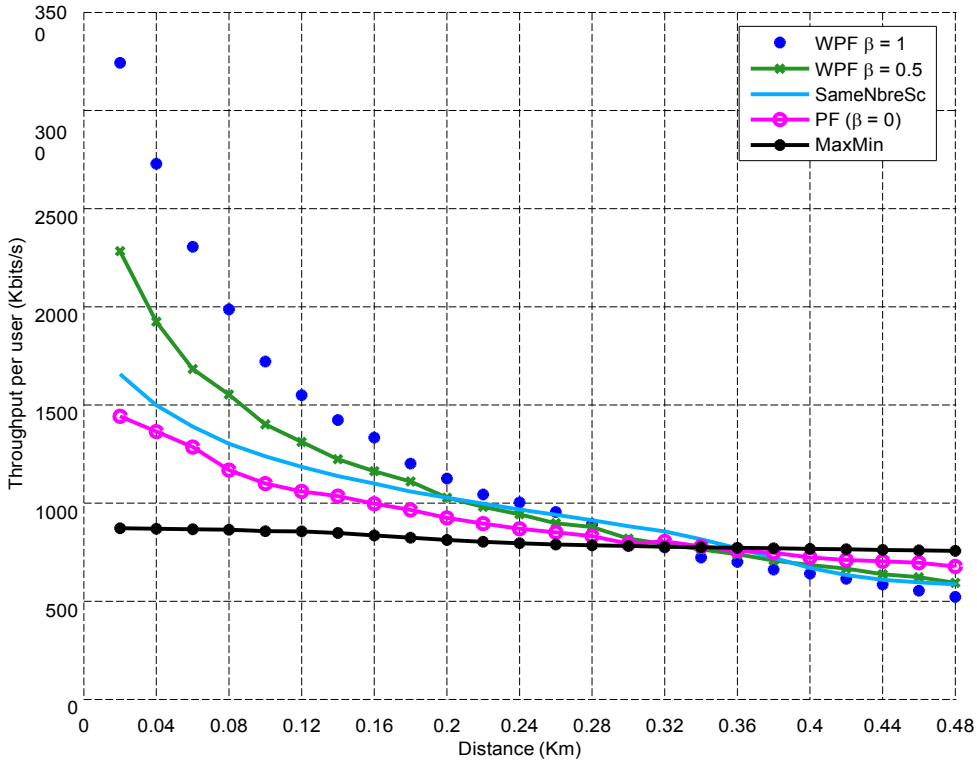

Figure 3.3: Rate versus Distance when P = 21 dBm

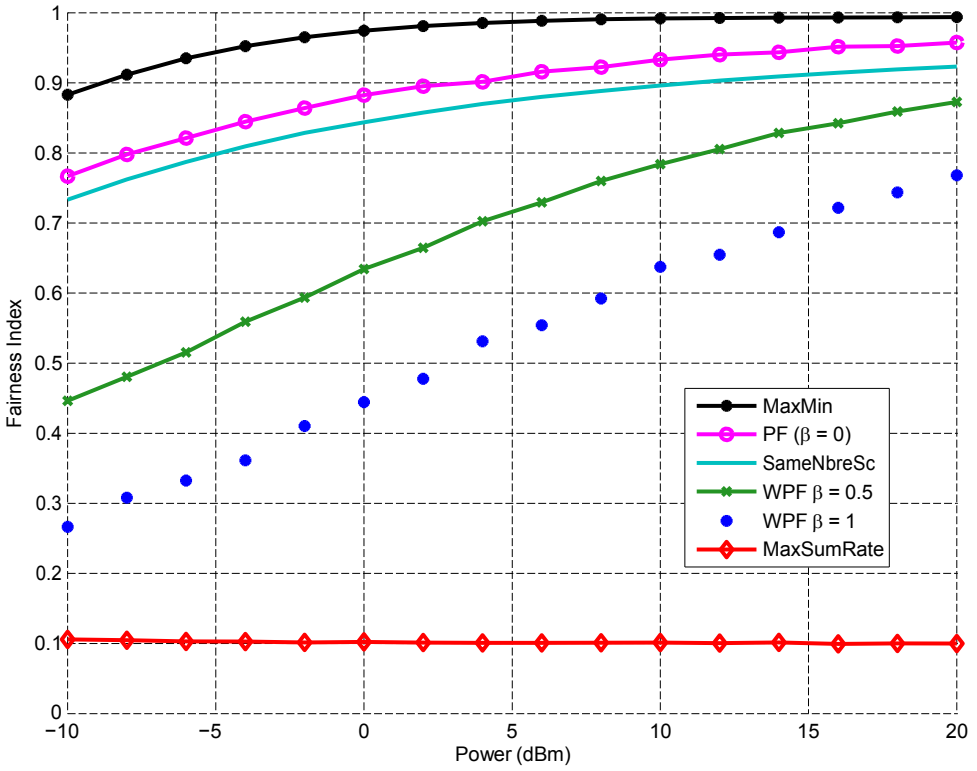

Figure 3.4: Fairness Index

Figure 3.4 shows the fairness indexes for the different algorithms. We can perceive that the **MaxSumRate** algorithm is totally unfair, the **MaxMin** is the upper bound for fairness indexes and the **WeightedPF** algorithm achieves 87% of fairness for $\beta = 0.5$ and 77% for $\beta = 1$ for high transmit power values. Compared with the standard **PF** algorithm, the proposed **WeightedPF** algorithm loses some fairness but with Figure 3.3, we can remark that users at cell border loose only 15 % of their throughput when users in the cell center earn up to 45 % of their throughput.

3.6.3 Influence of β

The WPF offers a tradeoff between throughput and fairness and depending on the quality of service requirements, β can be adjusted. For different values of $\beta \in [0;1]$ and for $P = 21$ dBm, table 3.2 shows the corresponding throughputs and fairness indexes. P is chosen as the maximum transmit power of a mobile terminal according to the 4G cellular network characteristics [14].

β	0.1	0.2	0.3	0.4	0.5
Throughput (Kbits/s)	838.3	853.8	856.3	863	867.5
Fairness Index	0.94	0.93	0.91	0.89	0.87
β	0.6	0.7	0.8	0.9	1
Throughput (Kbits/s)	869	877	876.5	886.2	890.8
Fairness Index	0.86	0.83	0.82	0.79	0.76

Table 3.2: Throughput and Fairness Indexes for $\beta \in [0;1]$

3.7 Conclusion

In this chapter, we studied the most used resources allocation algorithms and focused on Proportional Fairness allocation. Then, we proposed a Weighted Proportional Fair algorithm to improve total system throughput with a low decrease of the system fairness. To compare the behavior of the proposed algorithm to the classical PF one, a theoretical analysis was performed. In fact, the PF algorithm assigns nearly the same number of subcarriers for all users ordered by pathloss. The proposed WPF aims to assign more subcarriers in the cell center than in the

cell border to exploit good channel conditions while keeping sufficient fairness between users.

A theoretical analysis and simulation results have shown that the proposed algorithm achieves a high system throughput near to the totally unfair upper bound. It also provides interesting values of the fairness index especially for high transmit power.

The proposed WPF criterion can be easily implemented in wireless networks and the β parameter can be adapted to the QoS requirements either statically or dynamically. In addition, decreasing the number of subcarriers assigned to users in the cell edge can reduce the inter-cell interference (ICI) in a multi-cell context. A such muti-cell system model will be studied in the next chapter.

Chapter 4

Resource Allocation in a multi-cell system model

4.1 Introduction

In this chapter, the resource allocation in a multi-cell system model is studied. The challenge is to have high system performance in such systems where the ICI can be important. Dividing the users in two areas per cell, cell center and cell edge as adopted in the LTE standard, we reduce the ICI by two different manners. First, the weighted proportional fair proposed in the previous chapter is applied in the multi-cell system. The system performances are compared to the classical Fractional Frequency Reuse (FFR) used by LTE considering theoretical expressions and simulations. Both throughput and fairness features are considered for comparison. Then, BS cooperation based on the interference indicators is investigated to reduce ICI. For this purpose, we present a novel Enhanced Interference Indicator (EII) for each subcarrier per cell to indicate its interference level. BSs cooperate by exchanging the EII table and try to assign subcarriers in a manner that avoids high ICI. The EII values are studied to efficiently estimate ICI levels per subcarrier to reduce interference in the cell edge without complex cooperation

between BSs. The resource allocation is then performed according to the PF criterion considering the EII as the interference estimation. Simulation results show that with low cost BSs communication, the EII improves the system performances. We also study the system fairness and show that the use of EII does not affect it.

4.2 State of the art

For multi-cell systems, users in the neighboring cells that are transmitting in the same frequency at the same time cause the ICI which deteriorates the system performance. To mitigate the ICI, several approaches exist in the literature. Many interference avoidance techniques are proposed but the most common approach is to use the FFR. In [48], the authors offer a probabilistic method to avoid interference by shutting down the subcarriers having a high level of interference. With the FFR pattern, the use of the same subcarriers in the adjacent cells can be avoided to eliminate interference especially in the cell border. We can find static and dynamic reuse schemes with different level of complexity. In general, static reuse schemes using FFR are adopted for mobile networks where the users are divided into two areas: the cell center and the cell border. For all the system cells, the same subset of subcarriers is used in the center area, however, different subsets of subcarriers are used in the border areas. The interference is lowered in the border cells which improves the system performance but the total resources are divided according to the adopted FFR scheme. New interference avoidance algorithms are proposed in [31] using Fractional Time Reuse (FTR) and Fractional Time and Frequency Reuse (FTFR). In [6], the author aims to find the optimal FFR to use in the cell border and to determine the resources to allocate in each area. We can also find cooperative models where the base stations communicate to avoid the interference effect [8][9]. In addition to the FFR models, the resource allocation can be performed depending on the system objective. The resource allocation algorithm is applied independently in each cell area considering the ICI. A dynamic FFR algorithm based on PF allocation is proposed in [49] to assign subcarriers in each cell area and to keep fairness between users.
Moreover, for BSs cooperation, multiple strategies are studied [7]. BSs may cooperate through wireless communication, which can generate heavy signaling load and decrease the system data rate. BSs may also communicate through backhaul

links, then the exchanged information do not affect the system performance. In [33], each BS communicates only with its adjacent cells with both unidirectional and bidirectional backhaul links to reduce communication cost. In [50], an iterative scheme is introduced where BSs exchange decoded messages iteratively to eliminate ICI. The uplink interference cancellation method is also presented in [34] where Base Station Controller (BC) collects information from BSs through the network to benefit of the 'unlimited' capacity of the backbone network comparing to the wireless air interface and aim at eliminating ICI.
BSs cooperation may lead to higher system performance compared to systems without cooperation but requires heavy communication between BSs. To benefit from the BS communication without high cost, the LTE standard [21] proposes different defined interference indicators to exchange through X2 interface. First, the reactive Overload Indicator (OI) [2] uses three levels (low, medium or high) to measure the interference. The BS can change its allocation according to the received indicators. Then, the proactive High Interference Indicator (HII) [2] that represented by a boolean value, indicates if a resource block is considered interfered or not. Using the HII, each BS communicates the resource blocks assigned in the cell edge. The standard does not specify explicitely how a BS should react to HII but the best reaction is that this BS avoids scheduling resources with high HII in the cell edge.

4.3 Chapter's Structure

In this chapter, the resource allocation for a multi-cell system model is studied. The challenge is to have high system performance in a such systems where the ICI can be important.
In the first part of this chapter (section 4.4), we apply the weighted proportional fair in a multi-cell context. In the previous chapter and in[51], we introduced the WPF algorithm in a single cell model and provided a theoretical analysis showing the gain performed comparing to the classical PF allocation. We aim in this chapter to enlarge our study and apply the WPF algorithm in a multi-cell system. In this scheme, the ICI can be reduced by favoring the users in the cell centers thanks to the user weights. To reduce the ICI and to maintain fairness in the system,

the user weights are adapted and the system performance is improved comparing to the classical FFR model. In section 4.4.1, the system model is presented. The proposed scheme is described in section 4.4.2. The system performance evaluation is made in section 4.4.3 and section 4.4.4 depicts simulation results.
The second part of this chapter (section 4.5) considers cooperation between BSs using the interference indicators. For this, we focus on a proactive indicator that each BS communicates to its neighboring cells to avoid high ICI in the uplink without increase of complexity. For this purpose, we propose a novel Enhanced Interference Indicator (EII) operating as the HII but with integer values, to evaluate interference levels more accurately. The cell edge in our scheme is divided in several sectors and a EII value corresponding to a given subcarrier depends on the sector in which the subcarrier is assigned in the neighboring cells. Considering the EII values from its neighboring cells, a BS assigns subcarriers to users with the aim to generate as low ICI as possible. The system performance can thus be improved without high amount of communication between BSs. The section 4.5 is organized as follows: 4.5.1 presents the adopted multi-cell system model, section 4.5.2 describes the proposed EII, explains in details how to use it and details the used allocation algorithm. Then, section 4.5.3 depicts the simulation results that compare the allocation process with the proposed EII, with the standard HII and without interference indicator at all.

4.4 Weighted PF for MultiCell System Model

In this section, the WPF algorithm introduced in the previous chapter is applied in a multi-cell system model considering the ICI.

4.4.1 System model

We consider an uplink multi-cell OFDMA transmission system with C cells. In each cell, we have one BS with an omnidirectional antenna, K users and N subcarriers. The users in a cell have an uniform distribution and each user k in a cell c experiences a pathloss $L_{k,c}$ and a shadowing $S_{k,c}$ with log-normal distribution. We also consider that a subcarrier has a bandwith Δf and is exclusively allocated

to one user per cell. The channel is assumed a frequency-selective Rayleigh fading channel with slow fading and the noise is AWGN. The channel gain coefficients for a user k and a subcarrier **j** in a cell c at TTI m can be expressed as shown in equation (4.1). We note by channel gain coefficients the Rayleigh gains divided by the product of pathloss, shadowing and the sum of the noise and the interference.

$$\gamma^{m}_{k,j,c} = \frac{g^{m}_{k,j,c}}{L^{k,c} S_{k,c} (N_{sc} + I_{j,c})} \qquad N_{sc} = \Delta f \, N_0 \tag{4.1}$$

Where $g^{m}_{k,j,c}$ is the square Rayleigh fading between user k and the BS of the cell c in subcarrier j, m is the TTI index, N_{sc} is the noise per subcarrier and N_0 is the noise power density. $I_{j,c}$ is the interference on subcarrier **j** for the cell c caused by the other cells. With a maximum power P_k for user k (equation(4.3)), the total throughput in bits/s of this user in the cell c is given by:

$$R^{m}_{k,c} = \Delta f \sum_{j=1}^{N} a^{m}_{k,j,c} \log_2 (1 + \gamma^{m}_{k,j,c} P^{m}_{k,j}) \tag{4.2}$$

$$P^{m}_{k} = \sum_{j=1}^{N} a^{m}_{k,j,c} P^{m}_{k,j} \tag{4.3}$$

Where $P^{m}_{k,j}$ is the power allocated in subcarrier j. $a^{m}_{k,j,c}$ is a boolean variable which equals 1 if the subcarrier **j** is assigned to user k in the current c, 0 otherwise. We assume that pathloss and shadowing do not vary during the considered time frame.

Moreover, we consider that users in a cell are equally divided into two areas: cell center and cell border. With the uniform distribution assumed, a user is considered in the cell center if his distance from the BS is $d_k < \frac{R}{\sqrt{2}}$ with R the cell radius (figure 4.1). Consequently, if the user's distribution in the cell is uniform, approximately half of the users are located in each area.

4.4.2 Proposed model

In this section, we present our proposed models for the frequency reuse and the resources allocation to improve the system throughput compared to the classical

LTE model.

4.4.2.1 Proposed FFR

The classical partial FFR used in LTE [15][16] consists on dividing the subcarriers into four sets F_1, F_2, F_3 and F_4 with equal number of subcarriers $N_{F_n} = \frac{N}{4}$ for $n \in [1..4]$. Then, the same set F_1 is used for all cells centers whereas a $FFR = 3$ is used for cells borders with different sets F_2, F_3 and F_4 (figure 4.1.a).
We propose to improve especially the cell center throughput by using only two sets F'_1 and F'_2 with $N_{F'_n} = \frac{N}{2}$ for $n \in \{1, 2\}$. Users in the center use then subcarriers in F'_1 and those in the border use subcarriers in F'_2 with $FFR = 1$ (figure 4.1.b).
Since the number of subcarriers is doubled in the cell center, the throughput in

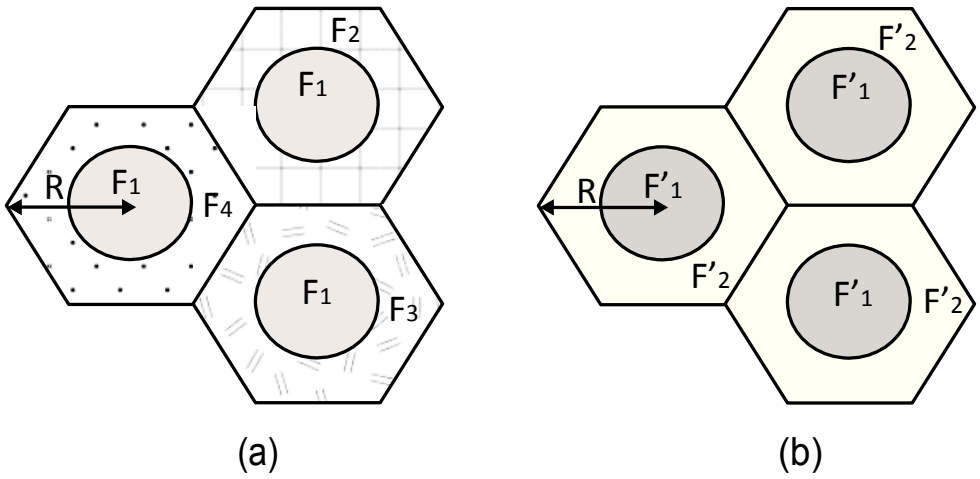

Figure 4.1: LTE FFR - Studied FFR

this zone and so the total cell's throughput will be improved. However, the used $FFR = 1$ in the cell border leads to more interference. We will show in the next sections that the throughput lost in the border area is low compared to the gain reached in the cell center.

4.4.2.2 Resource Allocation via WPF

In each zone of each cell, we adopt the WPF criterion to assign subcarriers to users. This allocation is based on the PF allocation to guarantee fairness between users and is improved by priorities depending on the users positions in the cell for a higher system throughput [51]. Consequently, in each cell c, a subcarrier **j** is

assigned to user k maximizing the incremental utility: $k^* = \arg\max_k U^m_{k,j,c}$
With:

$$U^m_{k,j,c} = \frac{R^m_{k,j,c}}{R^{m-1}_{k,c} + \sum_{i \in S^m_{sub,k,c}} R^m_{k,i,c}[w_{k,c}]}^{\beta} \quad (4.4)$$

and

$$w_{k,c} = \log_2\left(1 + \frac{P_k}{L_{k,c}S_{k,c}(N_{sc} + I_0)}\right) \quad (4.5)$$

Where $R^m_{k,c}$ is the cumulated rate of user k at the end of the m^{th} TTI, $S^m_{sub,k,c}$ is the set of subcarriers assigned to user k at the current m, $w_{k,c}$ is the weigth of user k. I_0 is an average interference calculated per user per subcarrier (see equation (4.10)). $\beta \in [0; 1]$, we remind that setting $\beta = 0$, we find the standard PF.

4.4.3 Theoretical expressions of throughput

To efficiently analyse the behaviour of our proposed model, we present the theoretical expressions of the throughputs in the cell center and in the cell border separatly. In this section, to simplify, we drop the time index m and the cell index c.

- **The cell center throughput**
  In the cell center, we can neglect the low interference with respect to the noise, the total throughput of this zone can then be expressed as:
  For the classical FFR = 3 (called FFR3 in the following):

$$R_{c1} = \sum_{k \in K_c} \sum_{j \in F_1} a_{k,j}\, \Delta f\, \log_2\left(1 + \frac{g_{k,j}P_{k,j}}{L_k S_k N_{sc}}\right) \quad (4.6)$$

  Where K_c is the set of the users in the cell center.
  For the proposed Model:

$$R_{c2} = \sum_{k \in K_c} \sum_{j \in F_1'} a_{k,j}\, \Delta f\, \log_2\left(1 + \frac{g_{k,j}P_{k,j}}{L_k S_k N_{sc}}\right) = 2\, R_{c1} \quad (4.7)$$

  Because we have the double of subcarriers for the proposed model: $N_{F_1'} = 2.N_{F_1}$.

With the same number of users, increasing the number of subcarriers upgrades the throughput and we can achieve the double of the rate provided by the classical FFR3. The gain provided in this center zone increases the total system throughput and allows better system performance.

- **The cell border throughput**

  In the cell border, the classical FFR3 can avoid high interference. The throughput, neglecting the interference term, can be expressed for high SNR as:

$$R_{b1} = \sum_{k \in K_b} \sum_{j \in F_n} a_{k,j} \Delta f \log_2 \frac{g_{k,j} P_{k,j}}{L_k S_k N_{sc}} \tag{4.8}$$

  $n \in [2..4]$ depending on the cell, K_b is the set of the users in the cell border. For the proposed Model:

$$R_{b2} = \sum_{k \in K_b} \sum_{j \in F_2'} a_{k,j} \Delta f \log_2 \frac{g_{k,j} P_{k,j}}{L_k S_k (N_{sc} + I_{proposed})} \tag{4.9}$$

  Where $I_{proposed}$ is the interference corresponding to the proposed model. The interference is approximated as an interference per user per subcarrier as:

$$I_0 = \frac{N_{interf}}{L_{interf}} \frac{P}{N_b} \frac{K_b}{} \tag{4.10}$$

With:

- N_{interf}: the number of the interfering users. In our system, we assume a 7 cells system model, we have then 6 interfering users for the cell border where the FFR used is equal to 1. Even if the number of cells is more than 7, we can consider that the potential interference is caused by only 6 neighboring cells.
- K_b: The set of the users in the cell border $K_b \simeq \frac{K}{2}$.
- N_b: The set of the subcarriers in the cell border $N_b = \frac{N}{2}$.
- P: The transmission power per user. $\frac{P\ K_b}{N_b}$ is then the average power per subcarrier.
- L_{interf} is the pathloss from the nearest user causing the interference. In fact, an interfering user can be situated all over the neighboring cell, but the interference it causes is high only if it is situated near to the considered cell. For this reason, we assume that the interfering user is located in the border of the cell with distance $d_I = R$ from his BS. We consider then the worst case of interference.

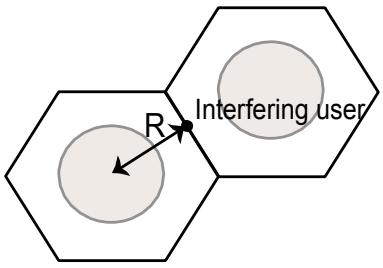

Figure 4.2: The position of the considered interfering user

To compare the two models, figure 4.3 shows the throughput in the border zone for low and high transmit powers corresponding to equations (4.8) and (4.9). For these theoretical results, the subcarriers' allocation is performed randomly and doesn't consider the WPF criterion which will be the case for the simulation results section. For low SNR, we can note that the two models have nearly the same performance, it is only for the high SNR where the proposed model is interference limited. In fact, the loss of performance in the cell border for the WPF is offset by the high gain in the cell center. In addition, we have note that interference is totally neglected in equation (4.8), even it is low, the interference exists when for equation

(4.9), the interference is estimated as the 6 potential interfering users are situated at the worst position with distance equal to R from the BS of the considered cell.

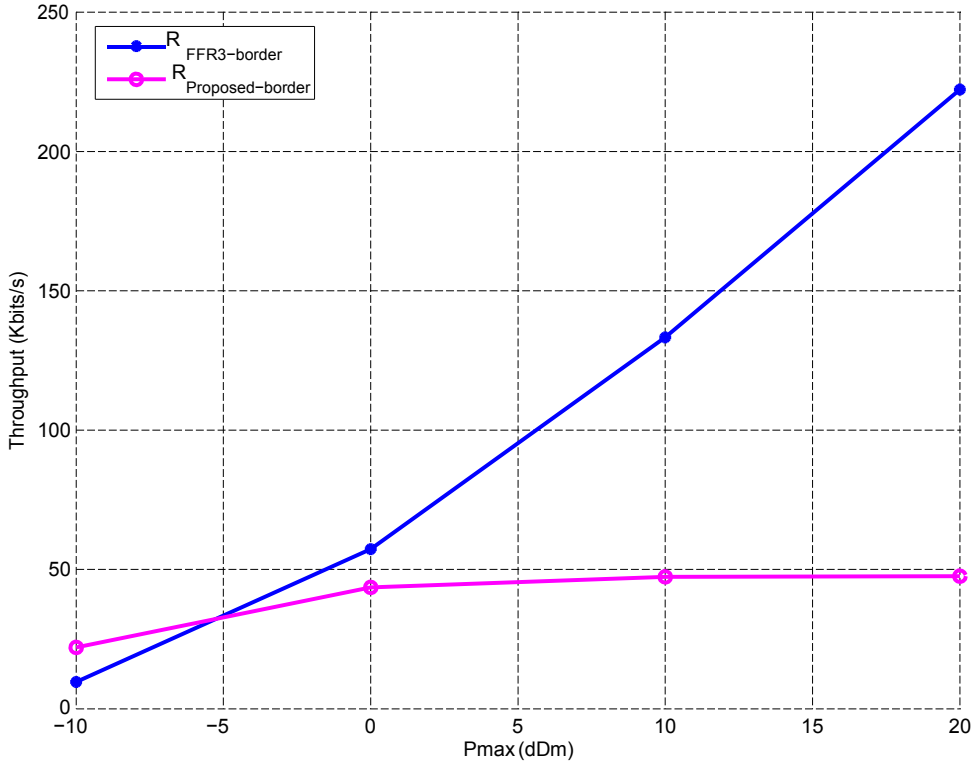

Figure 4.3: Throughput in the Border zone

4.4.3.1 The influence of the Weighted Proportional Fair

The WPF criterion is adopted for the ressource allocation which leads to priorities between users. According to the quality of service requirements, the weight can be ajusted by the β parameter (equation 4.4). Equation 4.5 shows that the weight depends on the users position in the cell and it presents a decreasing function of the distance. In this work, we study different values of β to evaluate the gain provided by the users priorities.

Figure 4.4 presents the user weights for different positions in the cell. With β = 0, we find the classical Proportional Fair algorithm where all the users have the same weight and will then acquire the same number of subcarriers whatever the distance. However, for β > 0, the system favors users near to the BS having good channel

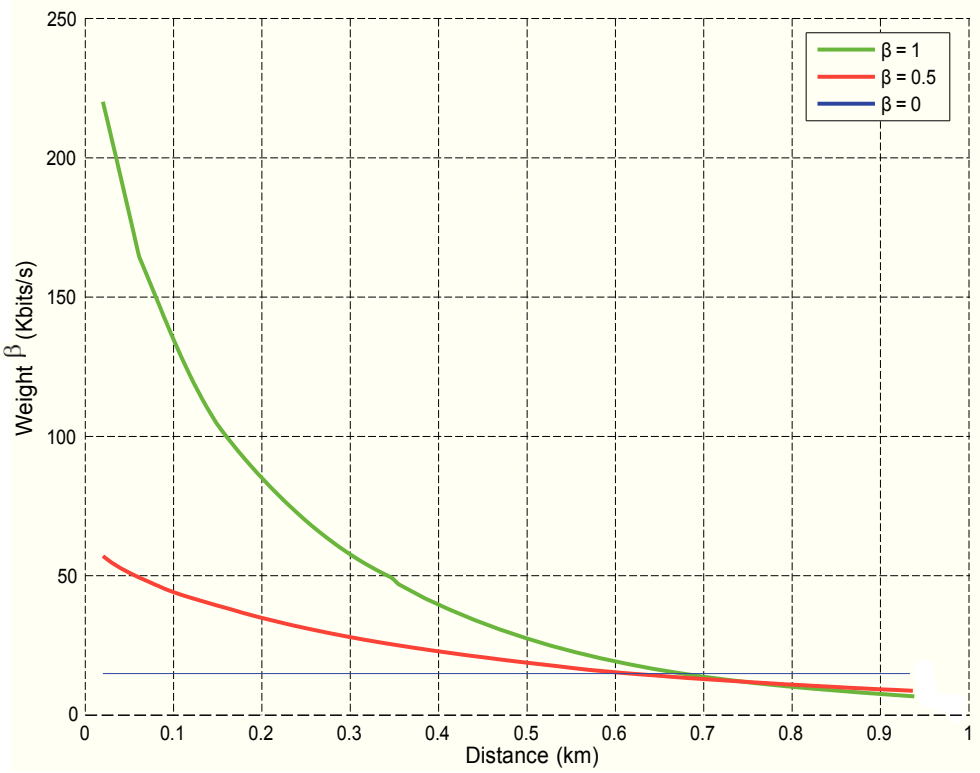

Figure 4.4: Weights versus Distance

conditions. The number of subcarriers allocated decreases with the users distance. The WPF criterion still maintains proportional fairness between the users and allows better system performance with the users' priorities considered.

4.4.4 Simulation results

We consider for the simulations a multi-cell model with 7 circular cells with radius of 1 km, each cell has one BS with an omnidirectional antenna, K = 20 users uniformly distributed and N = 72 subcarriers. The users are divided into two areas in each cell, users with distance d < $\frac{R}{\sqrt{2}}$ are in the cell center and the others are considered in the cell border. Per cell, we assume a total bandwidth B = 1.4 MHz and a bandwidth per subcarrier Δf = 15 KHz. We consider Rayleigh channels with Slow Fading and AWGN noise with power density N_0 = −174 dBm/Hz . The users experience a log-normal Shadowing with variance 6 dB and a pathloss according to the LTE model with frequency F = 2.6 GHz: $L_{k,dB}(d_k) = 128.1 + 37.6 \log_{10}(d_k)$ where d_k is the distance in Km of user k from

the BS.
We study two Frequency Reuse models for comparaison (figure 4.1):

- **FFR = 3:** The classical partial FFR adopted by the LTE model. 4 subbands are considered, one for all cells center and 3 for cells border. Each cell uses then only the half of the existing band to avoid inteference in the border area.
- **Proposed Model:** Our proposed FFR. Each cell uses all the available band divided equally for the two areas. Comparing to the FFR=3 model, the double of the resources is exploited.

For the WPF algorithm, we consider 100 TTIs, 500 simulations and study different values of β.

4.4.4.1 System Throughput

Figure 4.5 presents the system throughput per user in function of the transmit power. We study different valus of β and compare our proposed model to the classical FFR= 3 of the LTE. We can remark that the FFR3 model is an increasing function not limited by the interference but offers a lower throughput compared to the proposed model especially for low transmit powers. For all transmit power values, the proposed model allows a better or equal throughput system thanks to the resource allocation adopted. Its gain decreases when the transmit power increases because of the increased interference in the cell border, but the proposed model still offers good performance comparing to the FFR3 model.
Adding user priorities with β improves the system throughput by favoring users near to the BS. The gain provided by the proposed model varies from 8% to 45% for β = 1, from 5% to 41% for β = 0.5 and reaches 38% for β = 0 at low emitted power.

Figures 4.6 and 4.7 show the average throughput according to the users positions in the cell. For low transmit powers as presented in figure 4.6, the behavior of the FFR3 and the proposed model are similar in the cell border. However, the proposed model offers in the cell center a large gain up to 60% for β = 1 and up to 50% for β = 0. Moreover, for high transmit powers(figure 4.7), the gain in the cell center persists for the proposed model but the interference in the border

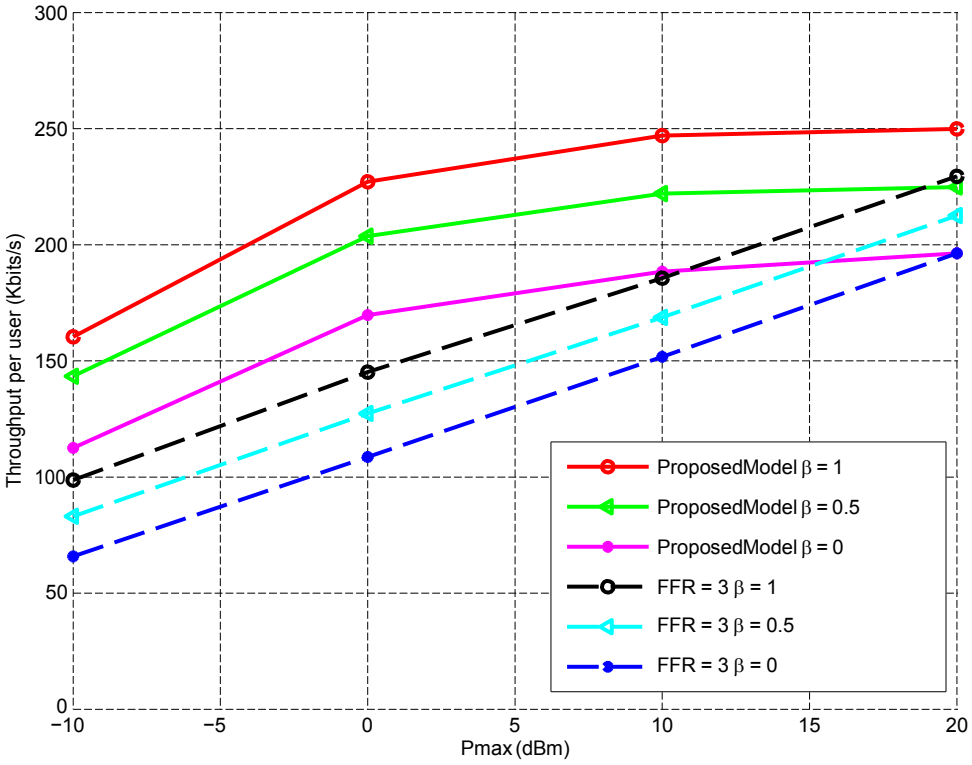

Figure 4.5: System Throughput

leads to some slight throughput decrease. Despite this low decrease, the total system throughput remains better for the proposed model as proven in figure 4.5. Comparing figures 4.6 and 4.7, we can also note that for very low distances, the throughput is better for low transmit powers. This can be explained by the number of subcarriers assigned and the interference suffered. Simulation results show that for $\beta = 1$, users with $d < 0.1$ Km can win up to 15 subcarriers for $P_{max1} = -10$ dBm comparing to only 8 subcarriers for $P_{max2} = 20$ dBm. In fact, with low transmit power, the throughput of these users remains low, they can then earn a high number of subcarriers thanks to their high weights comparing to users far from the BS. In addition, users transmitting with P_{max2} are more limited by the interference while interfering users transmit with the same power which lead to this difference of the throughput.

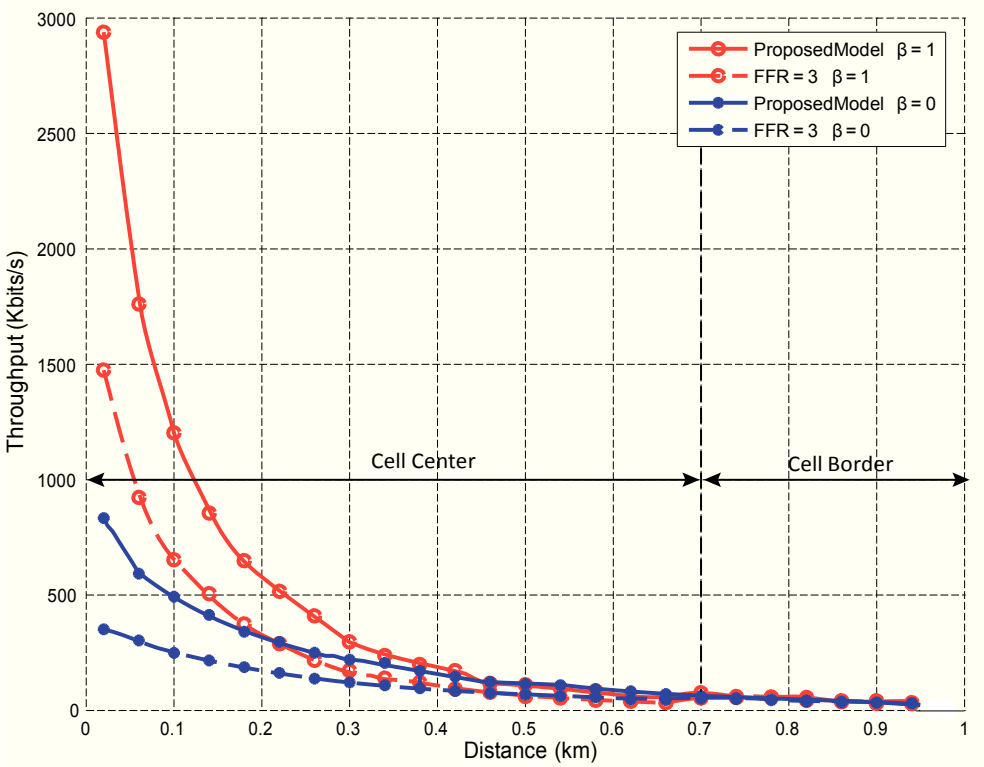

Figure 4.6: System Throughput versus Distance for $P_{max} = -10$ dBm

4.4.4.2 Fairness

To evaluate the fairness of our algorithm, we adopt the Fairness Index (FI) [13], The algorithm is more fair when its FI approaches 1 as explained by equation 3.15 Table 4.1 compares the fairness indexes for the FFR = 3 and the proposed model for low and high transmit powers. We note that the proposed model offers lower values of fairness compared to the classical FFR = 3 model but the decrease is kept quite low. The proposed model gives better system performance concerning overall throughput while maintaining the system fairness.

We also confirm, as in chapter 3, that increasing β leads to the decrease of the fairness. The β parameter can then be adjusted depending on the QoS requirements.

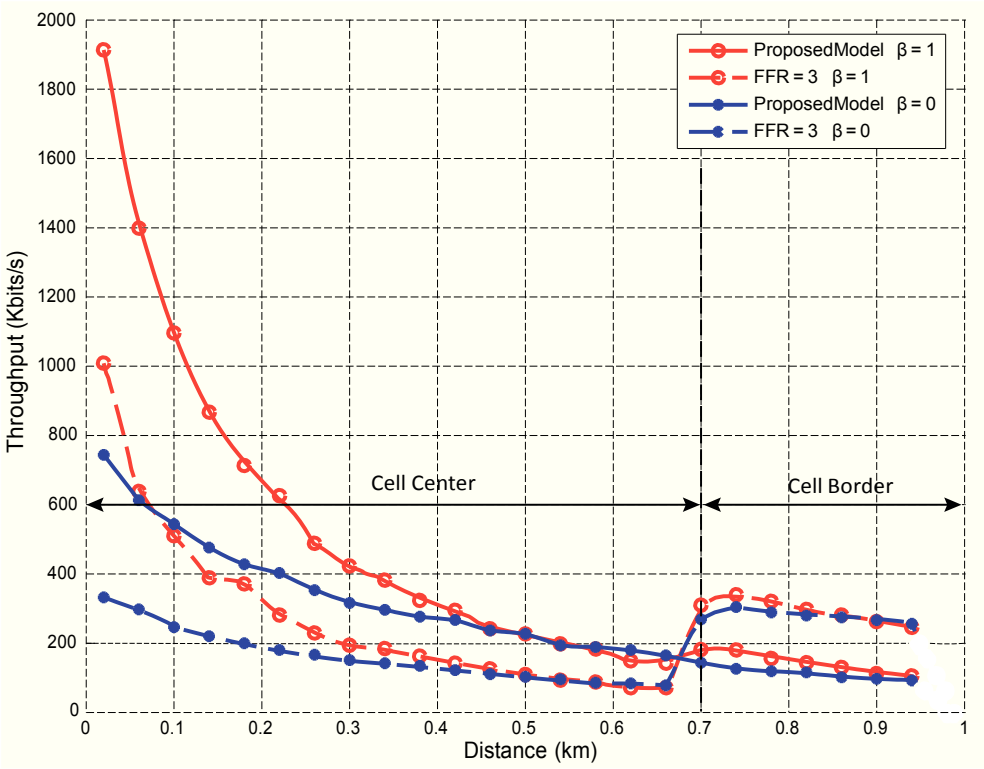

Figure 4.7: System Throughput versus Distance for P_{max} = 20 dBm

$P_{max} = -10$dBm			
	β = 0	β = 0.5	β = 1
FFR = 3	0.57	0.42	0.31
ProposedModel	0.5	0.37	0.28
$P_{max} = 20$dBm			
	β = 0	β = 0.5	β = 1
FFR = 3	0.75	0.72	0.61
ProposedModel	0.7	0.59	0.5

Table 4.1: Fairness Indexes depending on transmit power values

4.5 Enhanced Interference Indicator

In the last section, interference mitigation by the use of frequency reuse is studied. Resource allocation is then established in each cell independently without cooperation between BSs. In this section, the cooperation between BSs is studied to efficiently mitigate the ICI. Comparing to the FFR method, the total bandwidth is reused in all cells which increases the spatial diversity but ICI mitigation

needs communication between BSs. The cost of BSs cooperation depends on the exchanged data. Exchanging ICI indicators has the advantage to avoid high ICI level with low communication cost. In this section, interference indicators are studied and a novel interference indicator is proposed to reduce the ICI.

4.5.1 System model

We consider a multi-cell OFDMA system. Each cell has only one omnidirectional antenna BS, K users uniformly distributed and N subcarriers with a bandwidth Δf each. We focus in this work on the uplink transmission from users to BSs. The users experience both pathloss and shadowing. We consider a frequency-selective Rayleigh fading channel with slow fading and AWGN noise. Note that a subcarrier is allocated to only one user per cell. Using the Proportional Fair Algorithm, we consider a time period of m TTIs. If we note the user k, the cell c and the subcarrier j, the channel gain coefficient $\gamma_{k,j,c}$ at TTI m can be expressed by equation(4.1) and the total throughput (in bits/s) of user k in the cell c is given by equation (4.2). The users are uniformly distributed in the cell. In addition, we assume that each cell is divided into two areas: cell center and cell border. We have approximately the same number of users in the two areas: if the distance of user k, $d_k > \frac{R}{\sqrt{2}}$ with R the cell radius, k is considered in the cell edge. Moreover, for the resource allocation, we adopt a full frequency reuse with half of the subcarriers in each area. The same set of subcarriers F_1 is used in all cell centers and the allocation in this area is independent of the other cells. The same set of subcarrier F_2 is then used for all cell edges. The PF algorithm [52] is then considered to assign subcarriers to users as a tradeoff between throughput and fairness in the system.

The inconvenient of using the full FFR is the ICI in the cell border. In this work, we adopt a simple communication between BSs with exchange of Enhanced Interference Indicator (EII). The EII has several levels that indicate if the subcarrier **j** is not interfered, lowly interfered or very interfered for a better resource allocation. In the next section, the proposed EII will be explained in details.

4.5.2 Interference Indicator based Allocation

Based on the HII in the LTE standard notion [2], we introduce in this chapter an enhanced interference indicator with different integer values. Being a boolean variable, the standard HII only shows if the subcarrier is considered interfered or not. We aim to improve this indicator to have a more efficient cooperation between BSs. For this purpose, the cell edge is divided into different sectors like explained in figure 4.8. We treat here the users in the cell edge only. Each user is characterized by its sector and the EII is specified for one subcarrier in one cell. The EII value of a subcarrier **j** depends then on the sectors in which **j** is allocated in the neighboring cells. Since we focus on the uplink, the interference depends on the distance between the interfering user in the neighboring cell and the BS in the considered cell. For this reason, to specify the EII values, we analyze the dependencies between the sectors in the multi-cell model and calculate effective values of EII.

4.5.2.1 System dependencies

The EII aims at improving the resource allocation in the cell edges. To assign a specified subcarrier **j** to users, the EII's main objective is to decrease the utility of subcarrier **j** for the users which will be very interfered if they earn j. For example, figure 4.8 shows the dependencies of users in the central cell c1. These users will be highly interfered if they acquire a subcarrier **j** already allocated in the sector colored in red (val_1) because of the small distance to the central BS. With a high EII value of **j** they will be disadvantaged to earn it. In fact, the best allocation for users in c1 is to get subcarriers allocated in sectors with the high distance possible from the central BS which are sectors with the lowest EII: val_4 (sectors 2 of the cell 7 and sector 3 in cell 2 for example). To complete the same example, figure 4.9 shows a specific allocation for a given subcarrier j. In this case, the central cell is the last cell in the allocation process, which means that subcarriers have already been allocated in all other cells and subcarrier **j** is already allocated in the colored sectors. For users in cell 1, the EII value of **j** is $EII_{j,1} = 2val_1 + 3val_2 + val_3$. The EII is calculated with a heuristic method for all sectors to calculate then the PF criterion (see equation(4.11)).

The EII value of subcarrier **j** in cell c can then be expressed as:

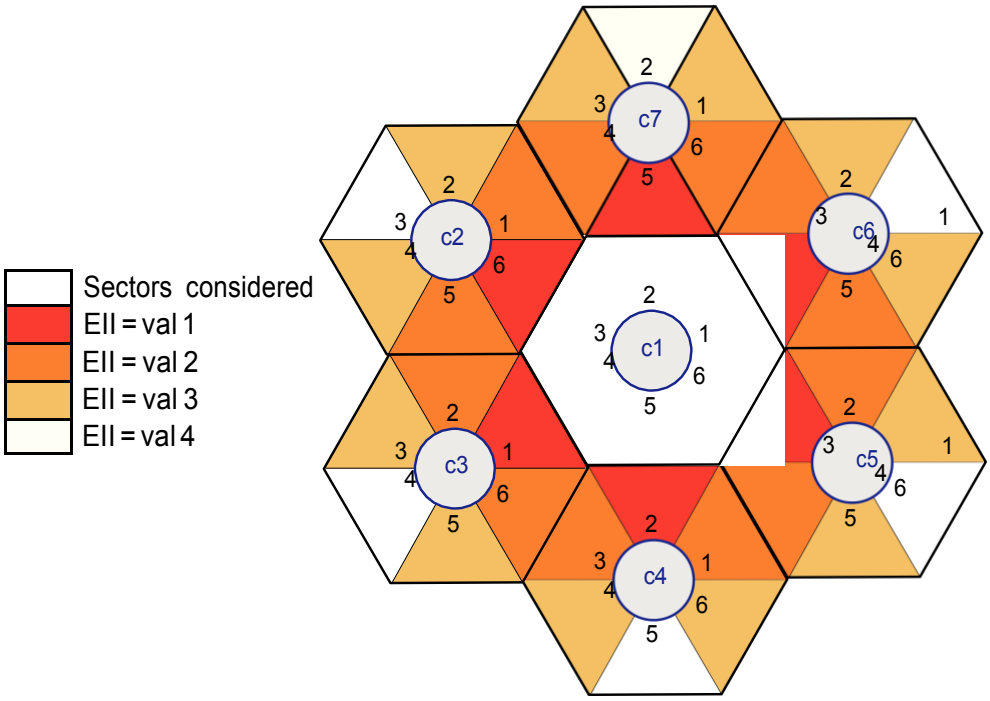

Figure 4.8: Example 1: System dependencies for the central cell

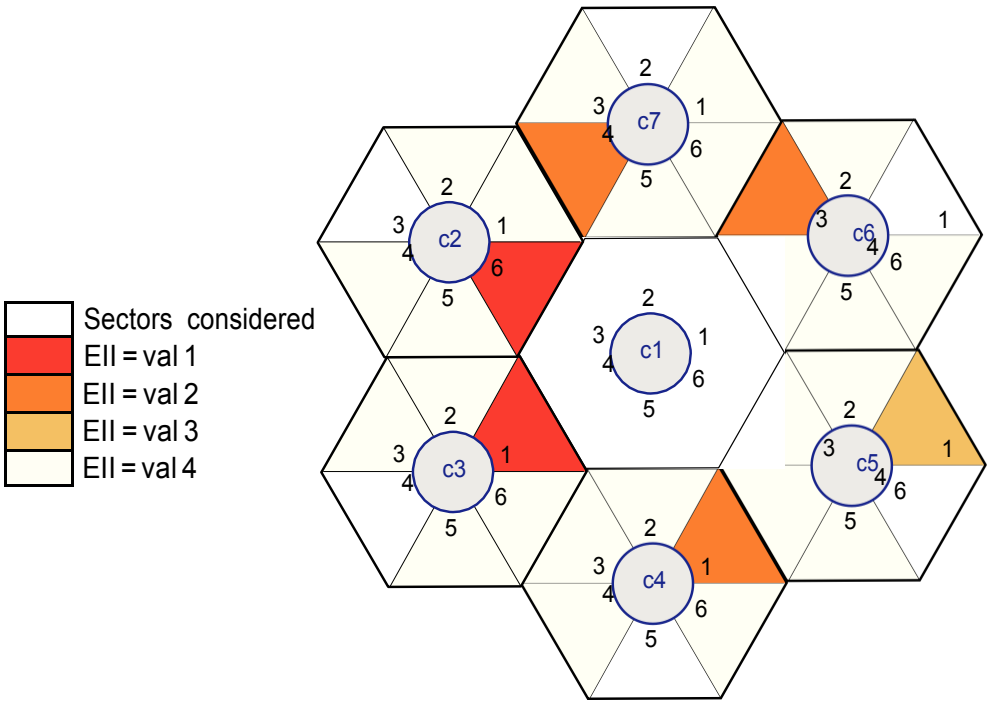

Figure 4.9: Example 2: The allocation is considered in the central cell, the discussed subcarrier **j** is already allocated in the colored sectors

$$EII_{j,c} = \sum_{c'/=c} \sum_{s=1}^{S} b_{s,j,c'} \cdot eii_{s,c',c} \quad (4.11)$$

where S the sectors number (= 6 in this case), $b_{s,j,c'}$ is a boolean variable that indicates if subcarrier **j** is allocated in sector s in the cell c' or not, $eii_{s,c',c}$ is the EII value of sector s in c' if the considered cell is c. $eii_{s,c',c} \in \{val_1, val_2, val_3, val_4\}$. The values of EII ($val_1$, val_2, val_3, val_4) will be calculated in the next section.

4.5.2.2 Interference Indicator Values

The EII values depend on the sector in which the current treated subcarrier is allocated in the neighboring cells. To have accurate values, we calculate the distances between a BS situated in a cell center and the sectors centers in neighboring cells d_1, d_2, d_3 and d_4 depending on the cell radius R, as shown in figure 4.10.

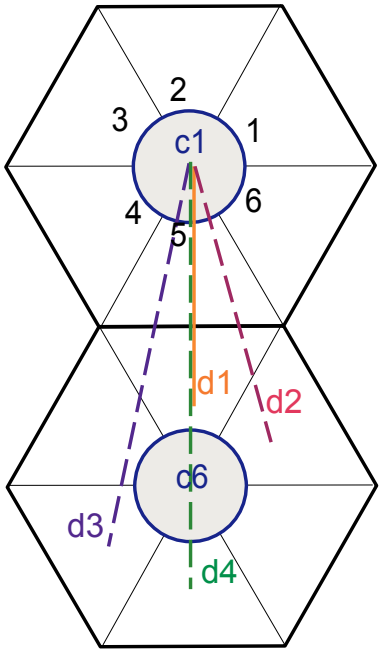

Figure 4.10: Distances: $d_1 = 1.3 \cdot R$; $d_2 = 1.56 \cdot R$; $d_3 = 1.98 \cdot R$; $d_4 = 2.16 \cdot R$

Then, depending on the pathloss's coefficient α, we compute $val_i = \frac{d_i}{d_4}^{-\alpha^\sigma}$, $i \in [1..4]$. In the studied case, α = 3.76 corresponding to the adopted LTE model and σ is a positive parameter σ has a low influence if it is equal to 1. If σ tends to infinity, val_4 = 1 while val_1, val_2 and val_3 are infinite, then, only subcarriers allocated in sectors with EII=val_4 will be allowed. We can deduce that when

increasing σ to infinity leads to a FFR = 6. To have an intermediate behavior, we choose to set σ = 2, EII values correspond thus to the relative values as: $val_1 = 36$, $val_2 = 9$, $val_3 = 4$, $val_4 = 1$. EII values will be used as interference terms in the resource allocation algorithm, as explained in the next section.

4.5.2.3 PF Allocation

To assign a subcarrier, we choose the best user considering the PF algorithm $k^* = \arg\max_k U^m_{k,j}$. Where $U^m_{k,j}$ the incremental utility of user k in subcarrier **j** at TTI m defined in equation (4.4) : Referring to the equation (4.1) to calculate the SINR of user k and subcarrier **j** in cell c, the ICI is estimated as:

$$I_{j,c} \quad \frac{EII_{j,c}}{L_{interf}} \cdot \frac{P \cdot K_b}{N_b} \tag{4.12}$$

where $EII_{j,c}$ is the EII value corresponding to subcarrier **j** in cell c, K_b the number of the users in the cell border, N_b the number of subcarriers allocated in the cell border, P the user transmission power and L_{interf} the pathloss from the nearest user k' causing the interference (with $d_{k'} = R$). In fact, we consider the worst case where the interfering user is in the extreme border. $\frac{P \cdot K_b}{N_b}$ is the average power per user per subcarrier.

The EII values aim to estimate the interference more accurately comparing to our previous work (equation (4.9))[53]. In equation (4.9), the interference estimation does not consider where the discussed subcarrier is allocated in the neighboring cells. We have considered that the subcarrier is allocated in all other cells and we have then the number of interfering users is equal to $N_{interf} = N_{cells} - 1$ where N_{cells} is the cells number. Furthermore, we have considered that interfering users are situated in the worst position at a distance = R from the BS of the considered cell. In this section, N_{interf} is substituted by the EII value which allows a more realistic estimation of the interference.

Moreover, we establish statistics for allocation in the central cell c1. To be realistic, c1 has not to be always the first cell for allocation, it is also not realistic if c1 is always the last cell for allocation. Thus, we adopt a rotating allocation method for the 7 cells in the system model. Each TTI, the order of the cells changes: for TTI = 1, we start with cell 1, cell 2 ... until cell 7, for TTI = 2, we start with cell

2, cell 1 becomes then the last cell to process, etc. This is used in order to have some fairness between all cells for the resource allocation process.

4.5.2.4 BS Cooperation

To realize this Enhanced Interference Indicator Algorithm, each BS communicates to neighboring BSs the sectors where subcarriers are allocated through the X2 interface in LTE, as for conventional HII. Instead of a boolean, BSs exchange a byte to indicate the EII value for a subcarrier. The dependencies between cells (figure 4.8) and the EII values are initialized in all cells and thus does not need any additional communication. A current BS has thus all the information to calculate the EII values for all subcarriers.
The proposed EII cooperation does not need a lot of information to communicate. In fact, BSs exchange boolean variables $b_{s,j,c'}$ to indicate if subcarrier **j** is allocated in sector s of cell c' or not (equation (4.11)). The total number of bits exchanged is then $S \times N \times (N_{cells} - 1)$ bits where S the number of sectors and N the number of subcarriers. In addition, BSs cooperate through the backhaul to reduce the exchange cost.

4.5.3 Simulation results

For the simulations, we consider the system model shown in figure 4.8 and the same assumptions of section 4.4.4, only the number of users changes K = 40 users. The algorithm considers 100 TTIs where the cells order is changed in each TTI. 1000 iterations are considered to randomly distribute users' positions, rayleigh fading and shadowing.
We compare our algorithm with EII to the standard HII and to the system performance without any interference indicator. For the standard HII which is introduced in section 4.5.2, a subcarrier is considered interfered if it is allocated in the nearest sector: refering to figure 4.8, if the central cell is the latest cell to process, a subcarrier **j** is considered interfered only if it is allocated in the sectors with $HII = val_1 = 36$. Otherwise, $HII = val_2 = val_3 = val_4 = 0$.

4.5.3.1 Instantanious Rate

We present in figure 4.11 the instantaneous rate for the central cell with EII, with HII and without interference indicator. Since the system runs for only one TTI, the central cell is the first cell to perform the resource allocation and the rotating allocation method does not occur in this instantaneous result. The HII offers then a gain comparing to the system without interference indicator, but our proposed EII leads to better results. Moreover, it will be shown in the next section that the HII loses this gain when the system considers more TTIs with the PF algorithm.

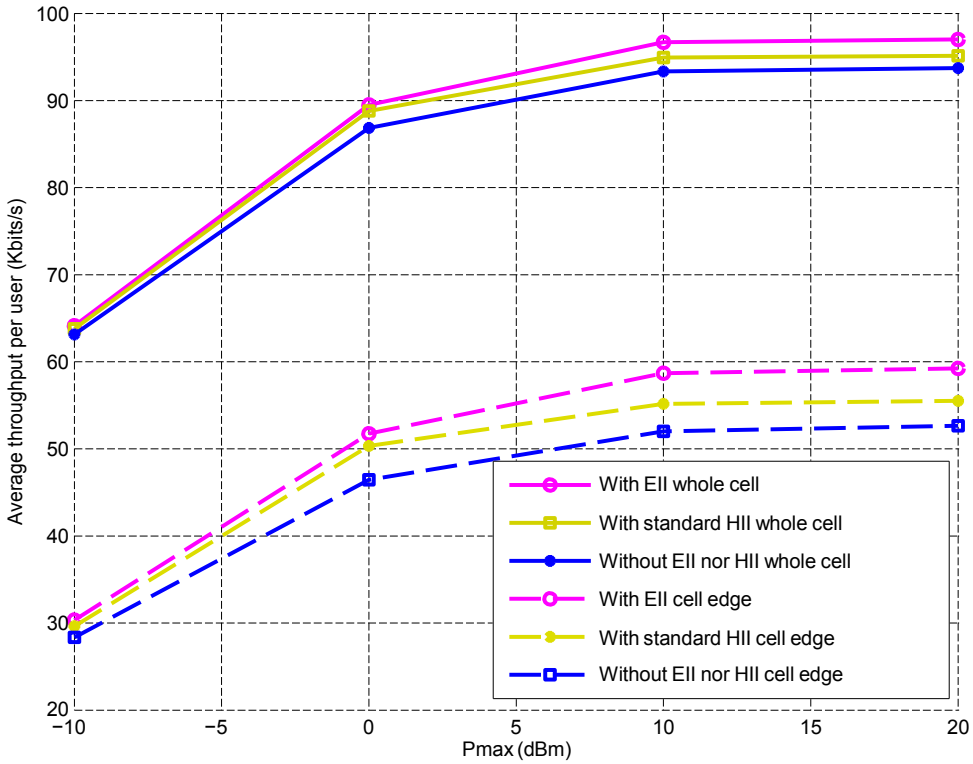

Figure 4.11: Instantaneous Rate

4.5.3.2 Throughput

Figure 4.12 shows for different transmit power values the average system throughput per user considering 100 TTIs. We differenciate the border area where the EII and the HII are used from the whole cell. Simulation results indicate the benefit of the EII in the cell border that reaches 13% for high transmit powers (figure 4.13)

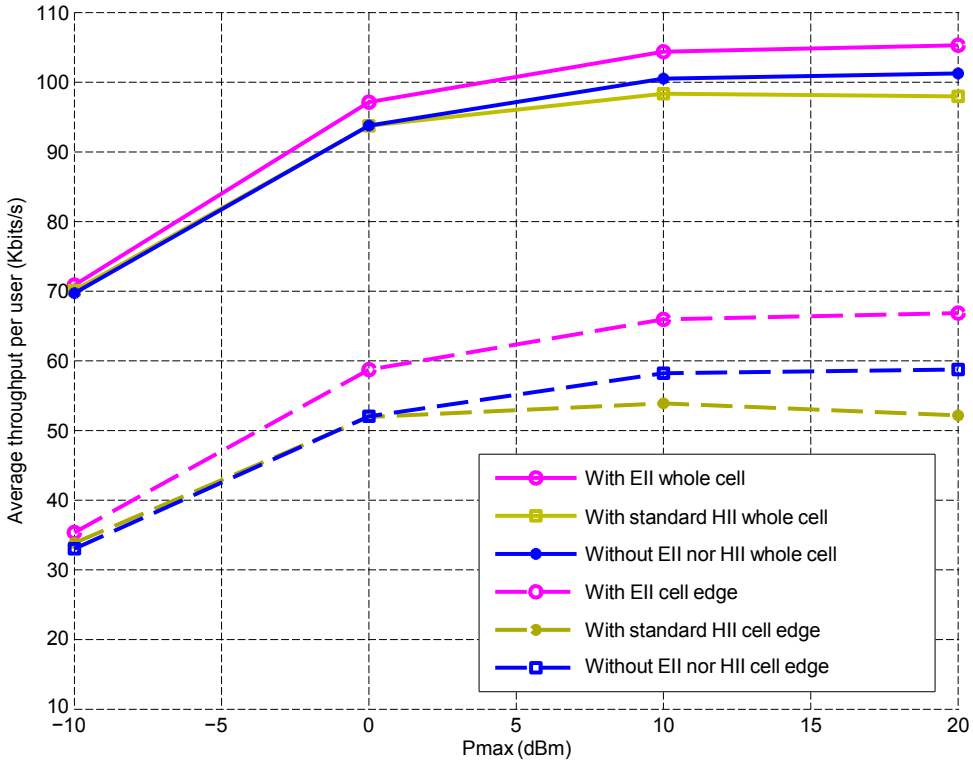

Figure 4.12: System throughput

compared to the system without interference indicator.

We also note that the standard HII does not offer always a gain especially for high transmit power. This loss of throughput can be explained by the decrease of diversity for the HII system. In fact, with the HII model, the system loses $\frac{1}{6}$ of user diversity because the users located in one sector per cell are prohibited from transmitting due to the high HII. Yet, some interfering users may still be selected in the other interfering sectors. With the temporal rotating process, the HII has worse results than the system without interference indicator caused by the decrease of user diversity and the presence of high interfering users. Since half of the users are in the cell edge, improving their throughput from 7% to 13% is interesting mainly since the system does not need a lot of communication between BSs.

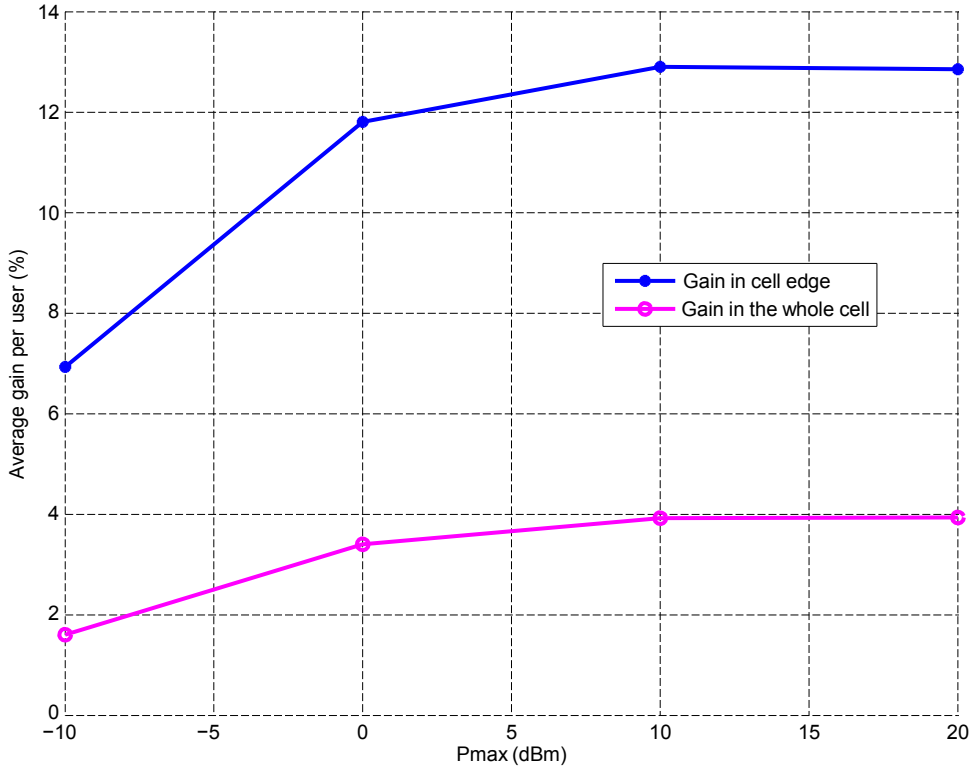

Figure 4.13: Average gain of the proposed algorithm with EII

4.5.3.3 Fairness

In this section, the system fairness is measured to prove the interest of the Interference Indicator by the fairness indicator introduced in equation(3.15). Table 4.2 compares the fairness indexes for the multicell model with and without EII for low and high transmit powers. We note that the use of the EII influences lowly the fairness index values. The EII allows then a better throughput while maintaining the system fairness.

The fairness is almost the same with and without the EII due to the number of

	$P_{max} = -10$ dBm	$P_{max} = 20$ dBm
Without EII	0.34	0.41
With EII	0.33	0.39

Table 4.2: Fairness Indexes

subcarriers per user which is the same for the two schemes. In fact, with the EII,

the choice of subcarriers per user is changed but the number of subcarrier assigned to each user still the same.

4.6 Conclusion

In this chapter, resource allocation for a multi-cell system model is investigated by applying the WPF. The main contributions of this chapter are the application of the WPF algorithm (presented in chapter 3) in a multi-cell system model. This is a method to reduce the ICI without any cooperation between BSs. Then, the second contribution is to propose an enhanced interference indicator that BSs exchange to mitigate the ICI.

First, using WPF allocation, we have provided an analysis of a proposed FFR schema combined to a WPF resource allocation. Comparing to the classical LTE model, we proved that the system throughput is improved in the cell center with a low decrease in the cell border. The WPF algorithm offers better results in increasing the β parameter by favoring users with good channel conditions. This parameter can be used to adjust the system throughput with the QoS required. We also depicted the fairness for different studied schemes and the simulation results show that the proposed model still maintains system proportional fairness. Moreover, in the second part of this chapter, we used a simple cooperation between BSs to improve the cell edge throughput. For this, we divide the users in different sectors per cell and during the resource allocation, each BS communicates the assigned subcarriers per sector to all surrounding BSs. In addition, based on Enhanced Interference Indicator concept, each BS has initially a dependencies table that indicates the EII values for each neighboring sector. Using this table and the information communicated by other cells, the current BS tries to efficiently assign subcarriers and to avoid high interference. We prove by simulation results that the BSs cooperation with EII can offer up to 13% of gain without high signaling exchange between them.

Chapter 5

Resource Allocation in Cooperative OFDMA with Multiplexing Mobile Relays

5.1 Introduction

In this chapter, relaying strategies are studied. In wireless cellular networks, relays are used to enhance mobile users performance especially in the cell edge where the pathloss due to users' location may lead to high signal attenuation. For such a system model, several feature are important as relay selection and protocols used in the relays. Relays can be fixed and deployed by cellular operators as a part of the network's infrastructure. This type of relays is standardized in the 4G wireless systems. Relays can also be mobile where simple mobile terminals may act as relays for other terminals and do not need then any additional infrastructure. This relay's type enhancing system performance without additional deployment cost is considered as a serious candidate for the 5G wireless system. We focus on mobile relays in this chapter and study the resource allocation for an uplink cooperative OFDMA system with multiplexing relays. Relays in our system are mobile users with favorable locations to relay some cell edge user. Potential relays multiplex then their own data to the relayed data to the BS. The system objective considered is to minimize the whole system transmit power to save battery life and

contribute to green communications reducing the overall environmental effects. A required data rate per user constraint is also considered. After an initialization step to associate source-relay pairs, the resource allocation is formulated as an optimization problem and resolved theoretically. Simulation results show that the proposed algorithm approaches the optimal solution and offers better results comparing to a system without relaying.

5.2 State of the art

Replying to quality of service requirement with always greedy data applications is still an important challenge for wireless cellular networks. Technical constraints pushes researchers and operators to provide solutions allowing users to acquire high performances independently of their geographical distance from the BS. In addition to the OFDMA technology, relays are among the principal features of the 4^{th} Generation (4G) wireless systems. Relaying technologies, inspired from ad hoc multihop networks, are currently receiving much attention to improve cellular network's performance where bandwidth and power are limited. Instead of deploying BS, relay stations become a solution to reduce high deployment costs and can provide capacity and coverage comparable to small cells. Relaying data aims to upgrade user's performance especially in cell border where users suffer from large signal attenuation. Relaying topology and behavior are standardized in both Long Term Evolution (LTE) Advanced [12] and International Mobile Telecommunication Advanced (IMT-Advanced). In these standards, relays have to be fixed in positions beforehand planned by the operators and become a part of the fixed access network. Each relay is then attached to a designated BS in a static topology. Moreover, relaying data can be considered for a single hop or for multihop using one or multiple relays to transmit information from source to destination. In this context, the LTE Advanced standard allows only two hops when the IEEE.802.s standard offers a multihop relaying scheme [54].

Many relay transmission schemes are proposed to relay information from source to destination in two time intervals [10][19]. A relay can use the Decode and Forward scheme (DF) where it decodes the received signal in the first Transmit Time Interval (TTI), re-encodes and then forwards it to destination in the second TTI [18].

A relay may also use Amplify and Forward scheme (AF) where it just forwards the received signal with an amplification factor. It is proven in [10] that DF scheme can achieve better performance than AF scheme, however, it is more complex. Several solutions using relays are proposed in the literature. We can differentiate relays used as virtual Multiple Input Multiple Output (MIMO) to exploit spatial diversity [11][18] which need combining techniques at the destination and relays used as repeaters where source has no direct link to destination [55].

Although only fixed relays' architecture is optimized in the standards, mobility is studied in the scientific community to offer dynamic relaying topology. Mobile relaying has been investigated in the Wireless World Initiative New Radio (WINNER) project [56] contributing in the development and the assessment of 3GPP LTE and IEEE 802.16 (WiMAX) [1] standards and in the Advanced Radio Interface Technologies for 4G Systems (ARTIST4G) project providing innovative concepts to cellular mobile radio communications [57]. Mobile relays can be considered as a serious candidate for future 5G wireless systems. A mobile relay can have the same technical characteristics as a fixed relay but its location dynamically changes. In [58], relaying use cases are studied to assess the relaying improvement brought by mobile relays. Some examples for this type of mobile relays are relays placed on transportation vehicles such as buses or trains. These relays can be placed to serve users traveling in theses vehicles or to serve users in the street. Another type of mobile relays is to use simple user terminals as relays. Users can have advantageous location and channel conditions to relay some cell border users. This type of mobile relay can upgrade system performance without additional infrastructure cost. An unpredictable dynamic topology is offered depending on sources and relays mobility [59].

Resource allocation for cooperative networks has been actively studied in the literature for both downlink and uplink. The principal features to discuss are relay selection, subcarriers allocation and power allocation that can be treated separately or jointly. The selection of relay partners is an important element to successful cooperative strategy [19]. The pairing step may be realized as a centralized process where the BS collects necessary channel and location information from users and relays and decides then to attach users to appropriate relays. Relay's selection may also be established in a distributed manner where users or relays decide to

make cooperative pairs [10]. The distributed decision can generally achieve better performance but needs more signaling overhead. Relay selection [19] can be made before transmission, aiming to achieve some required level of performance. It can also occur during the transmission time as a proactive selection or as an on-demand relay selection when the direct link's channel gain to the destination decreases. We note that for multihop relaying, relay selection strategy have to be repeated at each hop. In [59], the authors propose a relay selection method for user terminals as mobile relays where they minimize the set of candidate relays to reduce relay selection complexity.

Depending on the system objective and the constraints to respect, resource allocation for a system with relays is generally formulated as an optimization problem. The resource allocation problems are then solved via mathematical tools or heuristics to find the optimal or suboptimal solutions. In [55], the authors formulate an optimization problem to maximize the total system throughput. The proposed system model considers one source, one destination and a set of fixed AF relays where the source may use one or multiple relays to transmit data to the destination. In [60], resource allocation considering an uplink relaying system with one destination, several sources and several fixed relays is studied to maximize system throughput using AF and DF schemes with the constraints of minimum data rate and maximal transmission power per user. In [61], joint power allocation, relay selection and subcarrier assignment with a minimal data rate per user is discussed for a downlink system model with fixed relays. In [62], joint resource allocation is considered for uplink system where relays are fixed. It is solved via an iterative algorithm based on dual decomposition theory. The dual resolution method is adopted after problem's adaptations to solve the optimization problems in [59][55][60]. Dual decomposition [39] consists in dividing the global problem into subproblems to be solved independently. Dual method is a resolution method for convex problems [35] and can be adopted for non convex problems [37] in some cases without an optimality loss.

5.3 Chapter's structure

In this chapter, we propose a new resource allocation algorithm for an uplink multiuser OFDMA relay network in the context of green communications where we aim to save battery life by minimizing the consumed transmit power. We consider a relaying system model where DF relays are simple users with advantageous positions to relay cell-edge users. Relays forward to destination relayed data multiplexed to their own data in different RB. The objective considered is to minimize the total system transmit power while ensuring a minimum data rate per user. A cell edge user decides to use either its direct link to BS or an indirect link depending on the available relays by estimating the data rate that it can achieve with both methods. Then, we formulate an optimization problem with required quality of service per user to optimize both RB Allocation and Power Allocation. Dual Lagrange decomposition is adopted for theoretical resolution and an iterative algorithm is proposed to find optimal solution. In the literature, fixed relays are generally investigated. In addition, relays have not data to transmit to the BS. The major contribution of this work is that relays are mobile users and that have their own information to transmit. To the best of our knowledge, this is the fist work studying this system model where mobile relays multiplex their own data to the relayed data.

In section 5.4, Power allocation and RBs allocation are studied as the optimization variables, the source-relay pairing step is performed as an initialization. At the beginning, depending on its location and on available relays, each user estimates the achievable data rate among each link and decides then to cooperate or not. If cooperation is chosen, a user can be relayed by only one relay. A relay can relay one or more users. Once chosen, the association sources-relays remains constant during the whole optimization algorithm. In section 5.5, in addition to Power allocation and RBs allocation, relay selection is treated in the optimization problem and resolved dynamically. Contrary to the case treated in section 5.4, a user can be relayed by one or more relays in different RBs and the cooperative pairs can change along the resolution process. Finally, both methods are compared in section 5.6.

5.4 Joint Power and RB Allocation

5.4.1 System model

In this section, we present the adopted system model and assumptions. Then, we formulate the optimization problem and the associated constraints. We finally enumerate the resolution steps in the proposed algorithm.

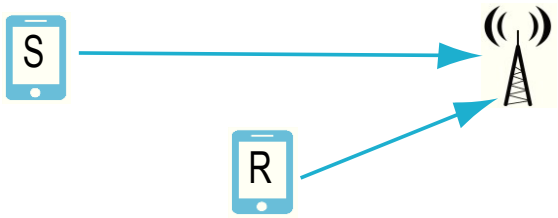

(a) Case 1: Not cooperative model

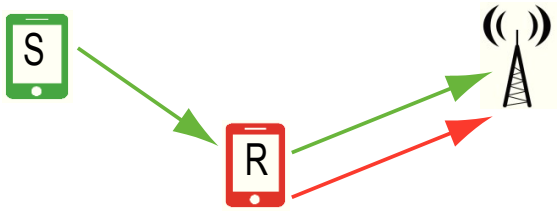

(b) Case 2: Cooperative model

Figure 5.1: Example 1: Transmission schemes

Relaying is used in this work to improve uplink system performance from users to BS. Simple mobile are used as relays and transmission can be made according to two possible schemes: direct transmission where each user transmit directly to the BS (figure 5.1a) or cooperative scheme where a user R can relay a source S in addition to its own data (figure 5.1b) thanks to its position approximately at the halfway between S and BS. We consider a single cell uplink OFDMA transmission system with one BS with an omnidirectional antenna, K users and N RBs. The channel is assumed a frequency-selective Rayleigh fading channel with slow fading and the AWGN noise. The users are uniformly distributed in the cell and experience pathloss and log-normal shadowing.

Our model is a cooperative system where some users can be relays for other users while still transmitting their own data. Source's relayed data and relay's data are then multiplexed by the relay and transmitted to the BS. Users are divided into three groups: Not Relayed Sources (NRS), Relays (R) and Relayed Sources (RS)

(figure 5.2). Relays in our model are simple mobile users whose location can be advantageous to relay some users located at the cell border.

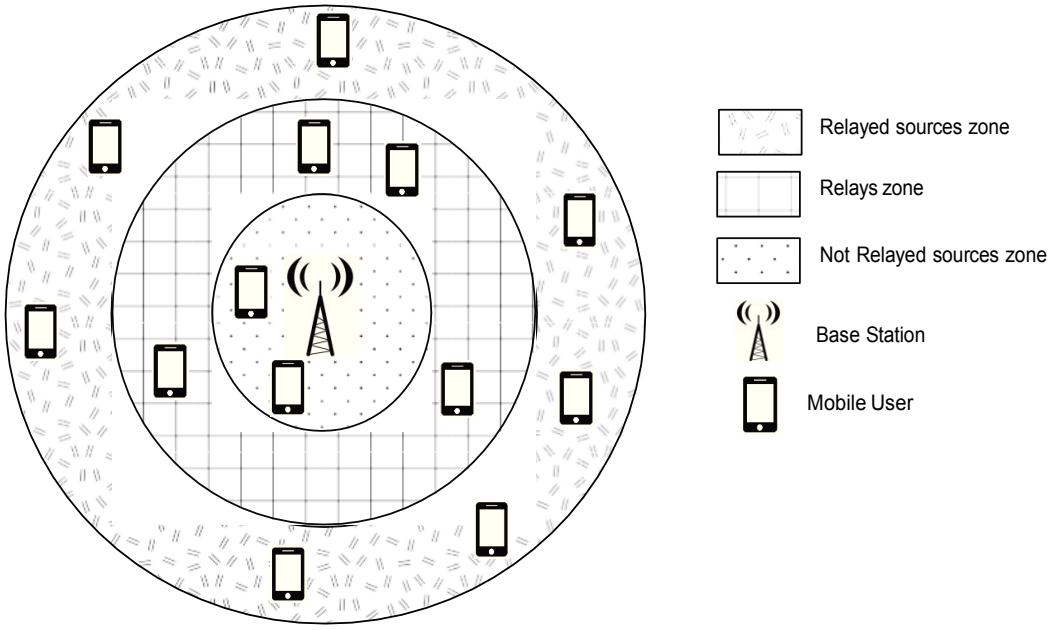

Figure 5.2: System Model

Let R be the cell's radius and $d_{k,k}$ the distance between user k and the BS. In order to simplify relay search, it has been decided the following:

- Users with distance $d_{k,k} < \frac{R}{3}$ will not have any advantage in being relayed because of their low distance to BS. Furthermore, they are far from cell border users so they are not seen as potential relays. Users with $d_{k,k} < \frac{R}{3}$ will be thus non relayed sources and will not act as potential relays.
- Users with distance $d_{k,k} > \frac{2R}{3}$ are in the cell border and will take advantage in being relayed if a user at mid distance from them and the BS exists. Users with $d_{k,k} > \frac{2R}{3}$ are thus potential relayed sources.
- Users with distance $\frac{R}{3} < d_{k,k} < \frac{2R}{3}$ can act as potential relays for users with $d_{k,k} > \frac{2R}{3}$. Because of their relative low distance from the BS, these users will not be relayed.
- A mobile user with $d_{k,k} > \frac{2R}{3}$ can have only one associated relay in order to lower signaling.

First, each user in the border finds its potential best relay and compares the data rate that it can achieve with the indirect link using this relay to the data rate with the direct link to the BS. It then decides between direct or indirect links. If the user chooses the direct link, it becomes a NRS even if it is in the cell border. An eventual Relay not used by any RS becomes also a NRS. At the end of this first step, we have initialized sets of NRS, R and RS depending on the users cooperation decision (see example 1 in figure 5.3). We assume that a relay can support one or more RS but a RS can have only one relay.

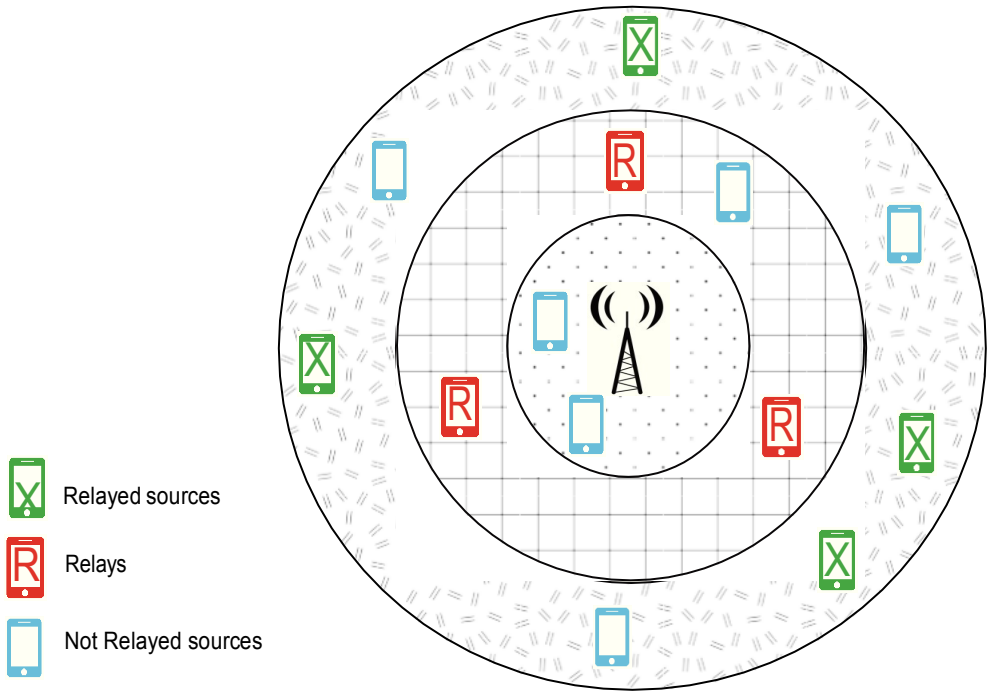

Figure 5.3: Example 2 : Initialized System Model

Mobile users are assumed half-duplex and thus cannot listen and transmit during the same TTI. Full duplex transmission would require that received and transmit data would use distant RBs in the frequency spectrum, to avoid inter-RB interferences. We will not consider that case in this section, but it wil be studied in section 5.5 in order to obtain an upper bound on the performances. The transmission process takes then two phases: In the first TTI, NRS transmit to the BS and RS transmit to their relays while relays are listening. In the second TTI, RS are silent, NRS and R transmit to the BS. R transmit at the same time their own

data and the data of their relayed sources thanks to multi-carrier transmission. For relayed data, the DF method is adopted at the relay.

The objective of our model is to outperform the system without cooperation in minimizing the whole system transmission power subject to a constraint of minimal rate per user. The objective has been chosen as optimizing energy consumption to reduce the overall environmental effects.

We note that the theoretical expressions are performed for a period of one TTI. A NRS k that transmits all TTIs has a transmit power of P_k^j in RB j. However, for a relay transmitting the half of the time, the rate is divided by 2 to have the average rate for one TTI. Considering an average transmit power and an average data rate per TTI, the user rate in bits/s/Hz using the DF scheme for user k and RB **j** can be expressed as:

$$R_k^j = \log_2\left(1 + P_k^j \gamma_{k,k}^j\right), \text{ if k is a not relayed source} \quad (5.1a)$$

$$R_k^j = \frac{1}{2}\min\left\{\log_2\left(1 + P_k^j \gamma_{k,r}^j\right); \log_2\left(1 + P_r^j \gamma_{r,r}^j\right)\right\}, \text{ if k is a relayed source with relay r} \quad (5.1b)$$

$$R_k^j = \frac{1}{2}\log_2\left(1 + P_k^j \gamma_{k,k}^j\right), \text{ if k is a relay} \quad (5.1c)$$

Where P_k^j is the transmission power of user k in RB **j** and $\gamma_{k,k'}^j$ is the channel coefficient gain expressed as:

$$\gamma_{k,k'}^j = \frac{g_{k,k'}^j S_{k,k'}}{L_{k,k'} N_{rb}} \quad (5.2)$$

$g_{k,k'}^j$ is the square Rayleigh fading in RB **j** between user k and user k' if $k \neq k'$, or between user k and the BS if $k = k'$. $L_{k,k'}$ and $S_{k,k'}$ are respectively the pathloss and the shadowing experienced by user k considering their direct links when $k = k'$ and considering the indirect links via user k' when $k' \neq k$. N_{rb} is the noise power per RB.

5.4.2 Problem formulation & Proposed Algorithm

5.4.2.1 Problem Formulation

Our objective is to minimize the whole system transmit power subject to several constraints. If we consider one NRS, one RS and one R having RBs j, j' and j'' respectively, table 5.1 details the consumed transmit power per user per TTI:

	NRS	RS	R
TTI 1	P_{NRS}^{j}	$P_{RS}^{j'}$	0
TTI 2	P_{NRS}^{j}	0	$P_{R}^{j''} + P_{R}^{j''}$
Average Power per TTI	P_{NRS}^{j}	$\frac{1}{2}P_{RS}^{j'}$	$\frac{1}{2}\left(P_{R}^{j'} + P_{R}^{j''}\right)$

Table 5.1: Power expended per user per TTI

The general optimization problem for a system model with K users and N RBs is expressed as:

$$\underset{\mathbf{a},\,\mathbf{b},\,\mathbf{P}}{\text{minimize}} \quad \sum_{k=1}^{K}\sum_{j=1}^{N}\left(1-\frac{b_k}{2}\right)a_{k,k}^{j}P_{k}^{j} + \frac{1}{2}\sum_{k=1}^{K}\sum_{r=1,r\neq k}^{N} b_k\, a_{k,r}^{j}\left(P_{k}^{j}+P_{r}^{j}\right) \tag{5.3a}$$

subject to

$$\sum_{k=1}^{K}\sum_{r=1}^{K} a_{k,r}^{j} \leq 1 \;\forall j, j = 1,..N \tag{5.3b}$$

$$\sum_{r=1}^{K}\sum_{j=1}^{N} a_{k,r}^{j}R_{k}^{j} \geq R_t \;\forall k, k = 1,..K \tag{5.3c}$$

$$a_{k,r}^{j} \in \{0,1\} \;\forall k, r, j \tag{5.3d}$$

$$b_k \in \{0,1\} \;\forall k \tag{5.3e}$$

$$P_{k}^{j} \geq 0 \;\forall k, j \tag{5.3f}$$

where

- $\mathbf{b} = [b_1, b_2, ..., b_K]^T$ is the vector of users decisions of cooperation.

- **P** is the power matrix per user in each RB:

$$\mathbf{P} = \begin{bmatrix} P_1^1 & P_1^2 & \dots & P_1^N \\ P_2^1 & P_2^2 & \dots & P_2^N \\ \vdots & \vdots & \vdots & \vdots \\ P_K^1 & P_K^2 & \dots & P_K^N \end{bmatrix} \tag{5.4}$$

- **a** is the RB allocation matrix per couple of (source, relay) and each RB j:

$$\mathbf{a} = \begin{bmatrix} a_{1,1}^1 & \dots & a_{1,K}^1 & a_{1,1}^2 & \dots & a_{1,K}^N \\ a_{2,1}^1 & \dots & a_{2,K}^1 & a_{2,1}^2 & \dots & a_{2,K}^N \\ \vdots & \vdots & \vdots & \vdots & \vdots & \vdots \\ a_{K,1}^1 & \dots & a_{K,K}^1 & a_{K,1}^2 & \dots & a_{K,K}^N \end{bmatrix} \tag{5.5}$$

- Constraint (5.3e) represents the cooperative decision for user k, $b_k = 1$ if user k is involved in a cooperative manner (k is a relayed source or a relay), $b_k = 0$ otherwise.

- Constraints (5.3b) and (5.3d) represent the RB allocation constraints, $a_{k,k}^j = 1$ means that RB **j** is assigned to the transmission of user k towards the BS. $a_{k,r}^j = 1$ with $k \neq r$ means that RB **j** is assigned to the transmission of user k towards relay r in the first TTI and transmission of relayed data from r to BS in the second TTI. If $a_{k,r}^j = 1$, then $b_k = 1$ and $b_r = 1$.
  We highlight the difference between $a_{k,r}^j$ and $a_{r,k}^j$ for a RB j: for $a_{k,r}^j$, the transmission considers user k as RS and user r as relay. However, for $a_{r,k}^j$ user r is considered as RS when user k is considered as relay.

- Constraint (5.3c) indicates the required target data rate per user R_t.

- Constraint (5.3f) ensures that all powers are positive.

- The first item of the optimization problem (5.34a) represents both the transmit power for a NRS in two TTIs and the transmit power for a relay for its proper data for only one TTI (expressed by the $\frac{1}{2}$ factor). The second

item of the optimization problem represents the transmit power consumed to transmit relayed data.

In this work, the cooperation decision is considered performed as the first step of problem resolution. Then, the optimization problem considering the RB allocation and the power allocation will be solved using the Lagrangian method.
Relaying decision consists in comparing direct link to the BS to the best indirect available link. For this, a potential RS s chooses first the best relay r^* for it as follows:

$$r^* = \max_r \min(\tilde{\gamma}_{s,r}, \tilde{\gamma}_{r,r}) \tag{5.6}$$

with $\tilde{\gamma}_{s,r}$ the average channel coefficient gain between s and r defined as:

$$\tilde{\gamma}_{k,k'} = \frac{1}{L_{k,k'}\ S_{k,k'}\ N_{rb}}$$

Once r^* is found, s compares it with its direct link to the BS. If $\tilde{\gamma}_{s,s} < \min(\tilde{\gamma}_{s,r^*}, \tilde{\gamma}_{r^*,r^*})$, then relaying will be advantageous for s, relaying scheme via r^* is then adopted. Else, relaying is considered not advantageous and s will be a NRS.
The different natures of the constraints makes the problem difficult to solve. Having both continuous and boolean variables makes the problem a combinatorial optimization problem with excessive computational complexity to find the global optimal solution. To put our problem in a resolvable form, we relax the boolean variable $a^j_{k,r}$ to be continuous in $[0, 1]$ based on the time sharing process. A RB is then shared by several users that can have the same RB **j** but not at the same moment. It is proved that relaxing the optimization problem leads to an upper bound solution of the primal optimization problem [38]. It is also proved in [37][63] that the duality gap of an optimization problem is considered insignificant if the number of subcarrier is high[1].
To solve our optimization problem, we propose a suboptimal heuristic based on the dual method [37] that consists to find iteratively the optimal solution for the two following subproblems:

1. The Sub-Optimal Power Allocation subproblem
2. The Sub-Optimal Resource Block Allocation subproblem

[1]We must note that in the final step of problem resolution, $a^j_{k,r}$ are converted to boolean variables (equation (11))

The algorithm 1 presents the proposed iterative algorithm, the details of each step will be detailed in the next sections.

Algorithm 1: Proposed Sub-Optimal algorithm for Relay selection, Resource Block and Power Allocation (Problem(5.3))

1 Sub-Optimal Power Allocation (subproblem (5.13a))
2 Sub-Optimal RB Allocation using resulting powers from step 1 (subproblem (5.20))
Update Lagrangian variable (equation (5.27))
3 **if** condition of convergence is verified (equation (5.28)) **then**
4 The sub-optimal solution is the RB Allocation resulting from step 2 with power values resulting from step 1.
5 **else**
6 return to step 1.

5.4.3 Problem Resolution

The dual method is adopted to resolve theoretically the optimization problem (5.3). Solving the hard primal problem in the dual domain begins by decomposing it into subproblems easier to solve. The master problem distributes to each subproblem the resources it can use and the price to pay. In turn, each subproblem returns to the master problem its solution with the amount of the resources it uses [39] (see figure 5.4).

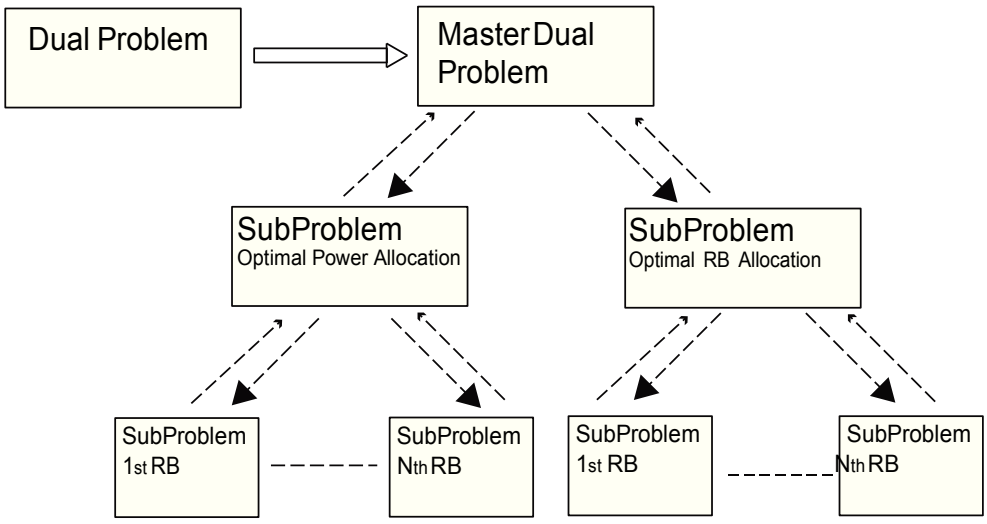

Figure 5.4: Hierarchy of the decomposed dual problem

5.4.3.1 Dual Problem

The Lagrangian function of problem (5.3) is written as:

$$L(\mathbf{a}, \mathbf{b}, \mathbf{P}, \lambda) = \sum_{k=1}^{K} \sum_{j=1}^{N} \left(1 - \frac{b_k}{2}\right) a_{k,k}^{j} P_k^j + \frac{1}{2} \sum_{k=1}^{K} \sum_{r=k}^{K} \sum_{j=1}^{N} b_k a_{k,r}^{j} (P_k^j + P_r^j) - \sum_{k=1}^{K} \sum_{r=1}^{K} \sum_{j=1}^{N} \lambda_k a_{k,r}^{j} R_k^j + \sum_{k=1}^{K} \lambda_k R_t \quad (5.7)$$

where $\lambda = [\lambda_1, \lambda_2, ..., \lambda_K]^T$ is the vector of dual variables associated to the required data rate constraints.

The Lagrangian dual function is then expressed as:

$$g(\lambda) = \begin{cases} \min\limits_{\mathbf{a},\, \mathbf{b},\, \mathbf{P}} L(\mathbf{a}, \mathbf{b}, \mathbf{P}, \lambda) \\ \text{subject to} \\ \sum\limits_{k=1}^{K} \sum\limits_{r=1}^{K} a_{k,r}^{j} \leq 1 \ \forall j \\ a_{k,r}^{j} \in [0..1] \ \forall k, r, j \\ b_k \in [0..1] \ \forall k \\ P_k^j \geq 0 \ \forall k \ \forall j \end{cases} \quad (5.8)$$

The problem can be solved by solving its dual problem as follows:

$$\begin{aligned} &\underset{\lambda}{\text{maximize}} \ g(\lambda) \\ &\text{subject to} \ \lambda_k \geq 0 \ \forall k \end{aligned} \quad (5.9)$$

The problem (5.9) is decomposed into N subproblems at each RB that can be solved independently. The subproblem for each RB **j** can be expressed as:

$$L_j(\mathbf{a}, \mathbf{b}, \mathbf{P}, \lambda) = \sum_{k=1}^{K} \left(1 - \frac{b_k}{2}\right) a_{k,k}^{j} P_k^j + \frac{1}{2} \sum_{\substack{k=1 \\ r=k}}^{K} b_k a_{k,r}^{j} (P_k^j + P_r^j) - \sum_{k=1}^{K} \sum_{r=1}^{K} \lambda_k a_{k,r}^{j} R_k^j \quad (5.10)$$

Subject to:

$$\sum_{k=1}^{K}\sum_{r=1}^{K} a^{j}_{k,r} \leq 1 \ \forall j$$

$$a^{j}_{k,r} \in [0..1] \ \forall k, r, j \tag{5.11}$$

$$b_k \in [0..1] \ \forall k \tag{5.12}$$

$$P^{j}_{k} \geq 0 \ \forall k \ \forall j$$

To solve problem (5.10), a second decomposition is necessary to solve independently the two subproblems (figure 5.4): Sub-Optimal Power Allocation and Sub-Optimal RB Allocation.

5.4.3.2 Sub-Optimal Power Allocation for a given Resource Block Allocation

For a given RB allocation, we aim in this section to find the optimal power allocation. Assuming $a^{j}_{k,r}$ fixed $\forall k, r, j$ and λ_k known $\forall k$, only positive power's constraint remains (equation (5.3f)) and the optimization problem can be expressed as:

$$\underset{\mathbf{P}}{\text{minimize}} \quad \sum_{k=1}^{K}\left(1-\frac{b_k}{2}\right)a^{j}_{k,k}P^{j}_{k} + \frac{1}{2}\sum_{k=1}^{K}\sum_{\substack{r=1\\ r\neq k}}^{K} b_k a^{j}_{k,r}\left(P^{j}_{k}+P^{j}_{r}\right) - \sum_{k=1}^{K}\sum_{r=1}^{K}\lambda_k a^{j}_{k,r} R^{j}_{k} \tag{5.13a}$$

$$\text{subject to } P^{j}_{k} \geq 0 \ \forall k \ \forall j \tag{5.13b}$$

Since only P is a variable, the optimization Lagrangian of this problem is convex by definition and can be written as:

$$L^{bis}_{j}(\mathbf{P}) = \sum_{k=1}^{K}\left(1-\frac{b_k}{2}\right)a^{j}_{k,k}P^{j}_{k} + \frac{1}{2}\sum_{k=1}^{K}\sum_{r\neq k}^{K} b_k a^{j}_{k,r}\left(P^{j}_{k}+P^{j}_{r}\right) - \sum_{k=1}^{K}\sum_{r=1}^{K}\lambda_k a^{j}_{k,r} R^{j}_{k} - \sum_{k=1}^{K} v^{j}_{k} P^{j}_{k} \tag{5.14}$$

where v^{j}_{k} is the Langrangian variable associated to the power constraint. Since the optimization problem (5.14) is convex, the KKT conditions are used to find

its global optimum:

$$\frac{\partial L_j^{bis}}{\partial P_k^j} = 0 \tag{5.15a}$$

$$\nu^j P_k^j = 0 \quad \forall k \tag{5.15b}$$

$$\nu_k^j \geq 0 \quad \forall k \tag{5.15c}$$

Considering the different types of users, we evaluate the optimal transmit power for each user in each RB. This is done by differentiating L_j^{bis} with respect to P, substituting equation (5.1) into equation (5.14) and applying the KKT conditions. Depending on the user's nature, the theoretical optimal power expressions are calculated as follows:

- k is a not relayed source or a relay transmitting its own data in RB j:

$$P_k^j = \left[\frac{1}{\ln(2)}\frac{\lambda_k}{\gamma_{k,k}^j} - 1\right]^+ \tag{5.16}$$

  with $[x]^+ = \max\{0, x\}$.

- k is a relayed source with relay r
  Let us first remind the throughput expression:

$$R_k^j = \frac{1}{2}\min\left\{\log_2\left(1 + P_k^j \gamma_{k,r}^j\right); \log_2\left(1 + P_r^j \gamma_{r,r}^j\right)\right\}$$

  In cooperative mode, the total transmit power is minimized when the source and the relay forward the same amount of data.. Consequently, the rate is the minimum of the rates on the two links (see the equation above). To achieve this, we assume that:

$$P_k^j \gamma_{k,r}^j = P_r^j \gamma_{r,r}^j \tag{5.17}$$

  - Solving problem (5.14) leads to the following expression for the power of the RS k in RB j:

$$P_k^j = \left[\frac{\lambda_k \gamma_{r,r}^j}{\ln(2)(\gamma_{k,r}^j + \gamma_{r,r}^j)} - \frac{1}{\gamma_{k,r}^j}\right]^+ \tag{5.18}$$

– From equation (5.17), we obtain that the power of the relay r for the relayed data of RS k is: :

$$P^j = \frac{\lambda_k \gamma^j_{k,r}}{\ln(2)(\gamma^j_{k,r} + \gamma^j_{r,r})} - \frac{1}{\gamma^j_{r,r}}^+ \tag{5.19}$$

Corresponding to users nature, optimal power expressions are calculated. We can notice that a relay has different power expressions for its own data (equation (5.16)) and for the data it relays (equation (5.19)).

5.4.3.3 Sub-Optimal Resource Block Allocation

The second subproblem to solve is the Optimal RB Allocation using the optimal power allocation studied above. The Lagrangian per RB **j** can be then written as:

$$L(\mathbf{a}, \lambda) = \sum_{k=1}^{K} (1 - \frac{b_k}{2}) a^j_{k,k} P^j_k + \frac{1}{2} \sum_{k=1}^{K} \sum_{r/=k}^{K} b^j_k a^j_{k,r} (P^j_k + P^j_r)$$
$$- \sum_{k=1}^{K} \sum_{r=1}^{K} \lambda_k a^j_{k,r} R^j_k + \sum_{k=1}^{K} \lambda_k R_t \tag{5.20}$$

subject to

$$(5.3b), (5.11) \text{ and } (5.12) \tag{5.21}$$

The Lagrangian dual function is written as follows:

$$g(\lambda) = \min_{\mathbf{a}}(L_j) = \max_{\mathbf{a}}(-L_j)$$

g(λ) can be written as:

$$g(\boldsymbol{\lambda}) = \underset{\mathbf{a}}{\text{maximize}} \sum_{k=1}^{K} \sum_{r=1}^{K} a^j_{k,r} G^j_{k,r} - \sum_{k=1}^{K} \lambda_k R_t \tag{5.22}$$

where $G = [G^j_{k,r}]$ is a $K \times K \times N$ matrix representing the potential gain of couple (k, r) if it earns RB j. The gain function is expressed according to users nature as:

- if k = r and k is a not relayed source:

$$G^{j}_{k,r} = \lambda_k \log_2\left(1 + P^{j}_{k}\gamma^{j}_{k,k}\right) - P^{j}_{k} \tag{5.23}$$

- if k = r and k is a relay transmitting its own data in RB j:

$$G^{j}_{k,r} = \frac{\lambda_k}{2}\log_2\left(1 + P^{j}_{k}\gamma^{j}_{k,k}\right) - \frac{1}{2}P^{j}_{k} \tag{5.24}$$

- if k is a relayed source and k /= r:

$$G^{j}_{k,r} = \frac{\lambda_k}{2}\log_2\left(1 + P^{j}_{k,r}\gamma^{j}_{k,r}\right) - \frac{1}{2}\left(P^{j}_{k,r} + P^{j}_{r,r}\right) \tag{5.25}$$

The gains are calculated for each RB j, then, **j** is allocated to couple (k, r) maximizing its gain on it:

$$a^{j}_{k,r} = \begin{cases} 1 \text{ for } (k, r) = \arg\max\limits_{(k,\,r)} G^{j}_{k,r} \\ 0 \text{ otherwise} \end{cases} \tag{5.26}$$

5.4.3.4 Lagrangian Variable Update

The last step in our algorithm is to update dual variables and to test the convergence condition for solving problem (5.9). Using results of current iteration t, λ for iteration t + 1 is updated for each user as follows:

$$\lambda_k(t+1) = \left[\lambda_k(t) + \eta_k(t)\left(R_t - \sum_{r=1}^{K}\sum_{j=1}^{N} a^{j}_{k,r}(t)R^{j}_{k}(t)\right)\right]^{+} \tag{5.27}$$

where η is the diminishing step size as the update of dual variable is performed according to the diminishing step approach [17] for each user k. Equation (5.27) shows that if user k has a data rate higher than R_t, it has to reduce its λ_k and then to reduce its power consumed to achieve the required data rate. On the other hand, if user k has a lower data rate than R_t, the dual variable update allows it to increase its λ_k and so its powers' value, it can then reach R_t by earning more RB or by raising its consumed power amount.

The algorithm is considered to converge when the variation of λ_k is negligible for

all k as follows:

$$\frac{\lambda_k(t+1) - \lambda_k(t)}{\lambda_k(t+1)} < \varrho \ \forall k \tag{5.28}$$

where ϱ is set close to zero.

5.4.4 Performance Evaluation

Simulations are presented in this section to analyze the proposed approach's performance. We consider a single circular cell with radius R = 1 Km, K users and N RBs that we vary along simulations. We assume a total bandwidth[2] B = 20 MHz equitably divided between the RBs. Rayleigh channels with slow fading are considered and the power density for AWGN noise is $N_0 = -174$ dBm/Hz. Users are uniformly distributed in the cell and suffer from log-normal shadowing with standard deviation equal to 6 dB and from pathloss according to the LTE model with frequency F = 2.6 GHz: $L_{dB}(d_{k,k'}) = 128.1 + 37.6.\log_{10}(d_{k,k'})$ where $d_{k,k'}$ is the distance in Km from user k to user k'. If $k = k'$, $d_{k,k'}$ is the distance of user k to the BS.

Users are divided into different sets as explained in section 5.4.1 (potential RS, NRS and potential R) depending on their distance from the BS.

The step size for λ_k is set to $\eta_k = \frac{\lambda_k}{\sqrt{t}}$ for $t < 2000$ where t is the iteration index. When t exceeds 2000, η_k becomes invariant. ϱ from equation (5.28) is set to 0.001.

For classical mobile cellular networks, the transmit power of a mobile user is generally of the order of 21 dBm. Considering such emitted power and for cell radius of 1 Km, expected data rates for cell border users are lower than 2 bits/s/Hz. Based on this observation, R_t is varied in the simulations in the range [0.5..1.5] bits/s/Hz. Results are averaged over 1000 simulations to get realistic results.

In the following, the proposed solution is compared to the optimal exhaustive solution for a special case with low users and RB number for evaluation. Then, convergence of the proposed solution is studied and the achieved performances are presented.

[2]Please note that we do not use RB number compliant with the LTE standard and that the total bandwidth is fixed and does not vary for all simulations.

5.4.4.1 Optimality evaluation

To find the optimal solution, exhaustive research is necessary for both RB allocation and power allocation. The best solution minimizing the system transmit power is then equal to the optimal solution. The complexity of this research is high and grows with user and RB number. For a given number of users, all possible combinations of RB allocations have to be studied. Then, for each RB allocation, optimal power allocation for all users is established ensuring required target data rate. The optimal solution offering the lowest total system power is finally identified. All possible source-relay pairs must be considered which increases again the complexity of the optimal solution search.

With 2 users where user 1 is relay and user 2 is relayed source, the number of RB allocation's possible combinations is

$$M = \sum_{i=1}^{N-1} C_N^i = 2^N - 2 \tag{5.29}$$

where N is the number of RB. Having N = 8 RBs, we have M = 254, for N = 16 RBs, M = 65 534 and for N = 32 RBs. Thus M exceeds 10^9 possible RB allocation.

If we consider three users when one is a not relayed source, one is a relayed source and one is a relay, the number of RB allocation's possible combinations is

$$L = \sum_{i=1}^{N-2} C_N^i \sum_{j=1}^{N-i} C_{N-i}^j = 3^N - 2^N - 2^{N+1} + 3 \tag{5.30}$$

For N = 8 RBs, L = 5 796, for N = 16 RBs, L = 42 850 116 and for N = 32 RBs, L exceeds 10^{15} possible RB allocation.

The optimal power allocation via waterfilling method is then performed for each possible RB allocation respecting the required quality of service.

Finding the optimal solution requires high computational cost and high time period that can not be realized in realistic cellular networks. Suboptimal solutions are therefore involved to approach the optimal solution. Table 5.2 compares system transmit powers with our proposed solution and with the optimal solution for 2 users and 8 RBs. Both system models with and without relaying are considered. We can remark that the proposed solution approaches the optimal solution. The

difference of proposed model applied to system without relaying is only 1% comparing to the optimal solution. For the model with relay, the difference is 17%. The proposed solution can reduce the system transmit power by 39% comparing to the optimal solution without relaying. Applying the proposed solution to a system model with a higher number of users especially in cell edge can be very interesting in order to decrease system energy consumption[3].

Proposed With Relay	Exhaustive With Relay	Proposed Without Relay	Exhaustive Without Relay
7.16	6.24	9.39	9.34

Table 5.2: System transmission power (dBm)

5.4.4.2 Convergence Analysis

In this section, the convergence rate of the proposed algorithm is studied. A simulation is considered convergent if it respects the Lagrangian variable variation constraints (equation (5.28)) and the required data rate per user constraint as $R_k = R_t \pm 0.1\ R_t\ \forall k$. The convergence rate is studied for 18 users and different RBs numbers and R_t values. The minimal convergence rate is 30% for 60 RBs and R_t = 1.5 bits/s/Hz and it can reach 65% for 192 RBs for the same R_t. The convergence rates can be justified by the hard convergence constraints. If we relaxed these constraints by expanding the R_t admissible variation range for example, convergence rates would be improved. Then, we can observe that the convergence rate increases when the number of RBs grows, this can be explained by the growth of the frequency diversity. Indeed, users are more likely to find RB with good channel gains, and thus to achieve their required data rate.

5.4.4.3 Achieved Performances

The system transmit power for different users and RB numbers and various R_t values is presented in this section. Figures 5.5 and 5.7 show the system transmit power for respectively 18 and 30 users considering all simulations. Figures 5.6 and

[3]We note that gain values consider power values in mW and not in dBm.

5.8 show results for a set of simulations having at least one relay. This differentiation is made to highlight the gain of the proposed algorithm that can be partially hidden because some simulations can have zero RS user.

The gain offered by the proposed algorithm reaches 21% for 18 users, 192 RBs and R_t = 1.5 bits/s/Hz as global gain. If we consider only relaying cases, this gain achieves 51% in the same conditions. For R_t = 1 bits/s/Hz and N = 192 RBs, the global gain is 18% and the relay gain reaches 48%. The gain is more significant when the user number increases, this is due to the number of cell edge users transmitting in cooperation mode. This is shown by the important gain realized with 30 users (figure 5.9): the minimal global gain is 12.8% for R_t = 0.5 bits/s/Hz and N = 384 RBs. The system transmit power can be saved until 57% for R_t = 1 bits/s/Hz and N = 576 RBs for the relaying schemes.

We can also observe that the system transmit power decreases when the number of RB grows, this is produced thanks to the frequency diversity. When a high number of RB is available, the RB allocation step can be established more efficiently and the transmit power is then saved.

From simulation results, it is shown that the proposed algorithm offers better performance comparing to the model without relaying. The transmit power can be saved especially in the cell edge. This result can be exploited to reduce interference level in a multicell system model.

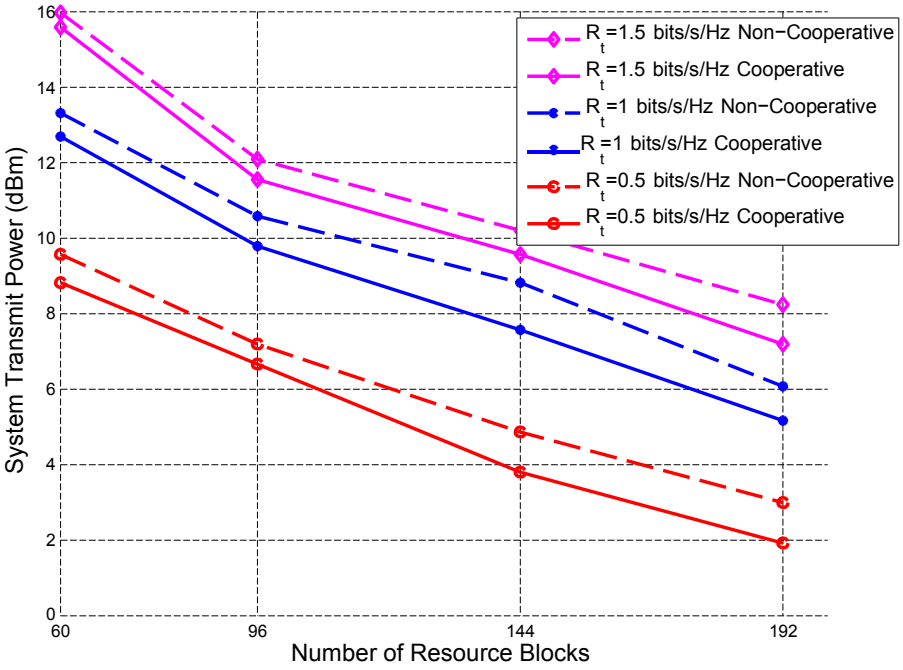

Figure 5.5: System transmit power for 18 users

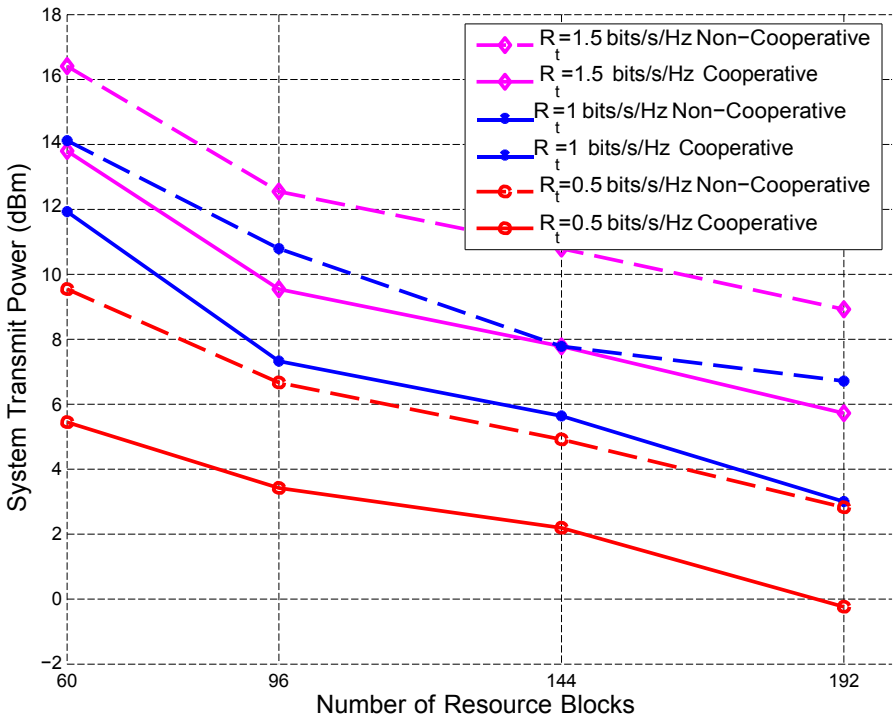

Figure 5.6: System transmit power for 18 users relaying only

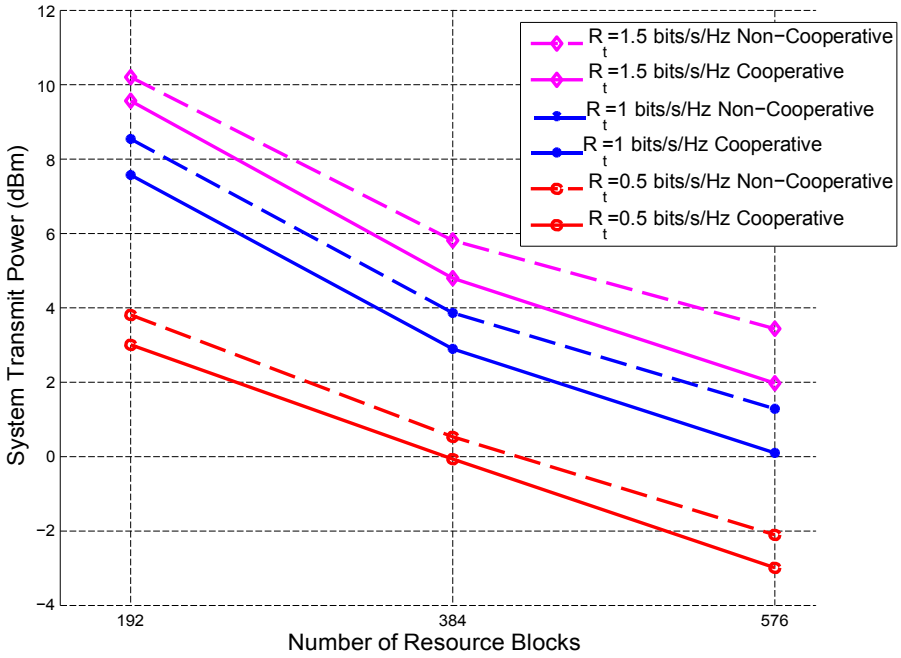

Figure 5.7: System transmit power for 30 users

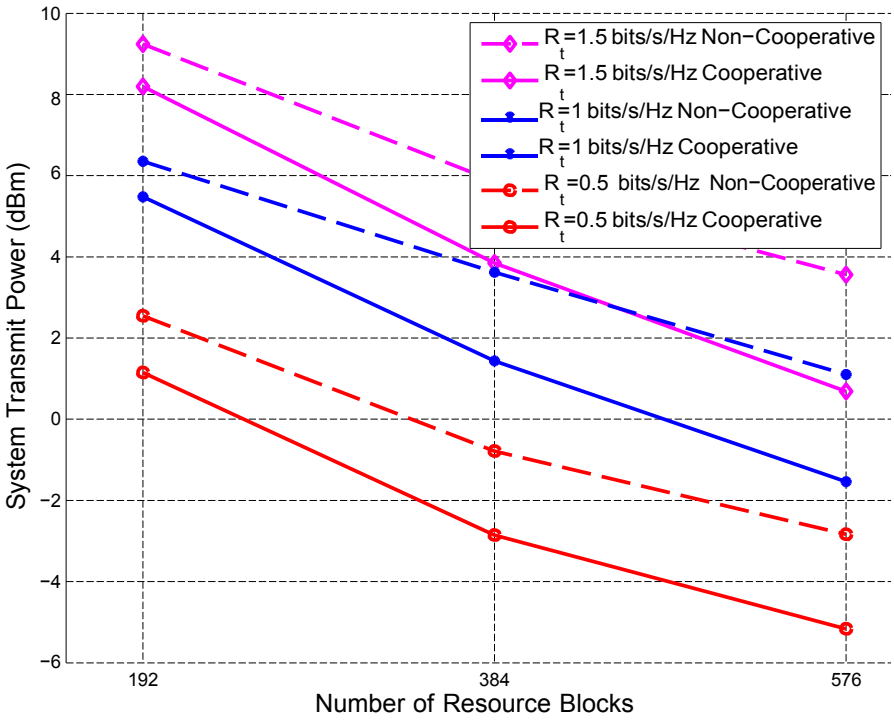

Figure 5.8: System transmit power for 30 users relaying only

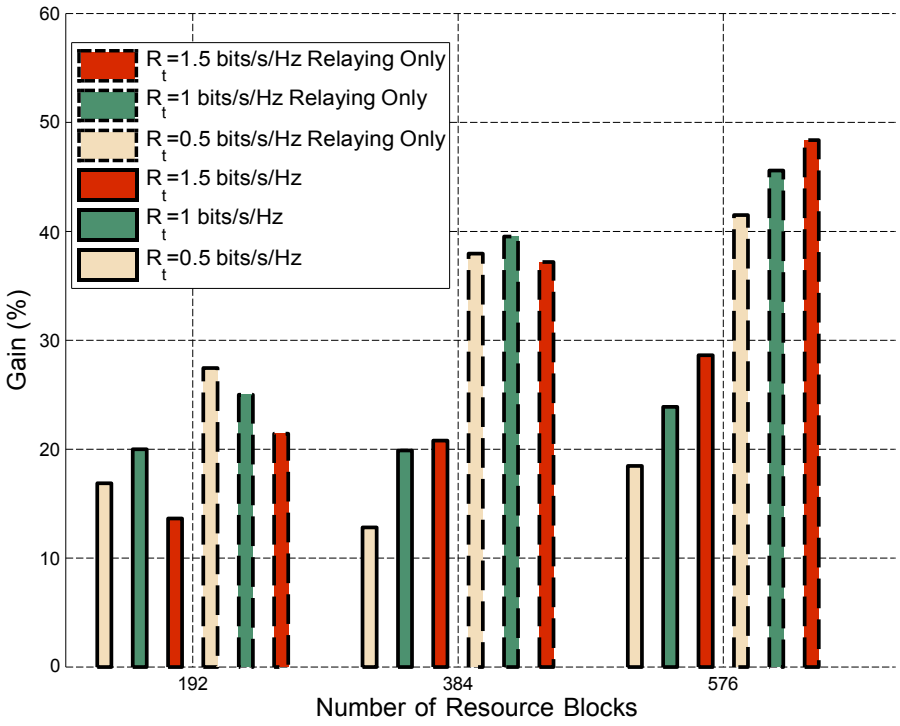

Figure 5.9: Gain for 30 users Global and Relaying only

5.5 Joint Power Allocation, Relay Selection and RB Allocation

5.5.1 System Model

In this section, Relay Selection is studied as an optimization variable in addition to power and RB allocation. It is not an initialization step as in the previous section. Users can transmit directly to the BS or via relay cooperation as explained in figure 5.1. In the joint relay selection and resource allocation, a relay can support one or more RS and a RS can be relayed by one or more relays but in different RBs. For a specific RB, only one relay is assigned for cooperation.

Transmission is studied for two cases: full duplex and half duplex. In the full-duplex case (figure 5.10b), relays can listen and transmit in the same TTI but in different RBs. Thus, a NRS transmits during all TTIs. One R can also transmit its own data during all TTIs in its RBs. Cooperative transmission requires two TTIs, in the first TTI, RS transmits to R. In the second TTI, R uses the same

RB to transmit relayed data to the BS.

Moreover, in the half-duplex case (figure 5.10a), a user can not listen and transmit in the same TTI. NRS do not need cooperation and transmit data to the BS in all TTIs. However, cooperative transmission is performed in two TTIs: in the first TTI, RS transmit to their relays, while relays are listening. In the second TTI, RS are silent and relays transmit to the BS their own data multiplexed to the source's relayed data. RBs used by the source in the first TTI are used by the relay in the second TTI to carry relayed data to the BS.

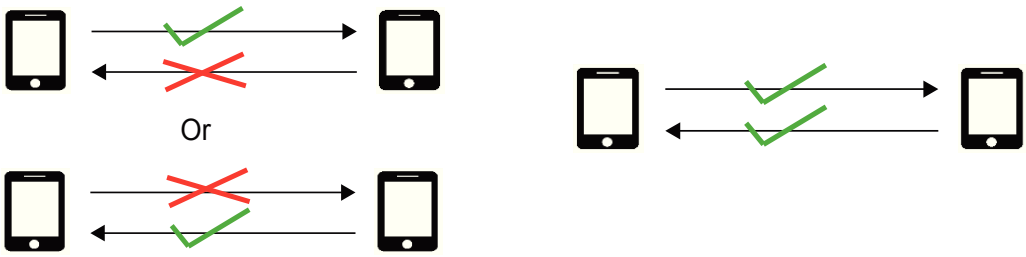

(a) Half Duplex Communication

(b) Full Duplex Communication

Figure 5.10: Duplex Communication

The full-duplex case is advantageous comparing to the half-duplex case since relays can transmit their own data while listening to RS. In the theoretical expressions, we introduce the HF variable that indicates the considered case: HF= 1 for full-duplex and HF= $\frac{1}{2}$ for half-duplex. If we consider one NRS, one RS and one R having one RB each, respectively j, j' and j'', table 5.3 details the necessary power to transmit data to the BS for both half and full-duplex cases.

	Half-duplex			Full-duplex		
	NRS	RS	R	NRS	RS	R
TTI1	P_{NRS}^{j}	P_{RS}^{j}	0	P_{NRS}^{j}	P_{RS}^{j}	$P_{R}^{j''}$
TTI2	P_{NRS}^{j}	0	$P_{R}^{j} + P_{R}^{j}$	P_{NRS}^{j}	0	$P_{R}^{j} + P_{R}^{j}$

Table 5.3: Power expended per user per TTI

The optimization objective is always to minimize the transmit system power while ensuring a minimal data rate per user. The user rate using the DF scheme for

user k and RB **j** can be expressed as:

- k is a not relayed source

$$R_k^j = \log_2\left(1 + P_k^j \gamma_{k,k}^j\right) \tag{5.31}$$

- k is a relay and RB **j** is used to transmit its own data

$$R_k^j = HF \log_2\left(1 + P_k^j \gamma_{k,k}^j\right) \tag{5.32}$$

- k is a relayed source by relay r

$$R_k^j = \frac{1}{2} \min\left\{\log_2\left(1 + P_k^j \gamma_{k,r}^j\right); \log_2\left(1 + P_r^j \gamma_{r,r}^j\right)\right\} \tag{5.33}$$

The same notation of previous section are used.

5.5.2 Problem Formulation

As the relay selection will be resolved in the optimization problem, the general optimization problem for K users, K potential relays and N RBs cas be expressed as follows:

$$\underset{\mathbf{a,\ b,\ P}}{\text{minimize}} \quad \sum_{k=1}^{K}\sum_{j=1}^{N}\left(1-b_k(1-HF)\right)a^{j}_{k,k}P^{j}_{k}+\frac{1}{2}\sum_{k=1}^{K}\sum_{r=1,r\neq k}^{K}\sum_{j=1}^{N}b_k a^{j}_{k,r}\left(P^{j}_{k}+P^{j}_{r}\right) \tag{5.34a}$$

subject to

$$\sum_{k=1}^{K}\sum_{r=1}^{K} a^{j}_{k,r} = 1 \quad \forall j, j = 1,..N \tag{5.34b}$$

$$\sum_{r=1}^{K}\sum_{j=1}^{N} a^{j}_{k,r}R^{j}_{k} \geq R_t \quad \forall k, k = 1,..K \tag{5.34c}$$

$$a^{j}_{k,r} \in \{0,1\} \quad \forall k, r, j \tag{5.34d}$$

$$b_k \in \{0,1\} \quad \forall k \tag{5.34e}$$

$$P^{j}_{k} \geq 0 \quad \forall k, j \tag{5.34f}$$

The first term of problem (5.34) traduce the necessary transmit power for direct links to BS: NRS and relays transmitting their own data. The second term of (5.34) traduce the necessary power to transmit relayed data.

For resolution, the same assumptions are adopted and the boolean variables $a^{j}_{k,r}$ and b_k are relaxed to be continuous in [0..1] as detailed in section 5.4.2.1. To solve our optimization problem, we propose a suboptimal heuristic based on the dual method [37] that consists to find iteratively (figure 5.4) the optimal solution for the two following subproblems:

1. The Sub-Optimal Power Allocation subproblem
2. The Sub-Optimal Relay selection & Resource Block Allocation subproblem

The iterative proposed algorithm for resolution is presented in algorithm 2.

Algorithm 2: Proposed Sub-Optimal algorithm for Relay selection, Resource Block and Power Allocation (Problem(5.34))

1 Sub-Optimal Power Allocation (subproblem (5.34))
2 Sub-Optimal Relay Selection and RB Allocation using resulting powers from step 1 (subproblem (5.41))
3 Update Lagrangian variable (equation (5.27))
4 **if** condition of convergence is verified (equation (5.28)) **then**
5 The sub-optimal solution is the Relay Selection and RB Allocation resulting from step 2 with power values resulting from step 1
6 **else**
7 return to step 1

5.5.3 Problem resolution

5.5.3.1 Dual Problem

The Lagrangian function of problem (5.34) is written as:

$$L(\mathbf{a}, \mathbf{b}, \mathbf{P}, \lambda) = \sum_{k=1}^{K} \sum_{j=1}^{N} \left(1 - b_k(1 - HF)\right) a_{k,k}^{j} P_k^j + \frac{1}{2} \sum_{k=1}^{K} \sum_{r \neq K}^{K} \sum_{j=1}^{N} b_k a_{k,r}^{j} \left(P_k^j + P_r^j\right) - \sum_{k=1}^{K} \sum_{r=1}^{K} \sum_{j=1}^{N} \lambda_k a_{k,r}^{j} R_k^j + \sum_{k=1}^{K} \lambda_k R_t \tag{5.35}$$

where $\lambda = [\lambda_1, \lambda_2, ..., \lambda_K]^T$ is the vector of dual variable associated to the required data rate constraint.

The Lagrangian dual function is then expressed as:

$$g(\lambda) = \begin{cases} \min\limits_{\mathbf{a},\ \mathbf{b},\ \mathbf{P}} L(\mathbf{a}, \mathbf{b}, \mathbf{P}, \lambda) \\ \text{subject to} \\ a_{k,r}^{j} \in [0, 1] \ \forall k, r, j \\ b_k \in [0, 1] \ \forall k \\ \text{constraints (5.34b) and (5.34f)} \end{cases}$$

The problem can be solved by solving its dual function by maximizing $g(\lambda)$ subject to $\lambda_k \geq 0 \ \forall k$.

The problem (5.35) is decomposed into N subproblems at each RB that can be

solved independently. The subproblem for each RB **j** can be expressed as:

$$L_j(\mathbf{a},\mathbf{b},\mathbf{P},\lambda) = \sum_{k=1}^{K}(1-b_k(1-HF))a^j_{k,k}P^j_k + \frac{1}{2}\sum_{\substack{k=1\\ r\neq K}}^{K} b_k a^j_{k,r}(P^j_k + P^j_r) - \sum_{k=1}^{K}\sum_{r=1}^{K}\lambda_k a^j_{k,r}R^j_k \quad (5.36)$$

subject to

$$a^j_{k,r} \in [0,1]\ \forall k,r,j; \quad (5.37)$$

$$b_k \in [0,1]\ \forall k; \quad (5.38)$$

(5.34b) and (5.34f)

To solve problem (5.36), a second decomposition step is necessary to solve independently the two subproblems: Sub-Optimal Power Allocation and Sub-Optimal relay selection and RB Allocation.

5.5.3.2 Sub-Optimal Power Allocation for a given Resource Block Allocation

For a given RB allocation, we aim in this section to find the optimal power allocation. Assuming $a^j_{k,r}$, and b_k fixed $\forall k,r,j$, only the positive power constraint remains (equation (5.34f)) and the optimization problem can be expressed as:

$$\underset{\mathbf{P}}{\text{minimize}}(L_j)$$

$$\text{subject to (5.34f)} \quad (5.39)$$

Since only P is a variable, the optimization Lagrangian of this problem is convex by definition and can be written as:

$$L^{bis}_j(\mathbf{P}) = L_j(\mathbf{P}) - \sum_{k=1}^{K} v^j_k P^j_k \quad (5.40)$$

Where v^j_k is the Langrangian variable associated to the power constraint (5.34f). Using the Karush-Kuhn-Tucker (KKT) conditions, the optimal transmission power

is evaluated depending on users nature. Since users can have different natures for different RBs, power is estimated for all possibilities. For each RB, a user k has different power expressions whether it is a not relayed source, a relayed source or a relay. The power expressions are described by equations (5.16), (5.18) and (5.19) using the assumption (5.17) as detailed in section 5.4.3.2.
Power expressions will be used in the next section to find the best transmission scheme. Direct or cooperative transmission will be decided depending on the transmission power and the target rate required per user. For cooperative transmission, optimal relay selection is also performed to assign source-relay pairing.

5.5.3.3 Sub-Optimal Relay selection & Resource Block Allocation

In this section, both relay selection and RB allocation are studied. Knowing the power values, the Lagrangian dual function is written as follows:

$$g(\lambda) = \min_{\mathbf{a}}(L_j) = \max_{\mathbf{a}}(-L_j)$$

$$\text{subject to (5.34b), (5.37) and (5.38)} \tag{5.41}$$

$g(\lambda)$ can then be written as:

$$g(\boldsymbol{\lambda}) = \underset{\mathbf{a}}{\text{maximize}} \sum_{k=1}^{\bar{K}} \sum_{r=1}^{\bar{k}} a^{j}_{k,r} G^{\mathbf{j}}_{k,r} - \sum_{k=1}^{\bar{K}} \lambda_k R_t \tag{5.42}$$

where $G = [G^{j}_{k,r}]$ is a $K \times K \times N$ matrix presenting the potential gain of couple (k, r) if it earns RB j. Gain's expressions for RB $\mathbf{j}$ are detailed as follows:

- k is a not relayed source:

$$G^{j}_{k,k} = \lambda_k \log_2\left(1 + P_{k\,j}\,\gamma_{k,k\,j}\right) - P_{k\,j} \tag{5.43}$$

- k is a relay transmitting its own data:

$$G^{j}_{k,k} = HF\ \lambda_k \log_2\left(1 + P_{k\,j}\,\gamma_{k,k\,j}\right) - HF\ P_{k\,j} \tag{5.44}$$

- k is a relayed source by relay r

$$G^{j}_{k,r} = \frac{\lambda_k}{2}\log_2\left(1 + P^{j}_{k,r}\gamma^{j}_{k,r}\right) - \frac{1}{2}\left(P^{j}_{k,r} + P^{j}_{r,r}\right) \tag{5.45}$$

At the beginning, all users are considered NRS. For each RB j, potential gains are calculated for all possible pairs of source k and relay r. **j** is assigned to couple $(k,r)^*$ maximizing the gain:

$$a^{j}_{k,r} = \begin{cases} 1 \text{ for } (k,r)^* = \arg\max_{(k,r)} G^{j}_{k,r} \\ 0 \text{ otherwise} \end{cases} \tag{5.46}$$

If k = r, direct transmission is considered and $b_k = 0$, else if k /= r, then cooper-
ation is investigated, thus $b_k = 1$ and $b_r = 1$. Users nature are updated in each allocation.

5.5.3.4 Lagrangian Variable Update

As in section 5.4, Lagrangian variable update is performed corresponding to equation (5.27) based on the diminishing step method.

5.5.4 Performance evaluation

In this section, simulation results are presented for the joint relay selection, RB and power allocation problem. The same assumptions as in section 5.4.4 are considered for cell characteristics, users' distribution, pathloss, shadowing, fading and diminishing step range. Results are averaged over 1000 simulations for variant numbers of users and RBs.

Figures 5.11 and 5.12 show the system transmit power for 18 users for a target required data rate of R_t = 1 bits/s/Hz and R_t = 1.5 bits/s/Hz respectively. Simulations are performed for both system models considering full-duplex and half-duplex schemes in function of the number of RBs. Comparing to a non-cooperative model, system performances are improved with the proposed algorithm and the transmit power is clearly reduced. For the half-duplex case, the proposed algorithm offers a high gain up to 36% for R_t = 1.5 bits/s/Hz and up to 49% for R_t = 1 bits/s/Hz. Moreover, for the full-duplex case, the gain is around 62% for

R_t = 1.5 bits/s/Hz and around 70% for R_t = 1 bits/s/Hz.

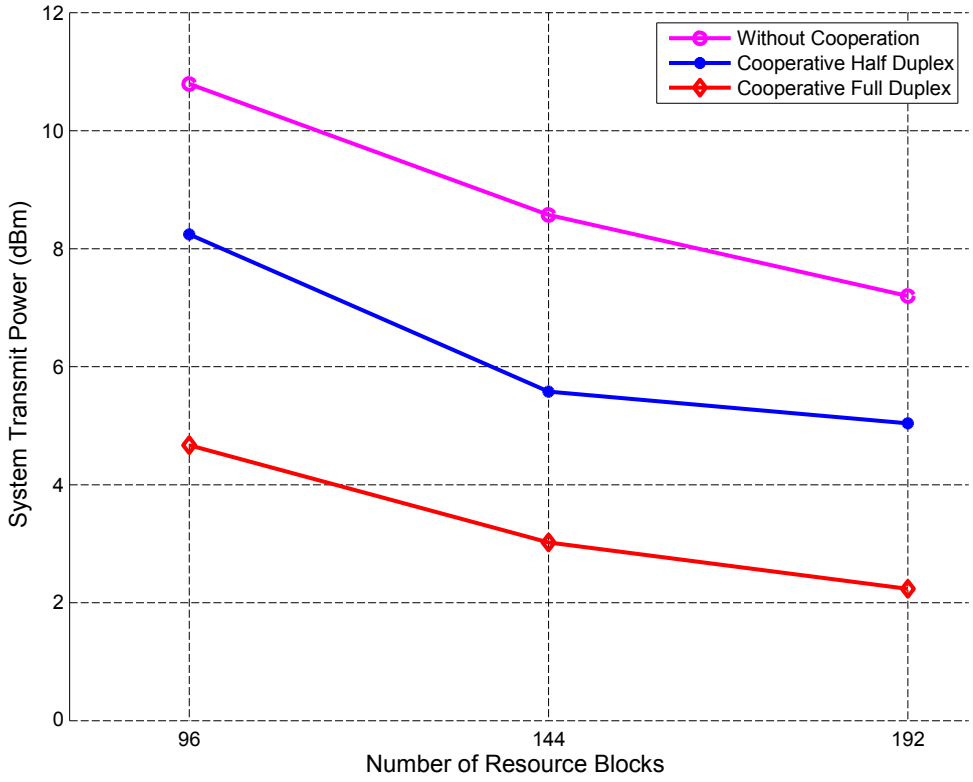

Figure 5.11: System Transmit Power: 18 users, R_t = 1 bits/s/Hz

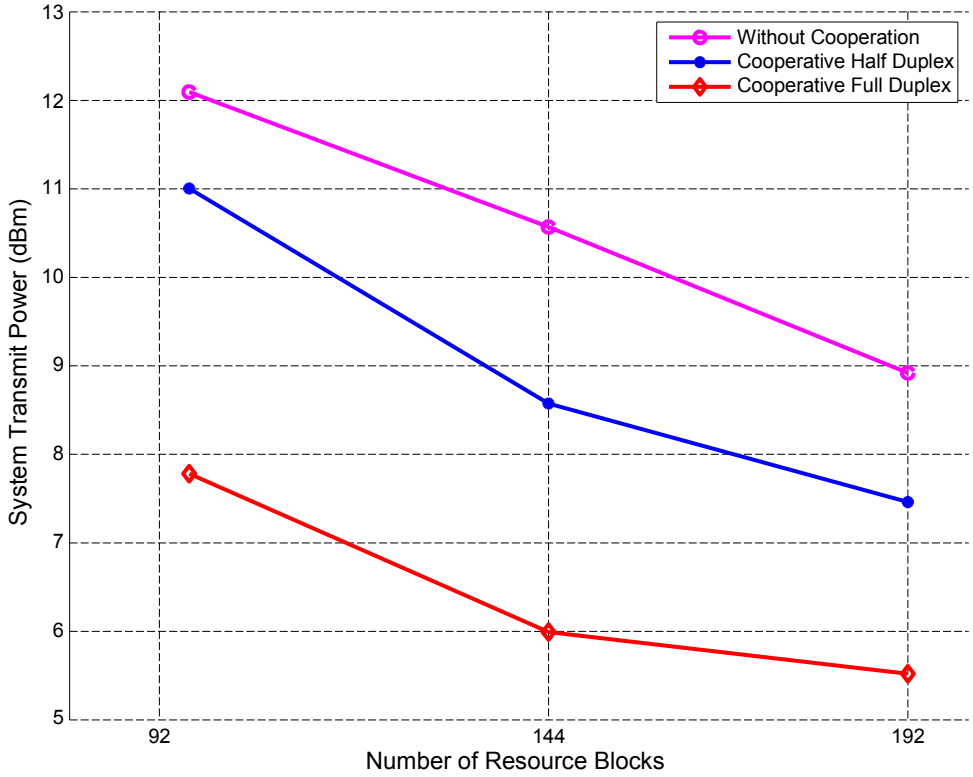

Figure 5.12: System Transmit Power: 18 users, R_t = 1.5 bits/s/Hz

The percentage of users nature are shown in table 5.4. For the same model (half or full-duplex), we can note that the percentage of relays remains invariant even if the number of RBs or the value of R_t change. However, when the required data rate R_t value grows, cooperation is more often required for the optimal solution minimizing the transmit system power, and then the number of relayed sources increases. The NRS number decreases consequently. Comparing half-duplex to full-duplex, table 5.4 shows that the number of NRS decreases considerably. This can be justified by the fact that a user is considered RS if it relays data in at least one RB.

5.6 Proposed Methods Comparison

In this section, the performances of the two proposed half-duplex methods are studied for comparison:

	RBs	NRS(%)	RS(%)	Relay(%)
Half-Duplex				
R_t = 1 bits/s/Hz	96	25	44	30
	144	20	47	31
	192	22	47	30
R_t = 1.5 bits/s/Hz	96	19	46	33
	144	21	48	30
	192	16	49	34
Full-Duplex				
R_t = 1 bits/s/Hz	96	15	48	37
	144	12	51	37
	192	11	52	37
R_t = 1.5 bits/s/Hz	96	12	49	39
	144	10	52	38
	192	9	52	38

Table 5.4: User nature percentage

- Proposed Method 1: The first proposed method is the **Joint power and RBs allocation** detailed in section 5.4. For this method, we remind that users are divided into three areas in the cell (see figure 5.2) where only users in the cell edge can be eventually relayed by users in the relays' area. According to this decomposition, the pairing step to associate relayed sources to their relays is performed as an initialization step based on the achievable data rate for direct link to the BS or indirect link through available relays. Then, the optimization problem to minimize the whole system power is formulated and resolved iteratively. The optimization aims to find the optimal power allocation and the RBs allocation to fixed pairs of source and relay.
- Proposed Method 2: The second proposed method is the **Joint Power allocation, Relay Selection and RBs allocation** studied in section 5.5. Comparing to the first method, the relay selection become an optimization variable and no longer an initialization step. All users can thus be relayed or not, independently of their location in the cell. The optimization problem is formulated aiming to the same objective of minimizing the transmit system power. Two subproblems are resolved iteratively to find the optimal power allocation and the optimal joint relay selection and RBs allocation.

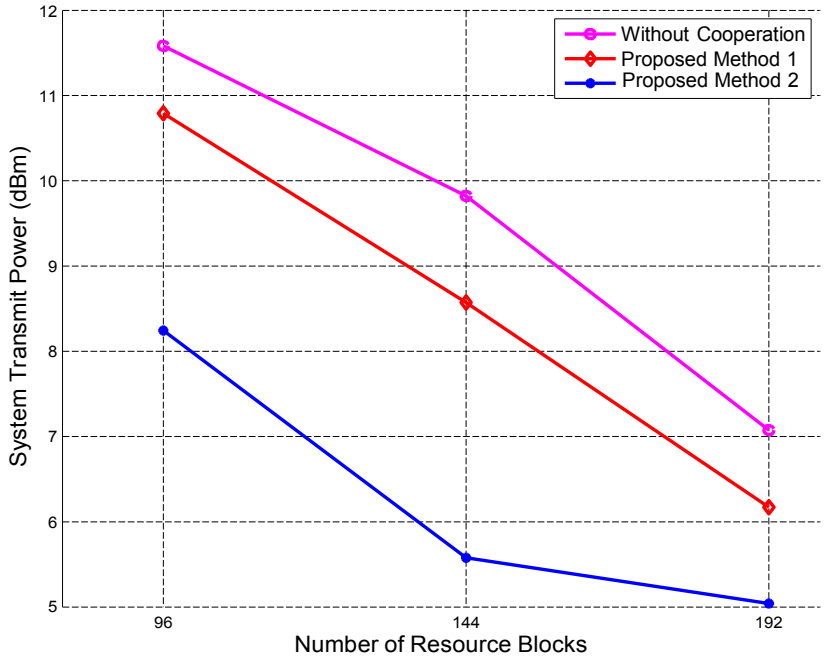

Figure 5.13: System Transmit Power: 18 users, R_t = 1 bits/s/Hz

The comparison is performed for 18 half duplex users (figure 5.10a) and varying RBs number. Figure 5.13 shows the system transmit power for the proposed methods studied in addition to the non cooperative scheme. Simulation results show that the proposed method 2 offers better results than the proposed method 1. This can be justified by the fact that optimizing the relay selection in the optimization process can be more efficient comparing to performing it before as an initialization. Optimizing all variables jointly offers then up to 40% of gain comparing to non cooperative scheme. We note that the proposed method 1 offers also a significant gain comparing to model without relaying up to 29%. However, adding the relay selection as an optimization variable makes resolution more complex.

5.7 Conclusion

In this chapter, we have studied resource allocation for relayed uplink transmission in OFDMA systems. Compared to previous published results, our system model considers mobile relays that have to transmit through frequency multiplexing their own data as well as relayed data. Two system models have been studied: a joint

power and RB allocation problem and a joint relay selection, RB and power allocation problem.

For the joint power and RB allocation problem, users are divided into sectors depending on their distance from the BS and as an initialization step, the BS determines users that will have direct transmission (Not Relayed Sources), users that will be relayed (Relayed Sources) and users acting as Relays for them. In this system, a RS can have only one associated relay in order to lower signalization load. When the BS has determined NRS, RS and R sets, a joint optimization problem minimizing the total system transmit power is proposed.

The second studied problem is a joint relay selection, RB and power allocation problem. The pairing step between relayed sources and relays is performed dynamically and resolved as an optimization variable without any initialization. A source can then be relayed by one or more relays. In this optimization problem, both half duplex and full duplex cases have been studied.

For the two considered problems, the optimization objective has been chosen to reduce environmental effects and save battery life by minimizing the system transmit power. Quality of service is also considered while power minimization is conducted with a constraint that all data rates must be higher that a certain threshold. For each problem to resolve, the primal optimization problem has been decomposed into subproblems solved in an iterative manner. Dual decomposition and subgradient methods have been used for this purpose. In the following chapter, the optimization problem will be extended to the multiple antennas case.

Chapter 6

Resource Allocation in Cooperative OFDMA MIMO system with Multiplexing Mobile Relays

6.1 Introduction

This chapter extends the results from Chapter 5 on resource allocation for an uplink OFDMA system with multiplexing relays. The system model is similar to that proposed in section 5.5 but with multiple antennas nodes. The objective of this chapter is to study the improvement gain of spatial diversity when users and BS are equipped by multiple antennas. The resource allocation optimization problem is formulated to minimize the transmit system power while ensuring a target data rate per user. The optimization aims to solve relay selection, power allocation and RBs allocation. The main contribution of this chapter is to solve these three features in the same optimization problem. In addition, the relays in the studied system model are mobile users having their own data to transmit to the BS. Resolving an optimization problem with such relays nature can be considered as a novelty. Moreover, for power optimization at each user, we compare different power control methods as equal power allocation and beamforming. In the next sections, Multiple Input Multiple Output (MIMO) are presented, the system model

is detailed as well as the resolution steps. Simulation resulats are finally shown and discussed.

6.2 State of the art

The wireless communication environment is very constrained. The transmitted data suffers from several environmental effects such as path loss effect, fading, interference, in addition to the limited available bandwidth. Wireless system nature yields then to a significant challenge to satisfy QoS requirements and to provide higher spectral efficiency. Wireless systems aims to provide high quality services at low cost.

In this context, relaying techniques are considered to improve system performances by deploying relay stations having a lower cost than BSs and covering areas suffering from bad channel conditions like the cell edges. Simple mobile users can also be investigated as relays and suggest an efficient solution without needing any additional infrastructure. Standards has specified topology and behavior of fixed relays [12] when dynamic mobile relays are an important feature for the 5^{th}G of wireless systems. Relaying technologies are detailed in the previous chapter (section 5.2).

Moreover, multiple antenna systems become the current trend in many of the wireless technologies. Comparing to Single Input Single Output (SISO) classical systems, MIMO systems can offer a great improvement. The capacity of a MIMO channel with n transmit and receive antennas is proportional to n [64]. Having multiple antennas in the system provides multiple propagation paths (see figure 6.1). If the same information is transmitted by the different antennas of the same user, MIMO systems offer spatial diversity and improve system reliability. However, if different portions of the data are transmitted in different antennas, spatial multiplexing is used to provide additional degrees of freedom and improve the system throughput. Diversity and degree of freedom can be expressed as

$$\text{diversity} = L_t \times L_r \tag{6.1}$$

$$\text{degree of freedom} = \min\{L_t, L_r\} \tag{6.2}$$

where L_t and L_r are the number of transmit and the receive antennas, respectively.

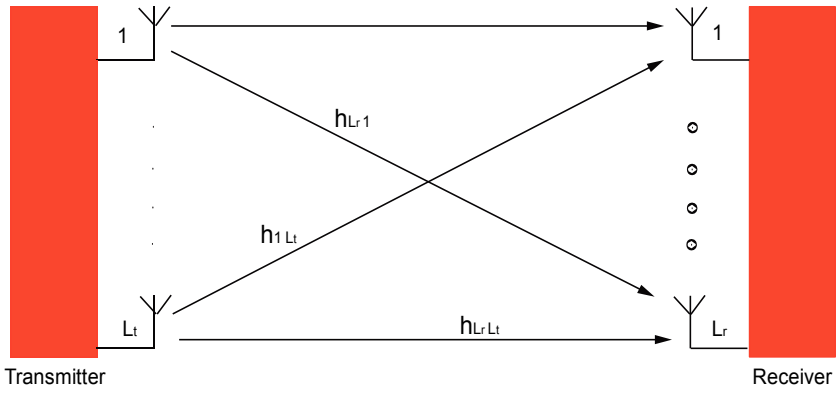

Figure 6.1: MIMO System Model

In MIMO systems, beamforming is an innovative technique improving system performance by directional signal transmission or reception. With beamforming, a single signal with high channel gain is transmitted comparing to MIMO systems where multiple signals are transmitted.

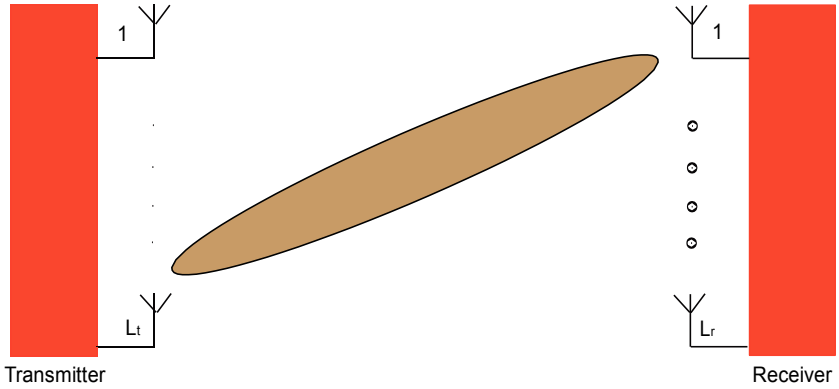

Figure 6.2: Beamforming System Model

Resource allocation remains critical for cooperative systems and even more for MIMO ones. In the literature, simplified models are studied with generally one source and one destination. One or more relays may be considered to transmit source's data to destination. In [65], the authors study the optimal power allocation at the source and each relay to maximize the end-to-end achievable rate for an AF cooperative MIMO. In [66], the authors propose a joint source and relay

beamforming for a system model with one source, one destination and multiple non regenerative relays. In [67] and [68], an heuristic algorithm for power allocation is proposed for a system model with a source, an AF relay and a destination to maximize the instantaneous data rate.

In this chapter, we focus on resource allocation for a multiple antenna system. This work extends the resource allocation studied on the previous chapter 5 where SISO systems were considered. A single cell model with one BS, K users and N RBs is then studied. All nodes are equipped by L_t antennas for the transmitter and L_r antennas for the receiver (see figure 6.3). The system is considered cooperative since users can act as relays for each others to improve system performance. The multiple antenna model is investigated to study the gain reached when data are transmitted and received by multiple antennas comparing to the SISO system model studied in section 5.5. Users are considered half-duplex (figure 5.10a), thus a cooperative transmission needs two TTIs. As explained in chapter 5, for a transmission time unit, NRS transmit in two TTIs when RS and R transmit only in one TTI each. RS transmits data to R in the first TTI and R transmits to BS in the second TTI. It is important to remind that relays are simple mobile users that have their own data to transmit to the BS. A user chosen as a relay multiplexes its own data to the relayed data before transmitting to BS. As in the previous chapter, DF scheme is considered at the relays. The resource allocation is formulated as an optimization problem aiming to minimize the whole system transmit power. The optimization considers the relay selection, the power allocation and the RBs allocation. QoS is traduced by a target data rate per user. For resolution, dual method and Lagrangian decomposition are investigated. The global optimization problem is decomposed into subproblems resolved in an iterative manner (see hierarchy in figure 5.4). At each user, different transmission strategies are considered and compared. First, equal power allocation is assumed when each user equally divides its power on the different antennas independently on their channel gains. Second, beamforming transmission is studied. User transmits only in the best direction to avoid those having high signal attenuation. Mutlipath gain may be lost but multiple antennas diversity leads to an improvement. Different power strategies are studied and their solutions are used by the global optimization problem of resources allocation. Global sub-optimal solutions are found and compared.

Comparing to existing works, the main contributions of our work are:

- Relays are simple mobile users with advantageous positions to relay cell-edge users and they have their own data to be transmitted to the BS. Therefore, a user chosen as relay multiplexes its own data to relayed data before transmitting to the BS. The multiplexing is established considering frequency division multiplexing.
- The resource allocation problem is formulated as an optimization problem to jointly solve all features: Relay selection, RB and power allocation. For resolution, dual method and Lagrangian decomposition are adopted. The global optimization problem is decomposed into subproblems resolved by an iterative manner.
- For the power allocation at each user, different transmission strategies are considered and compared. First, EPA is assumed when each user equally shares its power among the antennas independently on their channel gains. Second, beamforming transmission is studied. Users transmit only in their best direction to avoid those having high signal attenuation.

The remainder of this chapter is organized as follows. A theoretical analysis is performed to study the throughput expressions in section 6.3. The associated optimization problem is then formulated in section 6.4 and the proposed resolution steps are detailed in section 6.5. Simulation results are finally provided and discussed in section 6.6.

6.3 Theoretical Throughput expressions for MIMO system model

The channel per RB $\mathbf{j} \in [1, N]$ for transmission between user k and the BS or between user k and user k' is a point-to-point MIMO channel, subject to Additive White Gaussian Noise (AWGN). N_{rb} is the noise power per RB. It is expressed as [64]:

$$y^j = H^j x^j + z^j \tag{6.3}$$

where L_t the number of transmit antennas and L_r the number of antennas in reception. $x^j \in C^{L_t \times 1}$ is the transmitted signal vector, $y^j \in C^{L_r \times 1}$ is the received

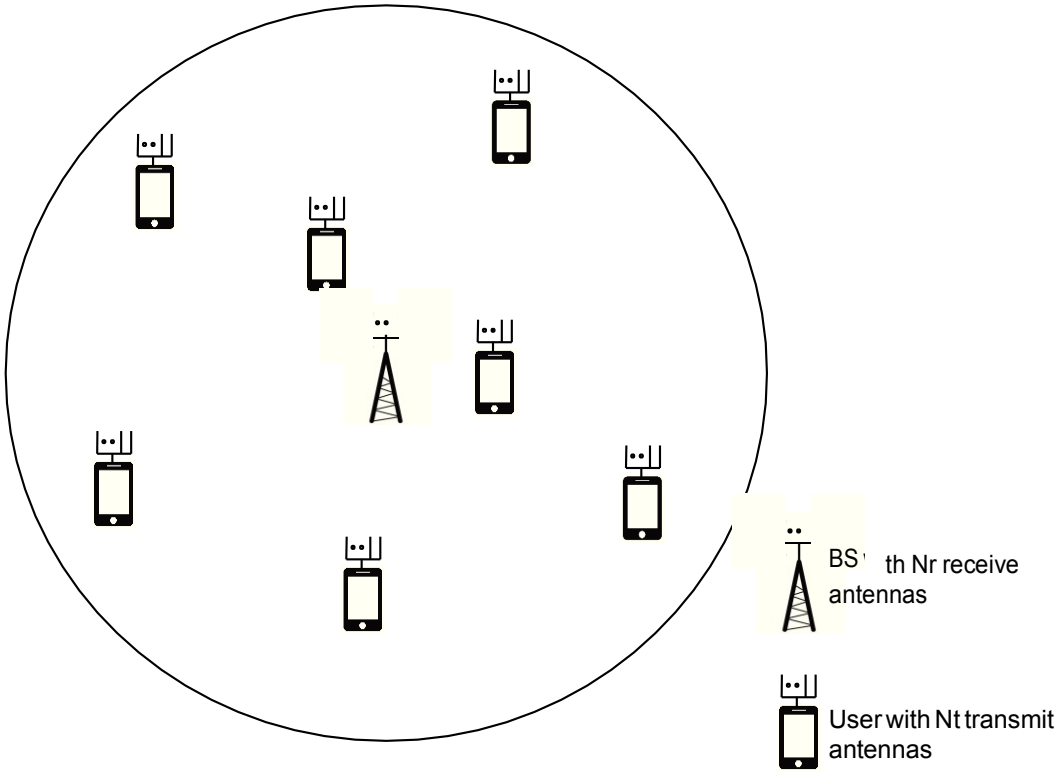

Figure 6.3: MIMO System Model

vector, $z^j \in C^{L_t \times 1}$ is an AWGN noise vector with variance N_{rb} and $H^j \in C^{L_r \times L_t}$ is the channel matrix expressed as:

$$\mathbf{H}^j = \begin{bmatrix} h^j_{11} & h^j_{12} & \cdots & h^j_{1L_t} \\ h_{21} & h_{22} & \cdots & h_{2L_t} \\ \vdots & \vdots & \vdots & \vdots \\ h^j_{L_r1} & h^j_{2_r1} & \cdots & h^j_{L_rL_t} \end{bmatrix} \tag{6.4}$$

where $h_{ii'}$ is the channel gain between the i'^{th} transmit antenna and the i^{th} receive antenna. It consists of pathloss, shadowing and fast fading. $\mathbf{H}^j$ is deterministic and assumed to be constant during two TTIs and known to both the transmitter and the receiver. The mutual information for a given channel realization $\mathbf{H}^j$ is [69]:

$$I(x^j; y^j \mid H^j) = \log_2 \det \left(I_{L_r} + \frac{1}{N_{rb}} H^j Q^j H^{jH} \right) \tag{6.5}$$

where I_{L_r} is the identity matrix with dimension L_r, $Q^j = E\{x^j x^{jH}\}$ is the covariance matrix of the transmit vector. The capacity can be computed by decomposing the vector channel into a set of parallel, independent scalar Gaussian sub-channels. The matrix H^j has a singular value decomposition (SVD) as:

$$H^j = U^j \Lambda^j V^{jH} \tag{6.6}$$

where $U^j \in C^{L_r \times L_r}$ and $V^j \in C^{L_t \times L_t}$ are unitary matrices, thus $U^j\, U^{jH} = I_{L_r}$ and $V^j\, V^{jH} = I_{L_t}$. $\Lambda^j \in R^{L_r \times L_r}$ is a diagonal matrix as:

$$\Lambda^j = \frac{1}{\sqrt{L_{k,k'} S_{k,k'}}} \begin{bmatrix} w_1^j & 0 & \dots & 0 \\ 0 & w_2^j & \dots & 0 \\ \vdots & \vdots & \ddots & \vdots \\ 0 & 0 & \dots & w_{L_{min}}^j \end{bmatrix} \tag{6.7}$$

The real diagonal elements $w_1^j \geq w_2^j \geq \dots \geq w_{L_{min}}^j$ are the ordered singular values of the matrix H^j, where $L_{min} = \min\{L_r, L_t\}$. $L_{k,k'}$ and $S_{k,k'}$ are respectively the pathloss and the shadowing experienced by user k through direct (if $k = k'$) or indirect link (if $k' \neq k$). If we set:

$$\tilde{x}^j = V^{jH}\, x^j;\ \tilde{y}^j = U^{jH}\, y^j;\ \tilde{z}^j = U^{jH}\, z \tag{6.8}$$

Using equations (6.3) and (6.6), we can write:

$$\tilde{y}_i^j = w_i^j \tilde{x}_i^j + \tilde{z}_i^j; \quad \forall i \in [1, L_{min}] \tag{6.9}$$

The capacity is finally expressed as follows:

$$R_k^j = \sum_{l=1}^{L_{min}} \log_2 \left(1 + \frac{P_k^{j,l}\, w_l^{j\,2}}{N_{rb} L_{k,k'} S_{k,k'}}\right) \text{ bits/s/Hz} \tag{6.10}$$

where $P_k^{j,l}$ are the power allocation for user k in RB j and direction l.

Based on the SVD decomposition and depending on users nature, the throughput expressions for MIMO users will be detailed in the next sections as well as the optimization problem. We define the channel gain coefficient for user k and k' in

RB **j** and antenna l as:

$$\gamma^{j,l}_{k,k'} = \frac{\omega^{j,l}_{k,k'}{}^{2}}{L^{k,k'} S_{k,k'} N_{rb}} \tag{6.11}$$

6.4 Optimization Problem Formulation

In this section, we formulate the optimization problem for the cooperative MIMO system model. The objective is to save battery life by minimizing the transmit system power. The optimization problem aims to find the optimal solution for power allocation, relay selection and RBs allocation. The optimal solution has also to satisfy QoS requirement by ensuring a target data rate R_t per user. Users as well as the BS are assumed equipped by the same number of antennas then $L_t = L_r = L$. Users are considered half-duplex so they not receive and transmit in the same TTI. If we consider one NRS, one RS relayed by R, having each one RB, respectively **j**, j' and j'', figure 6.4 details the consumed power per user and per TTI.

In the following, we will consider the power per TTI, by averaging over both TTIs. Considering K users and N RBs, the optimization problem is formulated as follows:

$$\underset{\mathbf{a,\ b,\ P}}{\text{minimize}} \quad \sum_{k=1}^{K}\sum_{j=1}^{N}\left(1-\frac{b^k}{2}\right)a^j_{k,k}P^j_k + \frac{1}{2}\sum_{k=1}^{K}\sum_{r=1,r\neq k}^{K}\sum_{j=1}^{N} b^k a^j_{k,r}\left(P^j_k + P^j_r\right) \tag{6.12a}$$

subject to

$$\sum_{k=1}^{K}\sum_{r=1}^{K} i_{k,r} = 1 \ \forall j, j = 1,..N \tag{6.12b}$$

$$\sum_{r=1}^{K}\sum_{j=1}^{N}\sum_{l=1}^{L} a^j_{k,r}R^{jl}_k \geq R_t \ \forall k, k = 1,..K \tag{6.12c}$$

$$a^j_{k,r} \in \{0,1\} \ \forall k, r, j \tag{6.12d}$$

$$b_k \in \{0,1\} \ \forall k \tag{6.12e}$$

$$\sum_{l=1}^{L} P^{jl}_k \geq 0 \ \forall k, j \tag{6.12f}$$

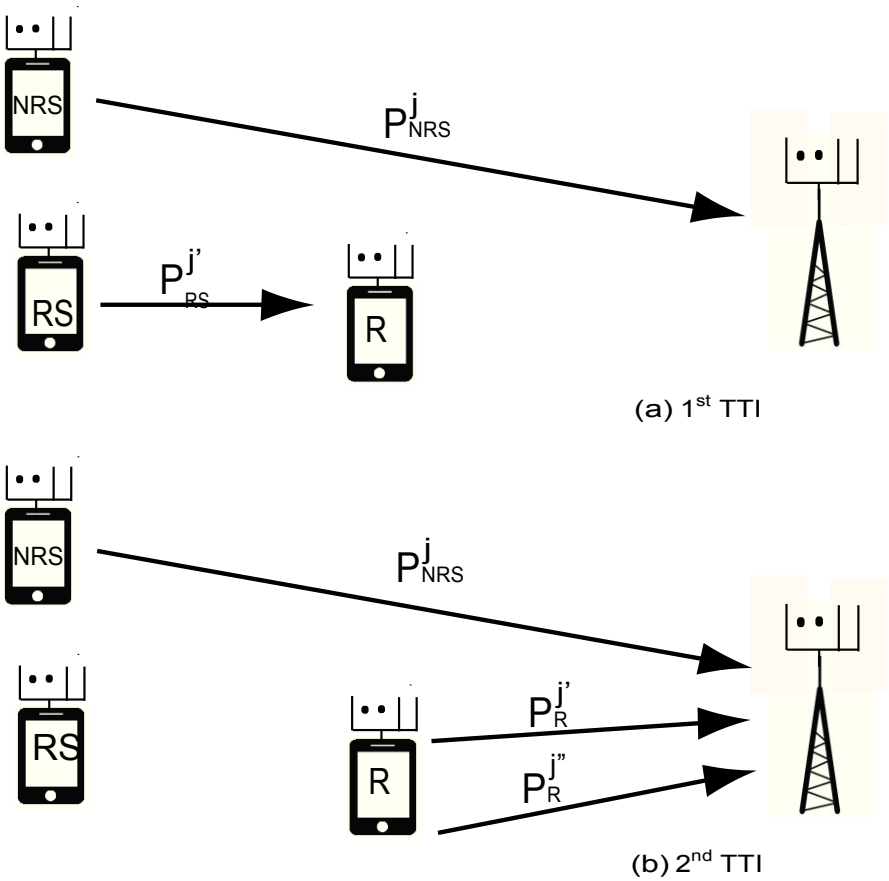

Figure 6.4: Example 1: Consumed power for 3 users and 3 RBs

where $P_k^{j,l}$ is the power allocated for antenna l of user k for the RB j. Constraint (6.12c) ensures a target data rate R_t per user. Constraint (6.12e) considers the cooperation decision, $b_k = 0$ for NRS that do not cooperate, $b_k = 1$ for RS and R since cooperation is involved. Constraint (6.12f) guarantees that all power values are positive. We note that the first term of problem (6.12a) considers direct links to the BS and thus NRS transmission as well as R transmission for their own data. The second part of (6.12a) considers the necessary power for cooperative transmission.

Dual decomposition is used for resolution to solve iteratively the two subproblems:

1. The Sub-Optimal Power Allocation
2. The Sub-Optimal Relay Selection and RBs Allocation

The power allocation is performed by user and RB independently of its antennas. Then the power per antenna is calculated by three different manners:

- Equal Power Allocation: for each user, optimal power is equally divided on all antennas, thus:

$$P_k^{j,l} = \frac{P_k^j}{L} \quad \forall l \tag{6.13}$$

- Beamforming: the whole user power p_k^j is allocated to the best direction l^* among the different available paths to maximize the achievable data rate.

$$P_{k,l^*}^{j,l^*} = P_k^j \tag{6.14}$$

$$P_k^{j,l} = 0 \quad \forall l \neq l^* \tag{6.15}$$

6.5 Problem Resolution

Based on dual Lagrangian decomposition, the Lagrangian function of problem (6.12) is written as:

$$L^{MIMO}(\mathbf{a}, \mathbf{b}, \mathbf{P}, \lambda) = \sum_{k=1}^{K}\sum_{r=1}^{K}\sum_{j=1}^{N}\sum_{l=1}^{L}\left(1-\frac{b_k}{2}\right)a_{k,k}^j P_k^j + \frac{1}{2}\sum_{k=1}^{K}\sum_{r\neq k}^{K}\sum_{j=1}^{N}\sum_{l=1}^{L} b_k a_{k,r}^j (P_k^j + P_r^j)$$
$$- \sum_{k=1}^{K}\sum_{r=1}^{K}\sum_{j=1}^{N}\sum_{l=1}^{L} \lambda_k a_{k,r}^j R_k^{j,l} + \sum_{k=1}^{K} \lambda_k R_t \tag{6.16}$$

where $\lambda = [\lambda_1, \lambda_2, ..., \lambda_K]^T$ is the vector of dual variables associated to the required data rate constraint.

The problem can be solved by studying its dual function as follows:

$$\begin{aligned} &\underset{\lambda}{\text{maximize}} \quad g^{MIMO}(\lambda) \\ &\text{subject to} \quad \lambda_k \geq 0 \quad \forall k \end{aligned} \tag{6.17}$$

with g the Lagrangian dual function is defined as:

$$g^{MIMO}(\lambda) = \begin{cases} \min\limits_{\mathbf{a},\,\mathbf{P}} L^{MIMO}(\mathbf{a},\,\mathbf{P},\,\lambda) \\ \text{subject to} \\ \sum\limits_{k=1}^{K}\sum\limits_{r=1}^{K} a_{k,r}^{j} \leq 1 \;\forall j \\ a_{k,r}^{j} \in [0..1]\;\forall k, r, j \\ b_{k}^{j} \in [0..1]\;\forall k \\ P_{k}^{j,l} \geq 0\;\forall k\;\forall j \end{cases} \tag{6.18}$$

The boolean variables $a_{k,r}^{j}$ and b_{k}^{j} are relaxed to be continuous in [0..1] according to the time sharing process [37][38]. The problem is decomposed in subproblems for each RB **j** independently $L_{j}^{MIMO}(\mathbf{a},\mathbf{b},\,\mathbf{P},\,\lambda)$ subject to:

$$a_{k,r}^{j} \in [0,1]\;\forall k, r, j; \tag{6.19}$$

$$b_{k} \in [0,1]\;\forall k; \tag{6.20}$$

(6.12b) and (6.12f)

The resolution of problem (6.18) consists in solving iteratively the power allocation and the joint relay selection and RBs allocation.

6.5.1 Sub-Optimal Power allocation

Having only the power as variable to optimize, the Lagrangian is convex. For resolution, assuming that $a_{k,r}^{j}$, and b_{k} are fixed $\forall k, r, j$, only positive power constraint remains (equation (6.12f)) and the corresponding Lagrangian can be expressed as:

$$\begin{aligned} L_{j,bis}^{MIMO}(\mathbf{P},\,\lambda,\nu) = & \sum_{k=1}^{K}\sum_{r=1}^{K}\sum_{l=1}^{L} \frac{1}{2}\left(1 - \frac{b_k}{2}\right) a_{k,k}^{j} P_{k}^{j,l} + \frac{1}{2}\sum_{k=1}^{K}\sum_{r/=K}^{K}\sum_{l=1}^{L} b_k a_{k,r}^{j}\left(P_{k}^{j,l} + P_{r}^{j,l}\right) \\ & - \sum_{k=1}^{K}\sum_{r=1}^{K}\sum_{l=1}^{L} \lambda_k\, a_{k,r}^{j}\, R_{k}^{j,l} - \sum_{k=1}^{K}\sum_{l=1}^{L} \nu_{k}^{j}\, P_{k}^{j,l} \end{aligned} \tag{6.21}$$

where ν_{k}^{j} is the Langrangian variable associated to the power constraint. Using KKT conditions, sub-optimal power expressions are computed for each MIMO power allocation technique.

6.5.1.1 Power allocation for EPA and Beamforming

For both EPA and Beamforming, the optimal power per user can be expressed depending on its nature as follows:

- k is a not relayed source:

$$P_k^j = \left[\frac{\lambda_k}{\ln(2)} - \frac{1}{\nu_{k,k}^j}\right]^+ \tag{6.22}$$

- k is a relay transmitting its own data in RB **j**

$$P_k^j = \left[\frac{\lambda_k}{\ln(2)} - \frac{1}{\nu_{k,k}^j}\right]^+ \tag{6.23}$$

- k is a relayed source with relay r, we assume that $P_k^j \gamma_{k,r}^j = P_r^j \gamma_{r,r}^j$,in order to minimize the transmit power, then:

$$P_k^j = \left[\frac{\lambda_k \nu_{r,r}^j}{\ln(2)(\gamma_{k,r}^j + \gamma_{r,r}^j)} - \frac{1}{\nu_{k,r}^j}\right]^+ \tag{6.24}$$

$$P_r^j = \frac{\nu_{k,r}^j}{\nu_{r,r}^j} P_k^j \tag{6.25}$$

where $\gamma_{k,k'}^j$ is different according to the adopted antennas power control manner :

- Equal power allocation (EPA): if users divide their power equally for antennas, $\gamma_{k,k'}^j$ is the geometric mean of the channel gains for different antenna per user:

$$\gamma_{k,k'}^j = \left[\prod_{l=1}^{L} \gamma_{k,k'}^{j,l}\right]^{\frac{1}{L}} \quad \forall k, k' \tag{6.26}$$

- Beamforming: if beamforming is adopted, $\gamma_{k,k'}^j$ is the best channel gain among all antenna as:

$$\gamma_{k,k'}^j = \gamma_{k,k'}^{*j,l} = \arg\max_l \gamma_{k,k'}^{j,l} \quad \forall k, k', j \tag{6.27}$$

6.5.2 Sub-Optimal Relay Selection & RBs Allocation

In this section, we aim to find the sub-optimal solution for relay selection and RBs allocation jointly. Based on power allocation studied on the previous section, the Lagrangian of the optimization problem (6.12a) is expressed as:

$$L^{MIMO}(\mathbf{a},\lambda) = \sum_{k=1}^{K}\sum_{r=1}^{K}\sum_{j=1}^{N}\sum_{l=1}^{L}\left(1-\frac{b_k}{2}\right)a_{k,k}^{j}\frac{P_k^j}{2} + \sum_{k=1}^{K}\sum_{r/=K}^{}\sum_{j=1}^{N} b_k a_{k,r}^{j}\frac{(P_k^j + P_r^j)}{2} - \sum_{k=1}^{K}\sum_{r=1}^{K}\sum_{j=1}^{N}\sum_{l=1}^{L} \lambda_k a_{k,r}^{j} R_k^{j,l} + \sum_{k=1}^{K}\lambda_k R_t \quad (6.28)$$

The corresponding dual function can be written as:

$$g(\lambda) = \underset{\mathbf{a}}{\text{maximize}} \sum_{k=1}^{K}\sum_{r=1}^{K} a_{k,r}^{j} G_{k,r}^{j} - \sum_{k=1}^{K}\lambda_k R_t \quad (6.29)$$

where $G = [G_{k,r}^{j}]$ is a $K \times K \times N$ matrix presenting the eventual gain of couple (k, r) if it earns RB j. This equation is different from equation (5.42) by the fact that MIMO system model is considered in this chapter. The gain expressions depend on user natures and are detailed in algorithms 3 and 4. The joint sub-optimal relay selection and RBs allocation is proposed for both equal power allocation and beamforming at users. To avoid confusion, the gain function is denoted E for the EPA case and F for the beamforming one.

First, all users are considered not relayed. Then, for each RB j, the gain is calculated for all possible pairing. Thus, for a NRS user, direct link gain is calculated as well as all possible indirect gains. Second, **j** is allocated to couple $(k,r)^*$ maximizing all gains for it. If $k = r$, user k remains a NRS, if $k /= r$, user k becomes RS
and user r becomes a relay. According to this, users sets are updated and the same instructions are repeated for all RBs. More details are explained in algorithms 3 and 4.

We note that the computation of potential gains and the decision allocation is performed for each RB. If $k = r$, direct transmission is considered and $b_k = 0$, else if $k /= r$, then cooperation is investigated, thus $b_k = 1$ and $b_r = 1$. Users nature
are updated in each allocation.

Algorithm 3: Proposed Sub-Optimal algorithm for Resource Block Allocation - MIMO - Equal Power Allocation

Initialize the users' sets: setNRS = {all users k}, setRS = { $\emptyset$}, setUsers = setNRS $\cup$ setRS $\cup$ setR,

for each RB **j** **do**

  Initialize $E1^{j}_{k,r} = 0, E2^{j}_{k,r} = 0, E3^{j}_{k,r} = 0, E4^{j}_{k,r} = 0 \ \forall k, r$ and using equation (6.13)

  for user k $\in$ setUsers¥setR **do**

    $E^{j}_{k,k} = \lambda_k \sum_{l=1} \log_2 1 + P^{j,l}_{k} \gamma^{j,l}_{k,k} - P^{j}_{k}$

  for user k $\in$ setR **do**

    $E^{j}_{k,k} = \frac{\lambda_k}{2} \sum_{l=1} \log_2 1 + P^{j,l}_{k} \gamma^{j,l}_{k,k} - \frac{1}{2} P^{j}_{k}$

  for user k $\in$ setRS $\cup$ setNRS and r $\in$ setUsers¥{k} **do**

    $E^{j}_{k,r} = \frac{\lambda_k}{2} \sum_{l=1} \log_2 1 + P^{j,l}_{k,r} \gamma^{j,l}_{k,r} - \frac{1}{2}(P^{j}_{k,r} + P^{j}_{r,r})$

  Find $(k, r)^* = \arg\max_{(k,r)} \{E1^{j}_{k,r}, E2^{j}_{k,r}, E3^{j}_{k,r}, E4^{j}_{k,r}\}$

  Allocation of RB j:

$$a^{j}_{k,r} = \begin{cases} 1 \text{ for } (k,r)^* \\ 0 \text{ otherwise} \end{cases}$$

  Update users' sets:

  if $(k^* \neq r^*)$ and $(k,r)^* = \arg\max_{(k,r)} E3^{j}_{k,r}$ $||$ $(k,r)^* = \arg\max_{(k,r)} E4^{j}_{k,r}$ **then**

    if $k^* \notin$ setRS **then**

      setRS = setRS $\cup \{k^*\}$

    if $r^* \notin$ setR **then**

      setR = setR $\cup \{r^*\}$

Algorithm 4: Proposed Sub-Optimal algorithm for Resource Block Allocation - MIMO - Beamforming

Initialize the users' sets: setNRS = {all users k}, setRS = { $\emptyset$},
setUsers = setNRS $\cup$ setRS $\cup$ setR,
for each RB **j** **do**
  Initialize $F1^{j}_{k,r} = 0, F2^{j}_{k,r} = 0, F3^{j}_{k,r} = 0, F4^{j}_{k,r} = 0 \ \forall k, r$ and using equations(6.14) and (6.27)
  for user $k \in$ setUsers¥setR **do**
    $F^{j}_{k,k} = \lambda_k \log_2 1 + P^{j}_{k} \gamma^{*jl}_{k,k} - P^{j}_{k}$
  for user $k \in$ setR **do**
    $F^{j}_{k,k} = \frac{\lambda_k}{2} \log_2 1 + P^{j}_{k} \gamma^{*jl}_{k,k} - \frac{1}{2} P^{j}_{k}$
  for user $k \in$ setRS $\cup$ setNRS and $r \in$ setUsers¥$\{k\}$ **do**
    $F^{j}_{k,r} = \frac{\lambda_k}{2} \log_2 1 + P^{j}_{k,r} \gamma^{*jl}_{k,r} - \frac{1}{2}(P^{j}_{k,r} + P^{j}_{r,r})$
  Find $(k,r)^* = \arg\max_{(k,r)} \{F1^{j}_{k,r}, F2^{j}_{k,r}, F3^{j}_{k,r}, F4^{j}_{k,r}\}$
  Allocation of RB j:

$$a^{j}_{k,r} = \begin{cases} 1 \text{ for } (k,r)^* \\ 0 \text{ otherwise} \end{cases}$$

  Update users' sets:
  if $(k^* \neq r^*)$ and $(k,r)^* = \arg\max_{(k,r)} F3^{j}_{k,r} \ || \ (k,r)^* = \arg\max_{(k,r)} F4^{j}_{k,r}$ **then**
    if $k^* \notin$ setRS **then**
      setRS = setRS $\cup \{k^*\}$
    if $r^* \notin$ setR **then**
      setR = setR $\cup \{r^*\}$

6.5.3 Lagrangian Variable Update

The last step in the resolution iterative algorithm is to update Lagrange variables. Based on power allocation resulted from section 6.5.1 and relay selection and RBs allocation resulting from section 6.5.2, λ_k are updated for all users. Equation 5.27 is then adapted for the MIMO system model as:

$$\lambda_k(t+1) = \lambda_k(t) + \eta_k(t)\left(R_t - \sum_{r=1}^{K}\sum_{j=1}^{N} a^j_{k,r}(t) R^j_k(t)\right)^+ \quad (6.30)$$

where η_k is the diminishing step size as explained in section 5.4.3.4. To decide from the convergence of the proposed algorithm, all users have to achieve R_t and the variation of λ_k has to be negligible for all k as follows:

$$\frac{\lambda_k(t+1) - \lambda_k(t)}{\lambda_k(t+1)} < \varrho \ \forall k \quad (6.31)$$

where ϱ is set close to zero.

The user throughput is expressed as:

- Equal Power Allocation
  - k is a not relayed source

$$R^j_k = \sum_{l=1}^{L} \log_2\left(1 + \frac{P^j_{k,k}}{L}\gamma^{j,l}_{k,k}\right) \quad (6.32)$$

  - k is a relay

$$R^j_k = \frac{1}{2}\sum_{l=1}^{L} \log_2\left(1 + \frac{P^j_{k,k}}{L}\gamma^{j,l}_{k,k}\right) \quad (6.33)$$

  - k is a relayed source through relay r

$$R^j_k = \frac{1}{2}\min\left(\sum_{l=1}^{L} \log_2\left(1 + \frac{P^j_{k,r}}{L}\gamma^{j,l}_{k,r}\right); \sum_{l=1}^{L} \log_2\left(1 + \frac{P^j_{r,r}}{L}\gamma^{j,l}_{r,r}\right)\right) \quad (6.34)$$

- Beamforming
  We remind that $\gamma^{*j,l}_{k,k} = \arg\max_l \gamma^{j,l}_{k,k} \ \forall k,k',j$
  - k is a not relayed source

$$R^j_k = \log_2\left(1 + P^j_k \gamma^{j,*j,l}_{k,k}\right) \quad (6.35)$$

  - k is a relay

$$R^j_k = \frac{1}{2}\log_2\left(1 + P^j_k \gamma^{j,*j,l}_{k,k}\right) \quad (6.36)$$

– k is a relayed source through relay r

$$R_k^j = \frac{1}{2} \min \left(\log_2 \left(1 + P_k^{j\,*j,l} \gamma_{k,r} \right) ; \log_2 \left(1 + P_r^{j\,*j,l} \gamma_{r,r} \right) \right) \quad (6.37)$$

The algorithm stops when all users achieve the required data rate R_t and the convergence condition is verified (equation (5.28)).

6.6 Simulation results

In this section, simulation results are presented and discussed. We consider a single cell with radius R = 1 km, one BS with 2 antennas. The number of RBs N is varied along simulations. The total bandwidth available considered is B = 20 MHz equitably divided between the RBs. Users suffer from log-normal shadowing with standard deviation equal to 6 dB and from pathloss according to the LTE model with frequency F = 2.6 GHz: $L_{dB}(d_{k,k'}) = 128.1 + 37.6.\log_{10}(d_{k,k'})$ where $d_{k,k'}$ is the distance in Km from user k to user k'. If $k = k'$, $d_{k,k'}$ is the distance of user k to the BS.

We also assume Rayleigh channels with slow fading and AWGN noise with density $N_0 = -174$ dBm/Hz.

For iteration t, the step size η_k from equation (6.30) is set to $\frac{\lambda_k}{\sqrt{}}$ if t does not exceed 2000, otherwise, η_k remains invariant. From equation (6.31), ϱ is set to 0.001. Results are averaged over 1000 simulations to get realistic results.

Figures 6.5 and 6.6 show the system transmit power for required target data rate of 1 bits/s/Hz and 1.5 bits/s/Hz respectively considering 18 users and 2 antennas per user. EPA and beamforming schemes are compared to MIMO system without cooperation and to cooperative SISO system. For the non-cooperative MIMO system, EPA is adopted for the power allocation.

Simulation results show that the cooperative MIMO system offers a considerable gain comparing to both cooperative-SISO and non-cooperative MIMO systems. Compared to non-cooperative MIMO system, cooperative EPA offers a gain of 80% and cooperative beamforming offers a gain of 90% for R_t = 1 bits/s/Hz. Cooperation is efficient where the optimization covers all resource allocation features and then the gain is maximized. We can also remark that beamforming system offers better results than MIMO EPA This is justified by the fact that

user in beamforming case allocates all its power to the best direction and does not waste any power in directions with bad channel conditions. Moreover, comparing to cooperative-SISO model, MIMO cooperation allows a gain of 80% for EPA scheme and beamforming offers a gain of 90% for R_t = 1 bits/s/Hz. For R_t = 1.5 bits/s/Hz, the gain is up to 85% and up to 90% for EPA and beamforming respectively. This gain is due to the spatial diversity offered by the MIMO model.

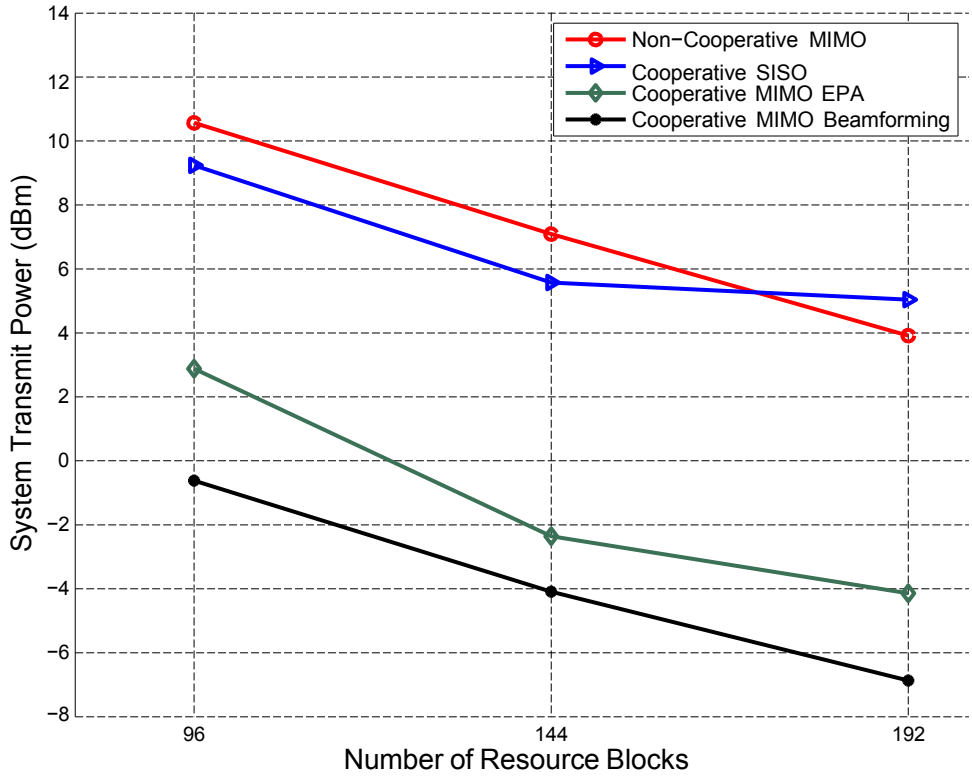

Figure 6.5: System Transmit Power: R_t = 1 bits/s/Hz

6.7 Conclusion

In this work, the resource allocation for an uplink cooperative MIMO OFDMA multiuser system for 5G wireless systems is studied. Mobile users are investigated as DF relays to relay other mobiles and minimize the system transmit power in the context of green communication. An optimization problem is formulated to find the optimal solution for relay selection, RB allocation and power allocation

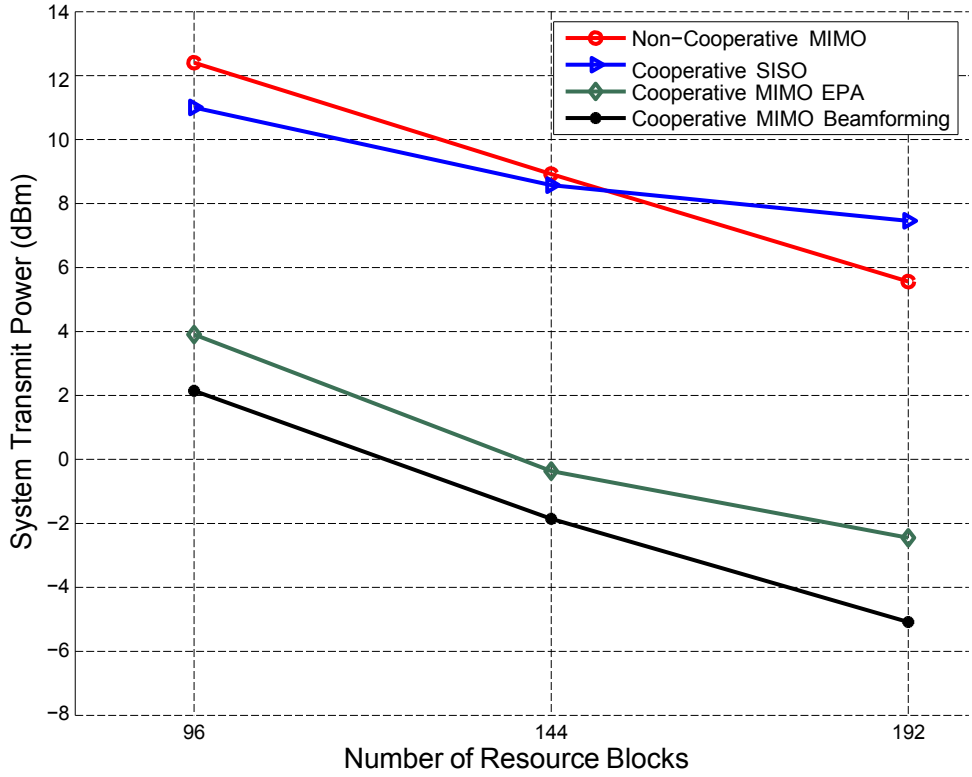

Figure 6.6: System Transmit Power: R_t = 1.5 bits/s/Hz

while ensuring a target data rate per user. For each user, both MIMO EPA and beamforming are performed to allocate power to the different antennas. Simulation results compare these two schemes to MIMO non-cooperative and to cooperative SISO systems and show that the proposed algorithm offers a high gain for both EPA and beamforming. Simulations also show that beamforming achieves better results than EPA by choosing to allocate the whole power to the best direction. This gain can be improved if users optimize their power in the different antennas depending on all antenna gains. This additional optimization will be our future work.

Chapter 7

Conclusions and Perspectives

7.1 Conclusions

The thesis has mainly considered the resource allocation problem for an uplink OFDMA system model. Our aim was to propose resource allocation strategies improving the system throughput while respecting QoS requirement and ensuring fairness between users.

First, we have investigated resource allocation in a single cell. We have studied the most used resource allocation algorithms, their associated utility function and have analyzed their impact for both throughput and fairness. Then, we have proposed a new WPF algorithm inspired from the classical PF algorithm where users have weights based on their distances from the BS that influence their priority to earn subcarriers. In fact, contrary to the classical PF algorithm which allocates approximately the same number of subcarriers to all users, the WPF assigns more subcarriers to users with good channel conditions while keeping sufficient fairness in the cell. A theoretical analysis has been established to compare the behavior of the WPF and the classical PF algorithms. Simulation results have shown that the proposed WPF approaches the upper bound for the system throughput while keeping fairness between users. In addition, the WPF can be adjusted using the β parameter to be adapted to the QoS requirement.

Based on PF resource allocation, we have studied the resource allocation in a multi-cell system model where the ICI limits system performance. We have performed a state of the art about ICI mitigation strategies and have proposed two methods to reduce the ICI. First, we have focused on FFR method and have applied the WPF algorithm developped in chapter 3 in a multi-cell system model using FFR. Using this method, resource allocation is performed in a distributed manner for each cell without knowledge of allocations in neighboring cells. Theoretical expressions and simulation results have shown that the proposed FFR and WPF offer higher system performances compared to the classical FFR scheme used by the LTE standard. Moreover, we have proposed a second new strategy to reduce the ICI based on cooperation between BSs. Inspired from boolean interference indicators proposed by the LTE standard, we have proposed a novel Enhanced Interference Indicator (EII) allowing to efficiently estimate the level of interference of subcarriers. In the aim to reduce the ICI without high cooperation cost between the BSs, the EII has been chosen with integer values. For this, the cell edge areas have been divided into multiple sectors and the EII values has been computed for each subcarrier per cell corresponding to the sectors in which it is allocated in neighboring cells. Because we are interested in the uplink, EII values depend on the distance from the considered BS. Resource allocation is then performed considering the EII as interference estimation and according to the PF algorithm. Simulation results have shown that the proposed EII offers better system performances by reducing the ICI compared to the HII proposed by LTE and to a system without any cooperation between BSs.

In the remainder of this dissertation, we have focused on resource allocation with multiplexing relays and optimization problems. Considering the uplink in a single cell system model, we have assumed that mobile users with advantageous positions can relay other users in the cell border in addition to their own data. Relay's own data and relayed data are then multiplexed before transmission to the BS. The main parameters to optimize have been relay selection, RB allocation and power allocation. To contribute to green communication, we have chosen to minimize the system transmit power as objective for the optimization problem. Moreover, the QoS requirement has been traduced by a target data rate constraint per user. In a first step, we have assumed half-duplex users, DF relays and have treated the pairing step to associate users to potential relays as an initialization step where

a relayed source can be relayed by only one relay. The optimization problem has been formulated to solve RBs and power allocation using dual method. The global problem has been decomposed into sub-problems and a sub-optimal iterative heuristic has been proposed. We have detailed theoretical resolution steps and have presented simulation results which show a high gain compared to system without cooperation. In a second step, we have treated the paring step as an additional optimization step to RB and power allocation. In this case, both half and full-duplex users have been studied and compared. Comparing the two proposed methods for half-duplex users, we have concluded that optimizing the relay selection can reduce the transmit power but adds complexity to the optimization problem. Finally, we have extended the half-duplex resource allocation using optimization problems to a MIMO system model to study the influence of multiple antennas systems on the system transmit power. A theoretical analysis has been established to present sub-optimal expressions for RB and power allocation. Moreover, both equal power allocation and beamforming have been studied and compared to allocate power in the multiple antennas of a user.

7.2 Perspectives and future works

A number of interesting topics, based on the research issues studied in this thesis, could be addressed. We hereunder provide some suggestions of possible extensions to the work presented in this dissertation:

- In all chapters we have considered that the Base Station knows perfectly the channel gains (Path Loss, Shadowing and Rayleigh fading gains) for each resource block. Furthermore, for relayed transmissions, it is assumed that the BS knows also the gains between any pair of mobile terminal for relay/relayed-source association. One perspective of our work could be to study the proposed resource allocation algorithms when we don't have perfect CSI knowledge. Several cases of errors on the CSI could be studied: CSI for each RB available but with estimation errors, averaged CSI on groups of RBs and/or averaged CSI on several TTIs. Robustness of the proposed algorithms against these impairments should give an insight on their applicability to real cellular cases.

- Concerning chapter 4 and cooperation between neighboring cells, we have proposed new indicators, Enhanced Interference Indicator (EII), that are an extension of the classical HII proposed in the LTE standard. Instead of being coded on one bit as the HII, EII have different levels depending on the potential interference levels experienced by the RBs of neighboring cells. We have proposed a simple procedure for EII exchange between cells, where the allocation for a group of 7 cells follows a cyclic procedure. It could be interesting to study other exchange procedures for the EII in a more realistic cellular network. Furthermore, it could be interesting to quantify the amount of transmitted data due to EII and the impact of transmitting these indicators not every TTI but with a lower frequency.
- In chapter 5 we have studied resource allocation optimization using mobile terminals as mobiles relays. For the case of Joint Power Allocation, Relay Selection and RB Allocation we have studied two cases: half duplex and full duplex communications. The full duplex case means that a mobile relay is able to transmit its own data on one RB while, in the same time, listening on an adjacent RB the data coming from the relayed source. For state of the art mobile terminals this is not yet possible. Some research projects are currently studying the feasibility of full duplex RF transmissions and this kind of transmission could become a reality in following years. Nevertheless, interference will remain between emission and reception and it could be interesting to study the behavior of the resource allocation algorithm when there exist interference in the full duplex mode.
- In chapter 6, MIMO transmission did not allow multiplexing several users on the MIMO streams. Multiplexing of the source and relay's data has been performed on different RB, similarly to the strategy chosen in chapter 5. It could be interesting to add spatial multiplexing to frequency multiplexing in some cases, for instance if the relay is very close to the BS and does not need to use all its spatial streams to reach the required data rate. However, this would require additional complexity at the relay, since it would no longer just forward the source's data on the same RBs. It would also lead to an increase in the signaling load between the relay and the BS, in order for the BS to correctly demultiplex all data.

- OFDM modulation has been chosen throughout the thesis and all mobile users and BS have been assumed to be synchronous. Moreover, neighboring cells are also assumed synchronous. As other post-OFDM waveforms (mainly filtered multicarrier waveforms) are proposed for 5G standardization, it should be interesting to study the impact of such waveforms on the performances when perfect synchronization is relaxed. In particular, the frequency localization of post-OFDM waveforms can have in interest in a non synchronous system [70].
- Finally, in our work we didn't consider any traffic model for the data and no moving model for the mobile users. Resource allocation is thus done at each TTI using different Rayleigh fading gains for the links. Taking into account user velocity could result in a higher period (several TTIs) for resource allocation computation for low speed users. Studying the impact of the resource allocation periodicity versus user mobility could be an interesting perspective. Besides, all algorithms where designed for full buffer cases. The proposed algorithms could be adapted to more realistic traffic models, taking into account not only the users data rate but also their buffer size and the risk of buffer overflow.

Appendix A

Relative Appendix in Section 3.5

A.1 Proof of expressions (3.9), (3.10) and (3.11)

We assume that we are in high SNR and we use the approximation $\log_2(1+a) \approx \log_2(a)$. Equations (3.7) and (3.8) can then be written as:

$$A = \log_2\left(\alpha_2 g_{2,j}\frac{P}{N_2}\right) - \sum_{i\in S_{sub,1}} \log_2\left(\alpha_1 g_{1,i}\frac{P}{N_1}\right)$$
$$= V_2 - \sum_{i\in S_{sub,1}} V_1$$

$$B = \log_2\left(\alpha_1 g_{1,j}\frac{P}{N_1}\right) - \sum_{i'\in S_{sub,2}} \log_2\left(\alpha_2 g_{2,i'}\frac{P}{N_2}\right)$$

where V_1 and V_2 two independent random variables with means μ_{V_1} and μ_{V_2} and variances $\sigma_{V_1}{}^2$ and $\sigma_{V_2}{}^2$.
We remind that we set:

$$X = \log_2(\alpha_1 g_{1,j} P) \sim L_X(\mu_1, \sigma_1{}^2)$$
$$Y = \log_2(\alpha_2 g_{2,j} P) \sim L_Y(\mu_2, \sigma_2{}^2)$$
$$Z = \log_2(\alpha_1 g_{1,j} P)\log_2(\alpha_2 g_{2,j} P) \sim L_Z(\mu_3, \sigma_3{}^2)$$

and that:

$$\mu_3 = \mu_1\mu_2;$$
$$\sigma_3^2 = \sigma_1^2\sigma_2^2 + \sigma_1^2\mu_2^2 + \sigma_2^2\mu_1^2$$

Applying the central limit theorem [47], A and B follow normal distributions with means μ_A and μ_B and variances σ_A^2 and σ_B^2. We aim to compute means and variances expressions.

$$V_1 = \log_2 \left(\alpha_1 g_{1,i} \frac{P}{N_1}\right)$$

$$V_1 = \log_2(\alpha_1 g_{1,i} P) - \log_2(N_1)$$

Then

$$\mu_{V_1} = \mu_1 - \log_2(N_1)$$

and

$$\mu_{V_2} = \mu_2 - \log_2(N_2) \tag{A.1}$$

Computation of $\sigma_{V_1}^2$ and $\sigma_{V_2}^2$

We have the formula:

$$\sigma_{V_1}^2 = E[V_1^2] - E^2[V_1] \tag{A.2}$$

$$E^2[V_1] = \mu_1^2 - 2\mu_1 \log_2(N_1) + \log_2(N_1)^2 \tag{A.3}$$

$$\begin{aligned} E[V_1^2] &= E\left[\log_2(\alpha_1 g_{1,i} P)^2 - 2\log_2(N_1)\log_2(\alpha_1 g_{1,i} P) + \log_2(N_1)^2\right] \\ &= \sigma_1^2 + \mu_1^2 + \log_2(N_1)^2 - 2\mu_1 \log_2(N_1) \end{aligned} \tag{A.4}$$

Substituting equations (A.3) and (A.4) in (A.2), we find:

$$\sigma_{V_1}^2 = \sigma_1^2 \tag{A.5}$$

In the same manner:

$$\sigma_{V_2}{}^2 = \sigma_2^2 \tag{A.6}$$

Computation of the mean and the variance of $\sum_{i \in S_{sub,1}} V_1$ and $\sum_{i \in S_{sub,2}} V_2$

With $|S_{sub,1}| = N_1$ and $|S_{sub,2}| = N_2$, we can write:

$$V_{1,bis} = \sum_{i \in S_{sub,1}} V_1 \sim L_{V_1}{}_{,bis}(\mu^V_{1,bis}, \sigma^V_{1,bis}{}^2) \tag{A.7}$$

$$V_{2,bis} = \sum_{i \in S_{sub,2}} V_2 \sim L_{V_2}{}_{,bis}(\mu^V_{2,bis}, \sigma^V_{2,bis}{}^2) \tag{A.8}$$

where

$$\mu_{V_{1,bis}} = N_1\mu_1 - N_1 \log_2(N_1) \tag{A.9}$$

$$\sigma_{V_{1,bis}}{}^2 = N_1\sigma^2_{V_1} \tag{A.10}$$

$$\mu_{V_{2,bis}} = N_2\mu_2 - N_2 \log_2(N_2) \tag{A.11}$$

$$\sigma_{V_{2,bis}}{}^2 = N_2\sigma^2_{V_2} \tag{A.12}$$

Using the formula for X and Y two independent random variables:

$$var(X.Y) = var(X)var(Y) + var(X)[E(Y)]^2 + var(Y)[E(X)]^2$$

we have:

$$\begin{aligned}\sigma_A{}^2 &= var(V_2.V_{1,bis}) \\ &= \sigma^2_{V_2}\sigma^2_{V_{1,bis}} + \sigma^2_{V_2}\mu^2_{V_{1,bis}} + \sigma^2_{V_{1,bis}}\mu^2_{V_2}\end{aligned} \tag{A.13}$$

Substituting equations (A.9) and (A.10) in (A.13), we find:

$$\begin{aligned}\frac{\sigma_A{}^2}{N_1} &= \sigma_1{}^2\sigma_2{}^2 + N_1\sigma_2{}^2\mu_1{}^2 - 2N_1\mu_1\sigma_2{}^2\log_2(N_1) + N_1\sigma_2{}^2\log_2(N_1)^2 \\ &\quad + \sigma_1{}^2\mu_2{}^2 - 2\mu_2\sigma_1{}^2\log_2(N_2) + \sigma_1{}^2\log_2(N_2)^2\end{aligned} \tag{A.14}$$

Similary:

$$\frac{\sigma_B^2}{N_2} = \sigma_1^2\sigma_2^2 + \sigma_2^2\mu_1^2 - 2\mu_1\sigma_2^2\log_2(N_1) + \sigma_2^2\log_2(N_1)^2 + N_2\sigma_1^2\mu_2^2 - 2N_2\mu_2\sigma_1^2\log_2(N_2) + N_2\sigma_1^2\log_2(N_2)^2 \quad \text{(A.15)}$$

Bibliography

[1] WiMax. 802.16m and wimax release 2.0. April 2010. URL http://www.ieee802.org/16/relay/.

[2] E. Dahlman, S. Parkvall, and J. Skold. 4G: LTE/LTE-Advanced for Mobile Broadbandd. Academic Press, 2011.

[3] F. Kelly. Charging and rate control for elastic traffic. European Transactions on Telecommunications, 8:33–37, Feb. 1997.

[4] AK Maulloo FP Kelly and DKH Tan. Rate control for communication networks: shadow prices, proportional fairness and stability. Journal of Operational Research Society, 49:237–252, 1998.

[5] E. Yaacoub and Z. Dawy. Achieving the nash bargaining solution in ofdma uplink using distributed scheduling with limited feedback. International Journal of Electronics and Communications (AEÜ), 65:320–330, 2011.

[6] M. Assaad. Optimal fractional frequency reuse (ffr) in multicellular ofdma system. In Vehicular Technology Conference, VTC-Fall, Calgary, Canada, Sep. 2008.

[7] G. Kramer, I. Maric, and R. D. Yates. Cooperative Strategies and Rates. Now Publisher Inc, 2006.

[8] H. Zhou, P. Fan, and J. Li. Cooperative interference-aware joint scheduling for the 3gpp lte uplink. In Personal Indoor and Mobile Radio Communications (PIMRC), Istanbul, Turkey, Sep. 2010.

[9] P. Frank, A. Muller, H. Droste, and J. Speidel. Cooperative proportional fairness scheduling for wireless transmissions. In International Wireless Communications and Mobile Computing Conference, New York, USA, Sep. 2009.

[10] Y. Yang, H. Hu, J. Xu, and G. Mao. Relay technologies for wimax and lte-advanced mobile systems. IEEE Communications Magazine, 47(10):100–105, October 2009.

[11] H. Rasouli, S. Sadr, and A. Anpalagan. A fair subcarrier allocation algorithm for cooperative multiuser OFDM systems with grouped users. In IEEE Global Telecommunications Conference GLOBECOM, New Orleans, LO, USA, Nov. 2008.

[12] 3GPP. Overview of 3GPP release 11 v0.2.0. Sept. 2014. URL http://3gpp.org/dynareport/36211.htm.

[13] T. Nguyen and Y. Han. A proportional fairness algorithm with qos provision in downlink ofdma systems. IEEE Communications Letters, 10(11), Nov. 2006.

[14] M. Terré, M. Pischella, and E. Vivier. OFDM and LTE. In Wiley-ISTE, editor, Wireless Telecommunication Systems. 2013.

[15] M. M. M. El-Tantawy, M. Aboul Dahab, and H. El-Badawy. Performance evaluation of frequency reuse schemes in lte based network. Telecommunications forum TELFOR, Nov. 2010.

[16] S-E. Elayoubi, O. Ben Haddada, and B. Fouresti. Performance evaluation of frequency planning schemes in ofdma-based networks. IEEE Transactions on Wireless Communications, 7, May. 2008.

[17] D. P. Bertsekas. Convex optimization algorithms. In Athena Scientific, editor, Convex Optimization Theory, pages 250–380. October 2009.

[18] K. Vardhe, D. Reynolds, and B.D. Woerner. Joint power allocation and relay selection for multiuser cooperative communication. IEEE Transactions on Wireless Communications, 9(4):1255–1260, April 2010.

[19] V. K. Shah and A. P. Gharge. A review on relay selection techniques in cooperative communication. International Journal of Engineering and Innovative Technology (IJEIT), 2(4):65–69, November 2012.

[20] R. Prasad. In Artech House, editor, OFDM for Wireless Communication Systems. January 2004.

[21] LTE Technical Specification. Lte: Evolved universal terrestrial, radio access network (e-utran); x2 application protocol (x2ap). 3GPP TS36.423 release 11, pages 63 – 64, 2014.

[22] N. Benvenuto and S. Tomasin. On the comparison between ofdm and single carrier modulation with a dfe using a frequency-domain feedforward filter. IEEE Transactions on Communications, pages 947 – 955, June 2002.

[23] B.E. Priyanto, H. Codina, S. Rene, and T. B. Sorensen. Initial performance evaluation of dft-spread ofdm based sc-fdma for utra lte uplink. pages 3175 – 3179, Dublin, April 2007.

[24] M.D Nisar, H. Nottensteiner, and T. Hindelang. On performance limits of dft spread ofdm systems. pages 1 – 4, Budapest, July 2007.

[25] T. S. Rappaport. In Cambridge University Press, editor, Wireless Communications: principles and practice. 1996.

[26] D. Pearson. In John Wiley and Sons Ltd, editors, The mobile radio propagation channel. 2000.

[27] D. Tse and P. Viswanath. The Wireless Channel. In Cambridge University Press, editor, Fundamentals of Wireless Communications, pages 10–48. Aug. 2005.

[28] F. Belloni. Fading models. In POSTGRADUATE COURSE IN RADIO COMMUNICATIONS, 2004.

[29] J. G. Proakis and M. Salehi. In McGraw-Hill Education; 5th edition, editor, Digital Communications. Nov. 2007.

[30] F. C. de Gouveia and T. Magedanz. Quality of service in telecommunication network. In TELECOMMUNICATION SYSTEMS AND TECHNOLOGIES.

[31] C. He, F. Liu, H. Yang, C. Chen, H. Sun, W. May, and J. Zhang. Co-channel interference mitigation in mimo-ofdm system. In Wireless Communications, Networking and Mobile Computing WiCom, Shanghai, China, Sep. 2007.

[32] A. Y. Tara. Fractional frequency reuse in lte networks. In Springer New York, editor, Understanding LTE and its Performance, pages 199–210. 2011.

[33] O. Simeone, O. Somekh, V. Poor, and S. Shamai. Local base station cooperation via finite-capacity links for the uplink of linear cellular networks. IEEE Transaction on Information Theory, 55, Jan. 2009.

[34] T. Mayer, H. Jenka. c, and J. Hagenauer. Turbo base-station cooperation for intercell interference cancellation. In IEEE International Conference of Communications, Istanbul, Turkey, June 2006.

[35] S. Boyd and L. Vandenberghe. Duality. In Cambridge University Press, editor, Convex Optimization, pages 215–273. March 2004.

[36] M. Chiang, S.H. Low, A.R. Calderbank, and J.C. Doyle. Layering as optimization decomposition: A mathematical theory of network architectures. IEEE Transactions on Wireless Communications, 95(1):255 – 312, Jan. 2007.

[37] W. Yu and R. Lui. Dual methods for nonconvex spectrum optimization of multicarrier systems. IEEE Transactions on Communications, 54:1310–1322, 2006.

[38] M. K. Awad, V. Mahinthan, M. Mehrjoo, X. Shen, and J. W. Mark. A dual-decomposition-based resource allocation for OFDMA networks with imperfect csi. IEEE Transactions on Vehicular Technology, 59(5):2394–2403, 2010.

[39] D. P. Palomar and M. Chiang. A tutorial on decomposition methods for network utility maximization. IEEE Journal on Selected Areas in Communications, 24(8):1439–1451, 2006.

[40] J. Huang, V. Subramanian, R. Berry, and R. Agrawal. Scheduling and resource allocation in ofdma wireless systems. In Orthogonal Frequency Division Multiple Access Fundamentals and Applications. Feb. 2009.

[41] M. Bohge, J. Gross, and A. Wolisz. The potential of dynamic power and sub-carrier assignments in multi-user ofdm-fdma cells. IEEE Globecom, 5: 2932–2936, Nov. 2005.

[42] G. Song and Y. G. Li. Cross-layer optimization for ofdm wireless networks-part ii: Algorithm development. IEEE Trans. Wireless Commun., 4(2):625–634, Mar. 2005.

[43] E. B. Rodrigues and F. Casadevall. Rate adaptive resource allocation and utility-based packet scheduling in multicarrier systems. Majlesi Journal of Electrical Engineering, 5(1), Mar. 2011.

[44] Z. Cao and E. W. Zegura. Utilitymax-min: An application-oriented bandwidth allocation scheme. IEEE International Conference on Computer Communications, 2:793–801, Mar. 1999.

[45] S. Shenker. Fundamental design issues for the future internet. IEEE Journal on Selected Areas in Communications, 13(7):1176–1188, Sept. 1995.

[46] G. Song and Y. G. Li. Cross-layer optimization for ofdm wireless networks-part i: theoretical framework. IEEE Trans. Wireless Commun., 4(2):614–624, Mar. 2005.

[47] A. Papoulis. Sequences of random variables. In J. M. Morriss R. L. Howell, editor, Probability, Random Variables, and Stochastic Processes, pages 214–215. Feb. 1991.

[48] E. Yaacoub and Z. Dawy. Proportional fair scheduling with probabilistic interference avoidance in the uplink of multicell ofdma systems. IEEE Globecom Workshop on Mobile Computing and Emerging Communication Networks, pages 1202 – 1206, Dec. 2010.

[49] P. Wang, C. Liu, and R. Mathar. Dynamic fractional frequency reused proportional fair in time and frequency scheduling in ofdma networks. International Symposium on Wireless Communication Systems, pages 745 – 749, Nov. 2011.

[50] M. Grieger, P. Marsch, and G. Fettweis. Uplink base station cooperation by iterative distributed interference subtraction. In Personal, Indoor and Mobile Radio Communications, PIMRC, Tokyo, Japan, Sept. 2009.

[51] S. Hamda, M. Pischella, D. Roviras, and R. Bouallegue. Analysis of weighted proportional fair resource allocation for uplink ofdma. Las Vegas, USA, Sep. 2013.

[52] G. Song and Y. G. Li. Cross-layer optimization for ofdm wireless networks-part i: theoretical framework. IEEE Trans. Wireless Commun., 4:614–624, Mar. 2005.

[53] S. Hamda, M. Pischella, D. Roviras, and R. Bouallegue. Fractional frequency reuse based on weigthed proportional fair for uplink ofdma. In IEEE Wireless Communications and Network Conference WCNC, Istanbul, Turkey, April 2014.

[54] G. R. HIERTZ, D. DENTENEER, S. MAX, R. TAORI, J. CARDONA, L. BERLEMANN, and B. WALKE. Ieee 802.11s: The wlan mesh standard. IEEE Wireless Communications, 17(1):104–111, Feb. 2010.

[55] W. Dang, M. Tao, H. Mu, and J. Huang. Subcarrier-pair based resource allocation for cooperative multi-relay OFDM systems. IEEE Transactions on Wireless Communications, 9(5):1640–1649, May 2010.

[56] A. Adinoyi, B. Bakaimis, L. Berlemann, J. Boyer, and al. EU FP6 IST-2003-507581 WINNER, d 3.4 definition and assessment of relay based cellular deployment concepts for future radio scenarios considering 1st protocol characteristics. October 2004.

[57] ARTIST. ARTIST4G presentation. ARTIST 4G Work Package 3 Advanced Relay Concepts.

[58] R. Balakrishnan, X. Yang, M. Venkatachalam Ian, and F. Akyildiz. Mobile relay and group mobility for 4G WiMAX networks. In IEEE Wireless Communications and Networking Conference WCNC, Cancun, Quintana Roo, March 2011.

[59] A. Papadogiannis, A. Saadani, and E. Hardouin. Exploiting dynamic relays with limited overhead in cellular systems. In IEEE Global Telecommunications Conference GLOBECOM, Honolulu, HI, Nov. 2009.

[60] H. Jeong, J. Hong Lee, and H. Seo. Resource allocation for uplink multiuser OFDM relay networks with fairness constraints. In IEEE Vehicular Technology Conference VTC Spring, Barcelona, Spain, April 2009.

[61] D. Zhang, Y. Wang, and J. Lu. Qos aware resource allocation in cooperative OFDMA systems with service differentiation. In IEEE International Conference on Communications (ICC), Cape Town, May 2010.

[62] M.S. Alam, J.W. Mark, and X. Shen. Relay selection and resource allocation for multi-user cooperative LTE-A uplink. In IEEE International Conference on Communications (ICC), Ottawa, ON, June 2012.

[63] I.C. Wong and B.L. Evans. OFDMA downlink resource allocation for ergodic capacity maximization with imperfect channel knowledge. In IEEE Global Telecommunications Conference GLOBECOM, Washington, DC, USA, Nov. 2007.

[64] D. Tse and P. Viswanath. MIMO I: Spatial multiplexing and channel modeling. In Cambridge University Press, editor, Fundamentals of Wireless Communications, pages 341–387. Aug. 2004.

[65] J. Liu, N. B. Shroff, and H. D. Sherali. Optimal power allocation in multi-relay mimo cooperative networks: Theory and algorithms. IEEE Journal on Selected Areas in Communications, 30(2):331–340, Feb. 2012.

[66] A. Toding, M. R. Khandaker, and Y. Rong. Joint source and relay optimization for parallel mimo relay networks. EURASIP Journal on Advances in Signal Processing, 174, Aug. 2012.

[67] I. Hammerström and A. Wittneben. Power allocation schemes for amplify-and-forward mimo-ofdm relay links. IEEE Transactions on Wireless Communication, 6(8):2798–2802, Aug. 2007.

[68] T. Kang and V. Rodoplu. Algorithms for the mimo single relay channel. IEEE Transactions on Wireless Communication, 6(5):1596–1600, May 2007.

[69] M. Chiani, M. Z. Win, and A. Zanella. On the capacity of spatially correlated mimo rayleigh-fading channels. IEEE Transactions on Information Theory, 49(10):2363–2371, Oct. 2003.

[70] H. Lin and P. Siohan. Multi-carrier modulation analysis and wcp-coqam proposal. EURASIP Journal on Advances in Signal Processing, May 2014.